Temperature Control of a High Vacuum Chamber

Tiago Miguel Salvador Rodrigues

Master's thesis

Supervisor at FEUP: Professor Doutor Fernando Gomes de Almeida

Supervisor at INEGI: Doutor Luís Miguel Pereira Pina

Master in Mechanical Engineering

2018

ABSTRACT

This MSc thesis theme is embeded in a larger project, developed by INEGI in partnership with Spin Works for ESA, whose objective is to develop and test a HDRM (Hold Down and Release Mechanism) for aerospace applications.

This work had as main goal the development of an automatic temperature control system for a thermal high vacuum chamber. For that, the chamber and associated system dynamics were studied, improvements suggested, and the temperature control system developed and implemented.

The modelling of the cooling and heating systems, as well as the chamber itself, were crucial for the objective of understanding the associated dynamics and to enable the development of an adequate temperature controller for the parts being tested inside the chamber.

Therefore, here are described all the steps taken for developing, implementing and assembling not only the temperature control system but also the monitoring and control software of the chamber. Finally, the results of the various tests conducted to validate the correct working of the temperature control system are presented.

The results of the work developed during this thesis will be used in other projects, for materials and space application components testing.

RESUMO

A presente dissertação enquadra-se num projeto mais alargado, desenvolvido em parceria do INEGI com a Spin Works para a ESA, que visa o desenvolvimento e teste de um mecanismo HDRM (Hold Down and Release Mechanism) para aplicações espaciais.

Este trabalho teve como objetivo o desenvolvimento de um sistema de controlo automático da temperatura no interior de uma câmara de alto vácuo. Para isso, foi estudado o comportamento da câmara e sistemas associados, sugeridas melhorias e desenvolvido e implementado o sistema de controlo de temperatura.

Foi essencial efetuar a modelação dos sistemas de aquecimento e arrefecimento, bem como da própria câmara, com o objetivo de perceber as dinâmicas associadas e de modo a tornar possível desenvolver um controlador adequado para controlar a temperatura dos componentes a serem testados no interior da câmara.

Estão então descritas todas as etapas de desenvolvimento dos modelos, da implementação e montagem dos sistemas de controlo de temperatura, bem como do software de controlo e monitorização da câmara. Finalmente são apresentados os resultados de ensaios realizados para validar o funcionamento do sistema de controlo de temperatura.

Os resultados do trabalho desenvolvido nesta dissertação virão a ser utilizados noutros projetos, para o ensaio de materiais e componentes para aplicações espaciais.

ACKNOWLEDGEMENTS

Firstly, I would like to thank Professor Fernando Gomes de Almeida and Dr. Luis Pina, for all their time and knowledge transmitted during this project.
To Jhonny Rodrigues and Fernando Silva for all the time spent helping me and guiding me.

To all the colleagues met at INEGI.
To all the professors that somehow contributed to my present and future success.

To my friends and family for the support provided throughout the years.
And to my parents and sisters, for the unconditional support and encouragement.

Thank you!

TABLE OF CONTENTS

TABLE OF FIGURES

TABLES

LIST OF ABBREVIATIONS

ESA – European Space Agency
GHe – Gaseous Helium
GN2 – Gaseous Nitrogen
GUI – Graphical User Interface
Kn – Knudsen number
LN2 – Liquid Nitrogen
N2 – Nitrogen
NASA – National Aeronautics and Space Administration
NEXA – Non-Explosive Actuator
PLC – Programmable logic controller
RGA – Residual Gas Analyzer
RUNE – Reusable and Non-Explosive Actuator
SCADA – Supervisory control and data acquisition
TMP – Turbomolecular pump
TVC – Thermal Vacuum Chamber

1 INTRODUCTION

1.1 Background

This MSc thesis theme arose from the need to test parts and components for aerospace applications for the European Space Agency (ESA), which requires very specific conditions. Before this project, the Thermal Vacuum Chamber (TVC) was manually controlled and had a poor setup temperature and pressure logging system. Therefore, this thesis will address these problems and propose solutions to solve them and improve the usability of the TVC.

1.2 The NEXA-Q / RUNE projects

This work is included in the NEXA-Q and RUNE projects, which are two parallel projects with the objective of developing a Hold Down and Release Mechanism (HDRM) and preparing it to be sent in space missions for the European Space Agency (ESA).

The main objective of the RUNE project is to perform the qualification test campaign for the device, whose objective "is to validate the performance of the mechanism under representative environmental conditions. The planned test sequence intends to preserve the order in which environments are encountered during the operational life, to detect potential failures and defects as early in the test sequence as possible, and to minimize the total time required for the test campaign." [1]

On the other hand, the NEXA-Q project is a project more focused in the testing of the device for improvement and optimization, where "the main goal of the project is to raise the mechanism's technology readiness level by implementing previously identified improvements, followed by demonstration and ground testing of a batch of mechanisms, in order to reach flight-qualified status (TRL 8). The project also aims at evaluating the commercial potential of the device and initiating the patent application process." [2]

1.3 Hosting Institution

Figure 1- INEGI [3]

The Institute of Science and Innovation in Mechanical and Industrial Engineering (INEGI), responsible for the proposal of this MSc thesis theme, presents itself as a National Reference Institution in technology-based innovation and the technology transfer area and aims to become a relevant player in the European Scientific and Technological System.

The institution describes itself as being a "Research and Technology Organization (RTO), bridging the University – Industry gap and focused on applied Research and Development, Innovation and Technology Transfer activities for the industry. It was founded in 1986, among what are now the Departments of Mechanical Engineering (DEMec) and of Industrial Engineering and Management (DEGI) of the Faculty of Engineering of the University of Porto (FEUP). Being a non-profit private association, recognized as of public utility and having its own team of 200 collaborators, INEGI is an active agent in the development and consolidation of a competitive model based on knowledge, on high product and process technological content and on technological innovation." [4]

Its mission is to be recognized as a national reference Institution in technology-based innovation and technology transfer area and become a relevant player in the European Scientific and Technological System.

1.4 Thesis layout

This thesis describes all the necessary steps in order to develop the system for the control of the temperature inside a thermal high vacuum chamber. It presents all the theory necessary to understand the various concepts addressed and the steps taken to obtain the final solution. Finally, the results are presented, as well as their analysis, and improvements for future projects are proposed.

In Chapter 1, the hosting institution and main goals are presented, as well as the methodology proposed for achieving such goals.

In Chapter 2, the project motivations, description of the problem and desired outcome are defined as well as the planning and applications of the project.

In Chapter 3, all the theoretical background required to better understand all the parts of the project is described. From the chamber itself, to supporting systems all are analysed in order to have knowledge of their working and limitations that may later affect the control.

In Chapter 4, a description of the previous system is done, and all the component are analysed and described. The component requirements and the various discussed solutions for the temperature control system are also presented and the solutions to adopt selected.

In Chapter 5, an analysis to the dynamics of the system is done. Simulation are performed, and the various control alternatives are studied.

In Chapter 6, the control strategies are defined, and explained.

In Chapter 7, the assembly of all the components and physical test of the systems is done, and the control strategy is refined.

In Chapter 8, the final results are shown, and the control strategy validated.

In Chapter 9, conclusions are presented and summarized, and improvements are suggested for future projects.

1.5 Main Goals

At the core of this study is the development and implementation of a temperature control system for a thermal high vacuum thermal chamber in order to achieve an accurate and autonomous sequence of thermal cycles necessary for component testing under space like conditions.

The goals can be summarized in 5 points:

- Improvement of the heat transferring system
- Development of an automatic temperature cycling controller
- Ensure robustness of the system for long duration tests
- Reduce human intervention in the testing process
- Creation of an adaptable solution for future changes in the testing needs

1.6 Methodology

To achieve the proposed objectives, the following steps were followed:

- Study of the existing temperature control system.
- Study and evaluation of existing thermal control inside high vacuum chambers.
- Design of control solutions that meet the requirements.
- Evaluation of these solutions and selection of the best design to implement.
- Acquisition of the necessary components.
- Installation and testing of each component individually.
- Integration and testing of all components in the DAQ and automatic control system.
- Study of the system dynamics.
- Development of the control strategy and control algorithm.
- Simulation of the control algorithm.
- Implementation in the vacuum chamber.
- Validation of the final automatic controller.

2 PROJECT ANALYSIS

2.1 Project motivations

The development of components for the aerospace industry is dependent on testing and simulation of conditions that will be experienced in their final application. This project arose from the involvement of INEGI in the testing of a component developed by a Portuguese company to be used in an aerospace application. This component needs to meet ESA standards and, for that, a series of tests need to be performed. INEGI is responsible, apart from others, for the thermal vacuum testing. The component is subjected to thermal cycles under vacuum and its behaviour is logged, in order to verify its suitability for final use.

These thermal cycles have very long durations, over 100 hours, so the temperature control system needs to be autonomous and robust.

This study is based on this need to control the temperature and to do it in a fast, reliable and autonomous manner.

2.2 Description and goals

There are a couple of problems that need to be solved in this project. One of these problems, is related to the heating system: although well controlled, the temperature being measured and used for the PID controller is in the oil bath inside the main unit, this meaning that the temperature on the furthest point, inside the chamber, is not the same as the one defined as setpoint for the controller. Other issue, is the use of the same copper serpentine for both heating and cooling systems. This has some implications in both the response time and structural integrity of the chamber. On one hand, when using the silicon oil-based heating system, which is a closed circuit there cannot be any contaminants interfering with the main unit. On the other, when using the liquid nitrogen cooling system, if there is any oil left on its path, it will freeze, possibly affecting the structural integrity of the copper serpentine. To solve this problem, there was the need to purge the serpentine, using compressed air to avoid any cross contamination of the systems. This had to be done manually which meant that the transition from cooling to heating would vary. Since the heating system was a closed circuit, any silicon oil purged from the system needed to be replaced in the main unit and could not be re-used, which meant a costly expense in a series of tests.

The other issue was the heat transfer from copper plate to the part, which is done due to conduction and radiation. The only way to heat or cool the part by conduction was through the contact areas of the copper plate, part support device and the part itself. On the other hand, the heat transfer due to radiation occurs mainly between the copper plate to the inside walls of the chamber. Since the main objective is to control the temperature of the part, there is the need to try and concentrate the radiation on it. Lastly, and from a control standpoint, the control of the system is being done in different ways, for the heating there is the possibility of using a PID or similar controller but for the cooling, since it is basically an on-off type of control, there are more limited control possibilities.

2.3 Planning

In order to keep the work organized, there was the need to establish a schedule for all the phases of the project. For that it was created a spreadsheet with the deadlines for all the tasks to be accomplished.

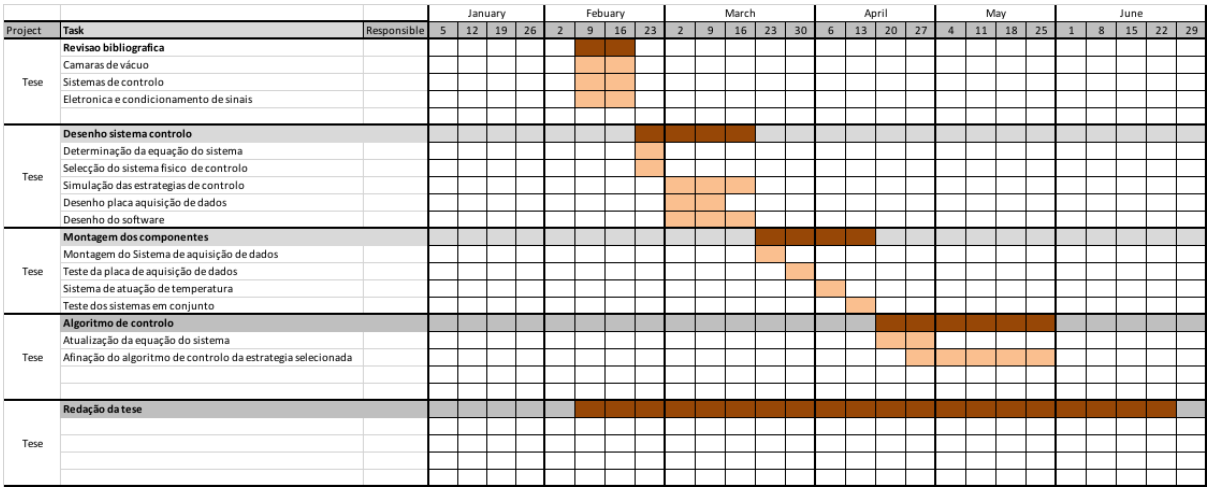

Figure 2- Dissertation planning

2.4 Applications

As stated earlier thermal vacuum testing is widely used in aerospace industry. This type of testing can be used to test final components as well as analyse and determine materials' behaviour. From either composites to metals, components used on satellites or airplanes, the tests need to be carried out and the control of conditions need to be the tightest possible.

3 STATE-OF-THE-ART

3.1 Thermal Vacuum chambers

High thermal vacuum chambers are pieces of equipment that allow the simulation of vacuum and temperature conditions found in space. These chambers are widely used in the aerospace industry and are used to test components for flight qualification or behaviour analysis. So, this chamber need to be able to simulate as closely as possible the environmental conditions experienced by spacecraft's and their components, both while in orbit and during take-off [5].

3.1.1 Vacuum

The vacuum state is characterized as the reduction in matter density in a gas, so, the measure of vacuum is given by the residual pressure of the matter remaining in vessel considered. This pressure can be expressed in various units, which relate to each other as follows:

$$1\ atm = 760\ torr = 1013\ mbar = 1.013 * 10^5 Pa$$

So, depending of the application, various vacuum ranges might be acceptable for use and they are characterized as follows:

Table 1- Vacuum ranges [6]

P (mbar)	10^3		1		10^{-3}		10^{-7}		10^{-12}	
		Low		Medium		High (HV)		Ultra-high (UHV)		Extreme high (EHV)
P (Pa)	10^5		10^2		10^{-1}		10^{-5}		10^{-10}	

3.1.1.1 Gas behaviour

A gas can be described as a group of molecules that move in random direction, constantly colliding and exchanging energy with each other which continually alters speed and direction of each molecule. For lower densities of particles, there is a reduction in the number of collisions and consequent reduction in interactions between molecules. This characteristic of a gas is quantified by a ratio known as the Knudsen number (Kn). This dimensionless number relates the mean free path (λ), which is the mean distance a particle can travel without interference from another molecule, and D, the characteristic dimension of its container, whose relation can be seen in equation 1.

$$Kn = \frac{\lambda}{D} \tag{1}$$

At atmospheric pressure, the value of λ is much lower than the one of D, which means that Kn<<1. So, the collisions between molecules dominate the gas behaviour, and it behaves as a fluid. Gases for which Kn << 1 are said to be in a continuum or viscous state. In the same way, when high vacuum is present, the mean free path, λ, is much larger than D, which means that Kn>>1. In the case of a vacuum chamber, this means that the interactions with the chamber walls dominate the gas behaviour and are more significant than the interactions between molecules, which is not fluid-like. Gas in these conditions is referred to as being in a molecular state [6].

3.1.2 Temperature

Current thermal vacuum chambers, such as the ones from ESA and NASA, use industrial refrigeration and heating systems. Mainly based in liquid nitrogen for the cooling, using different methods for such purpose. The heat exchange is done using shrouds that are either located around the chamber or directly over the part tested. There are also chambers prepared for radiation and sun simulation, but those are not the primary focus of this work.

3.1.3 Vacuum chamber designs

Vacuum chambers are the physical barrier between the exterior environment and the internal test conditions. There are several variants of vacuum chamber, depending on requirements and needs for each application.

Chamber shape

The vacuum chamber shape, allows the conservation of vacuum and thermal radiation phenomena, which are very important to simulate space environment characteristics.

There are several factors that limit the shape of the chamber, namely, the size of the test specimen, the vacuum level that is to be supported and also the thermal simulation system size. Therefore, different shapes have different level of structural rigidity, to avoid their collapse while under vacuum conditions. Figure 3 shows some of the most common shapes and their characteristics in terms of rigidity.

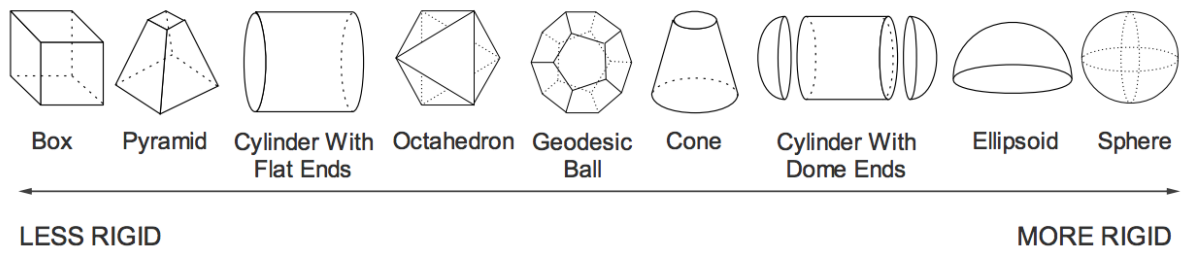

Figure 3- Vacuum chamber shapes in relation to their rigidity [5]

When using some of the less rigid shapes or designing a considerable size chamber, there is the possibility to reinforce the shape with supports, through the use of a stiffening ring for example, and in that way obtain better mechanical properties for the shape. The most common chamber type for space simulation is the cylindrical chamber with dome ends [5].

Materials

The most common material for construction of the chamber is stainless steel, but other materials are also used, such as aluminium. For use in the chamber or on supporting systems, there is also the need to be careful with the material choice, in order to avoid phenomena such as outgassing and vacuum leaks, so porous and dirty materials, such as the ones resulting from castings, must be avoided. The materials of choice for these applications are aluminium, mild steel, titanium, Inconel, Monel, glass, Teflon®, and polycarbonate [7].

Sealing

Sealing of surfaces must be another point of concern since vacuum leaks may occur through those locations. For this matter, gaskets are commonly composed of fluorocarbon (Viton-A®) but other materials are used, such as butyl, Buna-N, EPDM, Silicon, Chemraz and Kalrez. Silicon is only suitable for low vacuum levels; in the same way, for ultra-high vacuum applications, metal gasket, made of copper and aluminium, are often used [7].

3.1.4 Creating High vacuum

The process of obtaining vacuum is characterized as having a big variation in particle density throughout its duration. This process starts at atmospheric pressure and ends at the desired vacuum conditions. The most common way of achieving such conditions is the use of multistage systems, shown in Figure 4 ,that uses a roughing pump for atmospheric pressure pumping and a secondary pump to achieve high vacuum conditions. These pumps can either be connected in series or in parallel.

Although it is possible to use only one pump for both stages, the cost, dimensions and system weight make it an unviable solution [8]. The gas extraction system can also be run continuously or only until vacuum is achieved, from which point the chamber is sealed to avoid any vacuum leaks.

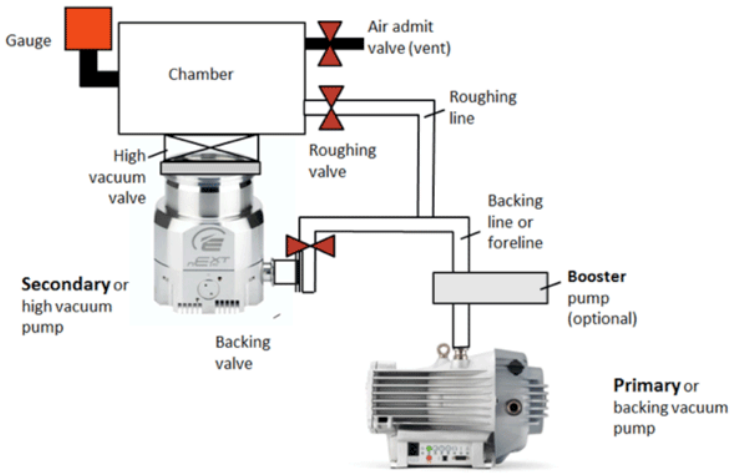

Figure 4- Dual stage vacuum system [9]

3.1.4.1 Turbomolecular pump (TMP)

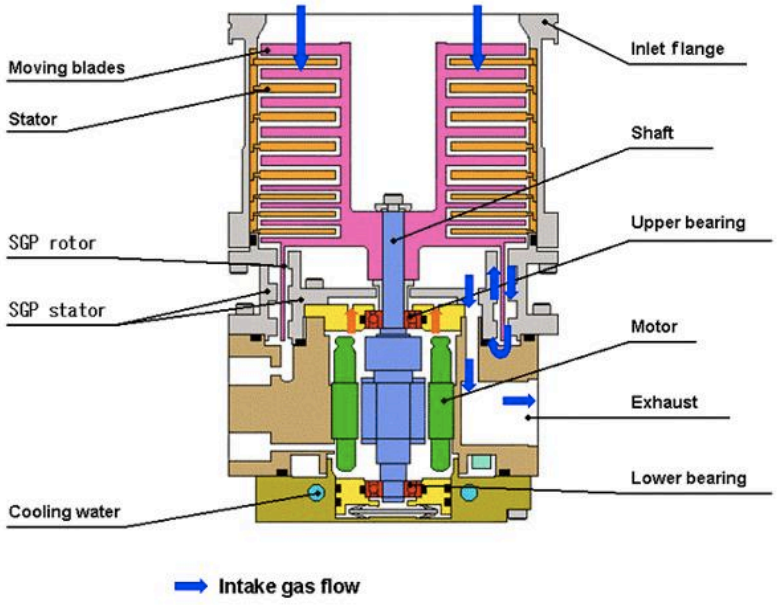

Figure 5- Cross-section of a turbomolecular pump [10]

The work principle of a TMP (Figure 5) is based on the momentum transfer from the rotating blades to the air molecules. The momentum of the rotor is transmitted to the particles by the superposition of the particle collision velocity and the velocity of the rotating blades. This way, a random motion of particles is transformed in a directional motion, creating the pumping action (Figure 6). For Kn values where the mean free path is bigger than the distance between blades, particle collisions occur mainly with the blades of the rotor allowing for an efficient pumping. When the Kn values get to the point where the mean free path is lower than said distance, cause by an increase in pressure, the interaction between molecules take bigger expression over the interaction with the blades and the effectiveness of the TMP is greatly reduced. Therefore, TMP are usually not able to pump against atmospheric pressure and must be backed up by a roughing pump.

This type of pump, coupled with a roughing pump, is the only mechanical pump that can achieve pressures in the range below 10^{-10} Torr [8].

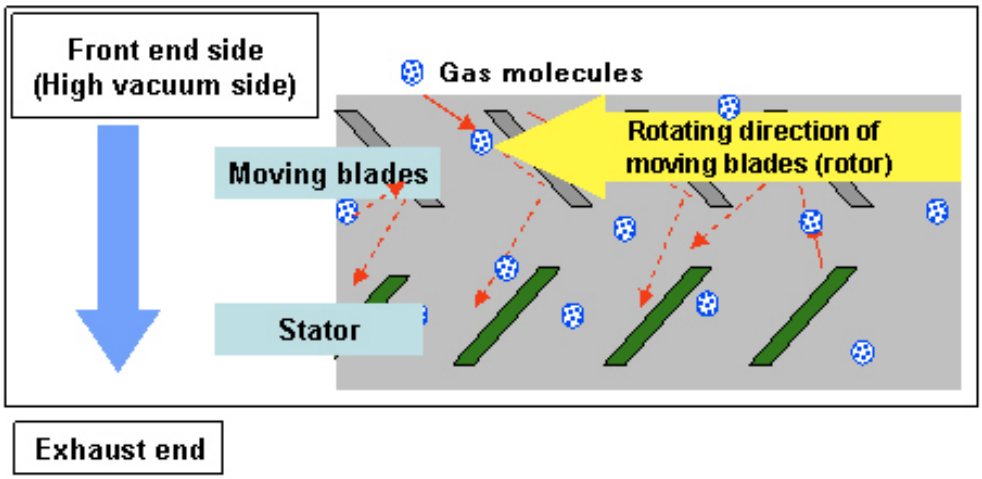

Figure 6- Inner workings of a turbomolecular pump [11]

3.1.5 Vacuum sensors

In order to monitor the pressure inside vacuum chambers, there is the need to use sensors that are capable of measuring pressures as low as 10^{-6} mbar.

Pressure is defined as the force exerted per unit of area (Equation 2), and its SI unit is the Pascal (Pa). As explained earlier, when referring to vacuum other units are more commonly used.

$$P = \frac{F}{A} \tag{2}$$

If pressure is measured via the force it exerts, then it is independent of the type of fluid that is exerting it. However, pressure measurement based on force has a limit due to forces becoming too small to be measured.

That being said, there is the need to measure these pressure drops with different methods, that are able to give accurate measures at such low pressures. Some of these methods use indirect measurements to determine the pressure. Also to note, is the fact that from these methods there is not one that can work for the entire pressure range [12].

For the selection of the different sensors, and measuring methods, the following parameters should be taken into account:

- Pressure range to be measured
- Gas composition (inert or corrosive)
- Desired repeatability and accuracy
- Environmental conditions (radioactive)

3.1.5.1 Piezoresistive gauge

This simple and extremely robust method is based in the piezoresistive effect, by which material changes electrical resistivity when subjected to a deformation. In the sensors, a piezoresistive element is incorporated in the diaphragm, which is being subjected to a reference

pressure from one side. When pressure is applied, the variation in resistance due to diaphragm deflection allied to the known reference pressure, allow for the calculation of the pressure being exerted. This sensor is characterized by its insensitivity to gas inrush and its high accuracy [13]. A representation of this gauge can be seen in Figure 7.

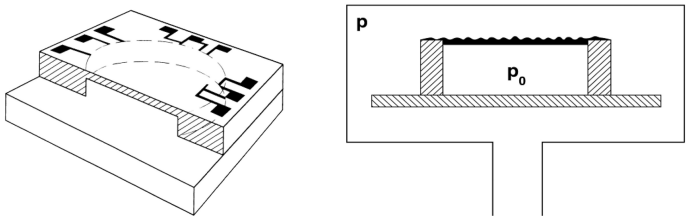

Figure 7- Piezoresistive gauge representation [13]

3.1.5.2 Capacitive gauge

The capacitive sensor (Figure 8) has a similar work principle to the previous one, but instead of being based on change of resistance, it relies on the variation of capacitance to measure the pressure. The deflection of the diaphragm is measured using the electrical capacitance between the thin metal diaphragm and some fixed electrodes. Capacitance manometers are the most accurate devices for measuring the differential or absolute pressure of all gases. The lower measurement limit is 10^{-5} mbar [13].

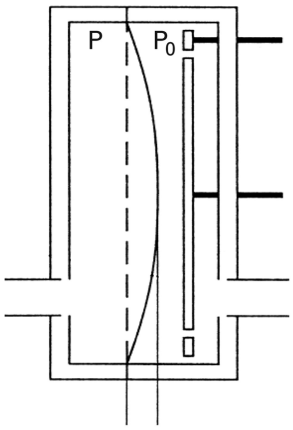

Figure 8- Capacitive gauge representation [13]

3.1.5.3 Pirani gauge

A Pirani vacuum gauge (Figure 9) utilizes the thermal conductivity of gases at pressures p of less than approx. 10 to 100 hPa. Wire (usually tungsten) that is tensioned concentrically within a tube is electrically heated to a constant temperature between 110°C and 130°C by passing a current through the wire. The surrounding gas dissipates the heat to the wall of the tube. In the molecular flow range, the thermal transfer is proportional to the molecular number density and thus to the pressure. If the temperature of the wire is kept constant, its heat output will be a function of pressure. However, it will not be a linear function of pressure, as thermal conductivity via the suspension of the wire and thermal radiation will also influence the heat output. Pirani's cover a pressure range from about 10 mbar to 10^{-5} mbar [14].

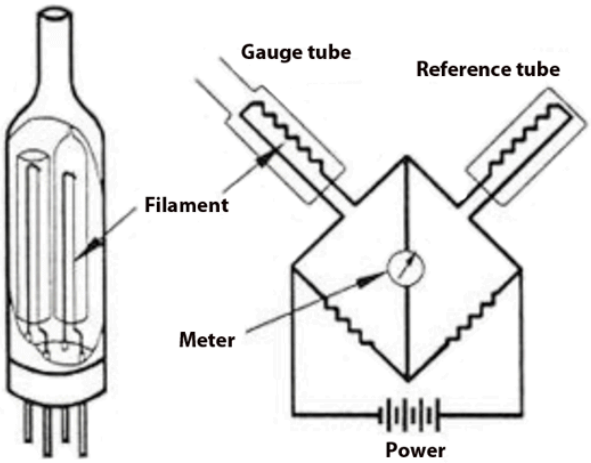

Figure 9- Representation of a Pirani gauge [15]

3.1.5.4 Ionization Gauges

With relatively minor differences, all ionization gauges use the same principle. Energetic electrons ionize the residual gases—the positive ions are collected at an electrode and the current is converted to a pressure indication. The idea is to ionize the gas because ions can be easily detected with a collector electrode. Therefore, electrons are accelerated to cause collision ionizations. This is possible in a wide pressure range from medium up to extreme high vacuum, where the particles have a sufficiently high mean free path [16].

3.1.5.5 Cold-cathode gauge

Cold cathode ionization vacuum gauges (Figure 10) essentially consist of only two electrodes, a cathode and an anode, between which a high voltage is applied via a series resistor. Negatively charged electrons leave the cathode through field emission, moving at high velocity from the cathode toward the anode. As they travel this path, they ionize neutral gas molecules, which ignites a gas discharge. The measured gas discharge current is a parameter for pressure [14].

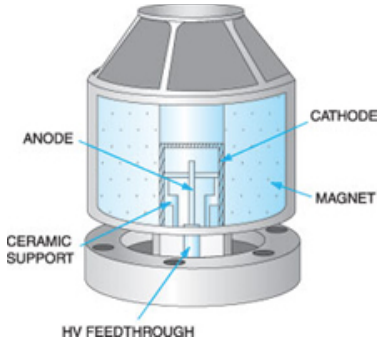

Figure 10- Cold cathode gauge [17]

Many electrode geometries have been used—cylinders, plates, rings, rods, in various combinations with the magnetic field direction and strength chosen to maximize the measured

current. If the gauge's central or 'end' electrodes are negative, the convention is to call this a magnetron. If the same electrodes are positive, the gauge is called an inverted magnetron [17].

3.1.5.6 Hot-cathode gauge

In this case electrons are generated with the aid of a heated cathode. A thin wire is placed in the middle of the cylindrical anode, as shown in Figure 11; this wire serves as the ion collector. A voltage of approximately 100 V is applied between anode and cathode. This accelerates all emitted electrons toward the anode and the emission current is measured in the anode circuit. This can be set using the heat output of the cathode. On their way to the anode electrons collide with gas molecules. The ions travel to the collector since it is at the same potential as the anode.

The measured collector current is a parameter for pressure. Since the emission current is proportional to the ion current, it can be used to set the sensitivity of the gauge [14].

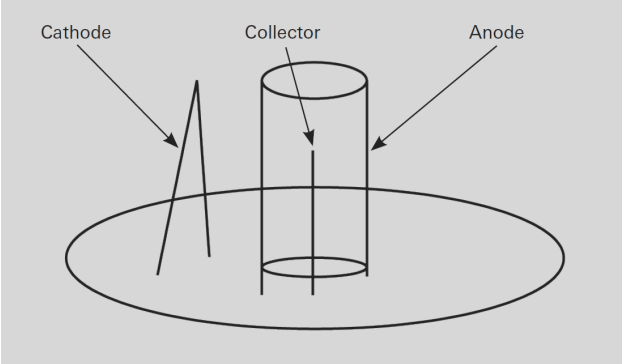

Figure 11- Hot cathode gauge [14]

3.2 Vacuum leak testing

Leaks can develop in different location in vacuum systems, such as feedthroughs, door seals, valves and any type of connection. The leaks detection method depends on the size of the leak.

Large leaks are usually obvious, as the system will not achieve full vacuum. There is the need to inspect all the previous mentioned spots, making sure all the flanges are fully tightened and uniform. A method used for this type of leak detection is the slight pressurization of the chamber with nitrogen and inspecting all connections with a liquid leak detector in order to detect defective seals.

For mid vacuum leaks, other processes are used. The use of methanol or isopropanol in suspected leaky area allows for detection of leaks by monitoring the vacuum gauge and detect any changes when these products are introduced. There may be an increase or decrease of the vacuum pressure, because the liquid may temporarily plug the leak and allow for better vacuum pressure.

Lastly, for high vacuum leaks more scientific methods are used. It is common the use of Residual Gases Analyzer (RGA), in these cases a very sensitive mass spectrometer tuned specifically to admit, ionize, and detect helium. The RGA is connected to one of the flanges of the chamber and it analyses the residual gas in the chamber after pump down. After an initial reading with the chamber depressurized, a flow of helium is put near the flanges and the values

read in the gauge are watched. If the count of helium particles increases, a leak has been found and helium is entering the chamber [18].

This gas is used because it has small molecules and fast moving, making the response time quicker and it is present in very low concentration in the ambient air. Its availability, nontoxicity, non-flammability and the fact that it is completely inert are other advantages of this gas [19].

3.3 ESA Thermal Vacuum Testing

In this section, it will be explained the procedure and requirements as per written by ESA in the testing protocol [20]. Thermal vacuum testing is done in order to demonstrate the ability of an equipment to withstand and perform its correct function in the worst in-orbit conditions, including a safety margin.

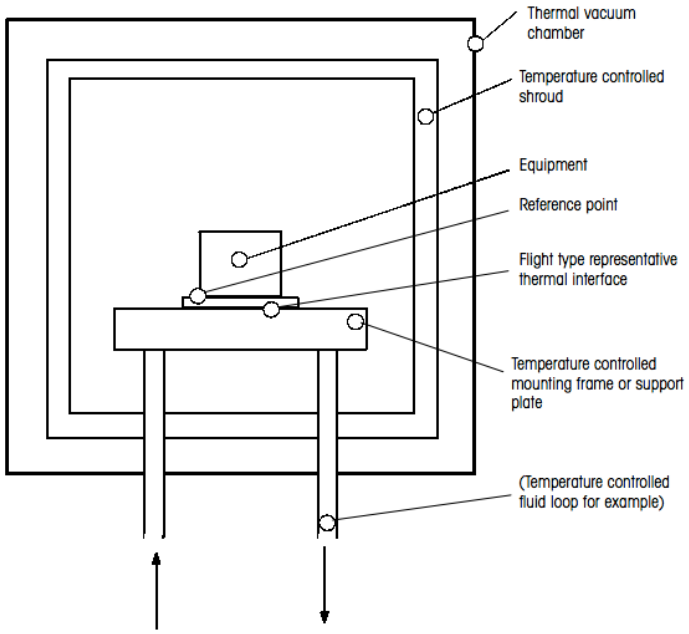

Figure 12- Vacuum chamber setup [20]

3.3.1 Test setup

According to the test procedure, the part must be mounted inside the chamber in a controlled temperature environment (Figure 12). This parameter must be selected and measured in order to guarantee that the temperatures used are equal or past the ones needed for qualification. The part to be tested also has to be mounted in a support that mimics its final mounting location.

3.3.2 Vacuum specification

The test must be carried out with a pressure of 10^{-5} mbar or less, although the first heating can start when the pressure is less then 10^{-4} mbar.

3.3.3 Thermal cycles

The part must be exposed to a thermal cycle, that allows for simulation of launch and in-orbit conditions. This sequence is graphically represented in the next figure:

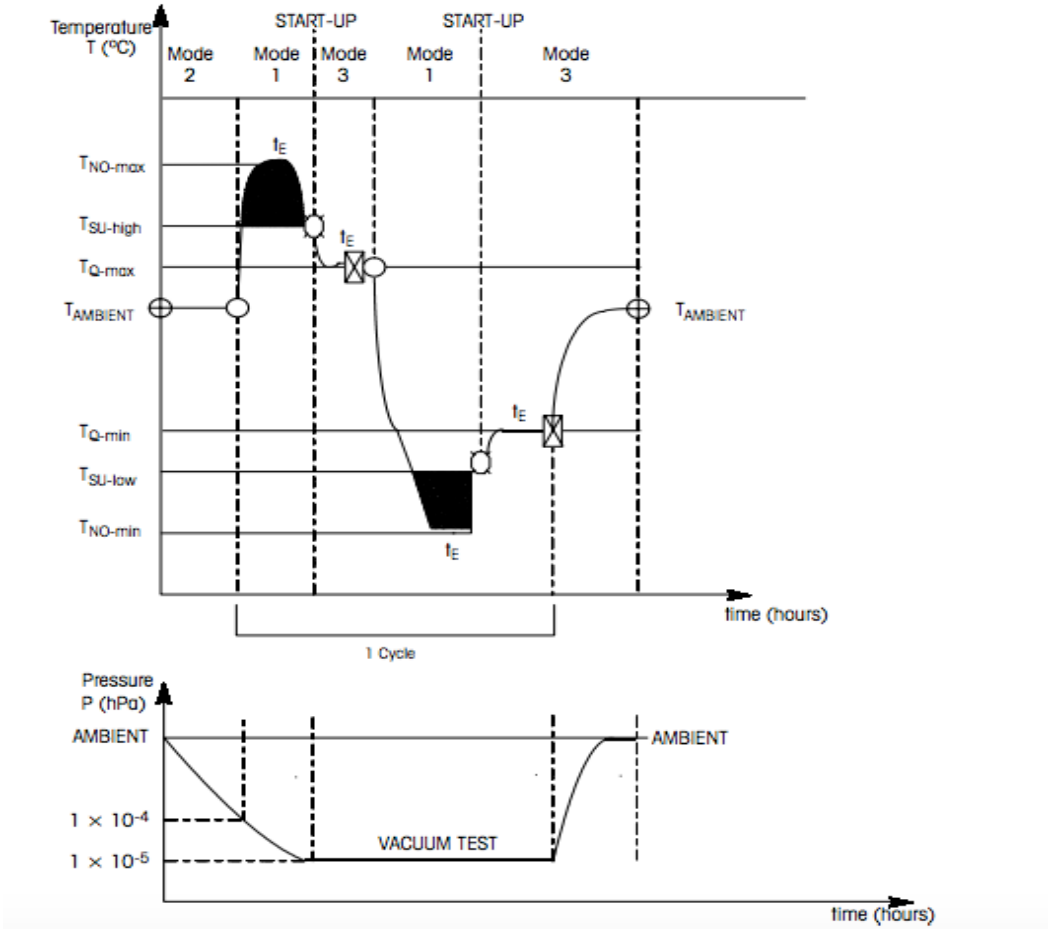

Figure 13- Thermal cycle [20]

With the variables being described as follows:

Symbol	Description
T	Test item temperature
$T_{AMBIENT}$	Ambient temperature
T_{NO-max}	Maximum non-operating temperature (highest design temperature for the equipment to survive not powered)
T_{NO-min}	Minimum non-operating temperature (lowest design temperature for the equipment to survive not powered)
$T_{SU-high}$	Maximum start-up temperature (highest design temperature of the equipment, at which the equipment can be switched on)
T_{SU-low}	Minimum start-up temperature (lowest design temperature of the equipment, at which the equipment can be switched on)
T_{Q-max}	Maximum qualification temperature (highest design temperature at which the equipment demonstrates full design ability)
T_{Q-min}	Minimum qualification temperature (the lowest design temperature at which the equipment demonstrates full design ability)
P	Pressure
MODE 1	Functionally inert (test item not energized). Normally applicable to the non-operating condition.
MODE 2	Partially functioning. Conditions as detailed in applicable design specifications, but normally applicable to conditions during launch.
MODE 3	Fully functioning (test item fully energized and fully stimulated). Normally applicable to conditions during orbit.
⊕	Initial and final "functional and performance test"
⊠	Intermediate reduced functional and performance test
t_E	Dwell time
⏻	Switch-on (Start-up)
⏻	Switch-off

Figure 14- Variables description [20]

The qualification requirements are:

Parameter	Condition / Value
Start cycle	Hot (Hot start for outgassing)
n (number of cycles)	1
t_E (dwell time at T_{hot}/T_{cold}) [a, b]	2 hours
dT/dt (temperature rate of change)	< 20 °C/min
Stabilization criterion	1 °C/1 hour
a $T_{hot} = T_{Q-max}$ or T_{NO-max}.	
b $T_{cold} = T_{Q-min}$ or T_{NO-min}.	

Figure 15- Qualification Requirements [20]

3.3.4 RUNE specific requirements

Depending on the device being tested, some of the requirements are changed. In the case of the RUNE, the specific requirements can be seen in Table 2.

Table 2- RUNE specific requirements

TEST REQUIREMENTS	
n (number of cycles)	8
Pressure (hPa)	$< 10^{-6}$
dT/dt (temperature change rate)	<50 ºC/h
Stabilization criterion	5 ºC/h
TOLERANCES	
Max_Hot.T	+85 ºC [*-0;+5*] *ºC*
Min_Cold.Op.T	-50 ºC [*-5;+0*] *ºC*
Min_Cold.NonOp.T	-100 ºC [*-5;+0*] *ºC*
Room.T	+21 ºC [*-5;+5*] *ºC*

3.4 Heat exchange in vacuum

In normal conditions, i.e., at atmospheric pressure, heat transfer occurs via three ways, conduction, convection and radiation, by which heat energy is transferred from higher to lower temperatures.

Conduction is the process by which heat is transferred from higher to lower temperatures by contact between surfaces. Convection is the process by which a gas in the surroundings of a hot surface is warmed by conduction, expand and becomes buoyant, relative to its surroundings and therefore rises, carrying the transferred energy with it.

Radiation, on the other hand refers to the process by which energy is absorbed, emitted and reflected by surfaces, and does not require a medium to occur [6].

Therefore, both conduction and convection need a medium to occur, which is almost inexistent in high vacuum conditions. So, in this type of conditions, heat transfer by radiation is the only option to exchange energy through the air, or lack of it. Although for some situations conduction can be used, as long as two parts are in contact, the various types of heat transfer are shown in Figure 16.

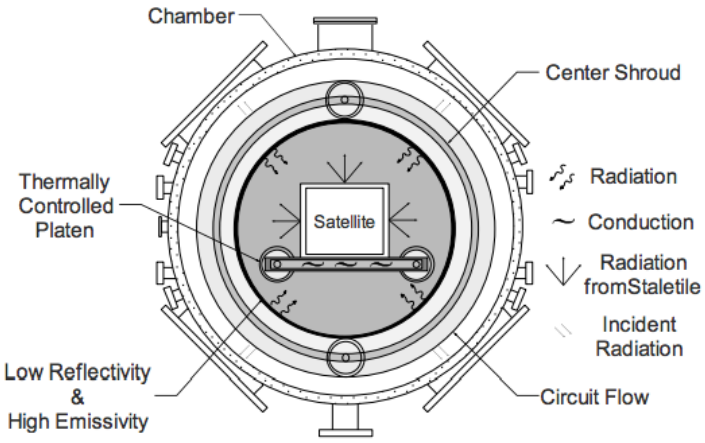

Figure 16- Heat transfer in a vacuum chamber [5]

3.5 Methods for Heating and cooling

Heat exchangers in vacuum chamber come in a variety of forms and shapes. The heat exchange and temperature control can be achieved resorting to shrouds, which surround the chamber and tested component and are used not only as heat exchangers but also as radiation shields, or the use of a platen, that normally also functions as a support for the test subject.

3.5.1 Heat transfer fluids

For operation that do not surpass a certain limit over room temperature, the use of heat transfer fluids, such as silicon oil, may be an appropriate. This type of fluids have the advantage of using a closed-loop circuit and a heater and/or chiller to control the temperature of the fluid. The increase of viscosity of these fluids limits their lower temperature limit to -70 °C, while the boiling and decomposition of the fluid limit its upper temperature limits, typical values are between 100 °C and 150 °C. The use of a closed-loop allows for uniform and controlled temperatures, and fairly rapid changes in temperature can be achieved by minimizing the thermal mass associated with it [21].

3.5.2 Gaseous Nitrogen (GN2)

Gaseous nitrogen, also known as GN2, allows for a wider range of temperature than liquids, with a range of -180 °C to 150 °C, and is used in recirculation systems. However, since gases have lower heat capacity than the latter, a larger volume of this fluid must be circulated in order to perform the heat exchange. That being said, in comparison to liquids, tubes and connections need to be larger. To maintain gas density the pressure of the GN2 loop is adjusted according to temperature. One advantage in regard to liquids is that the possibility of a leak inside the chamber will only represent the venting of a clean gas into the camber [21].

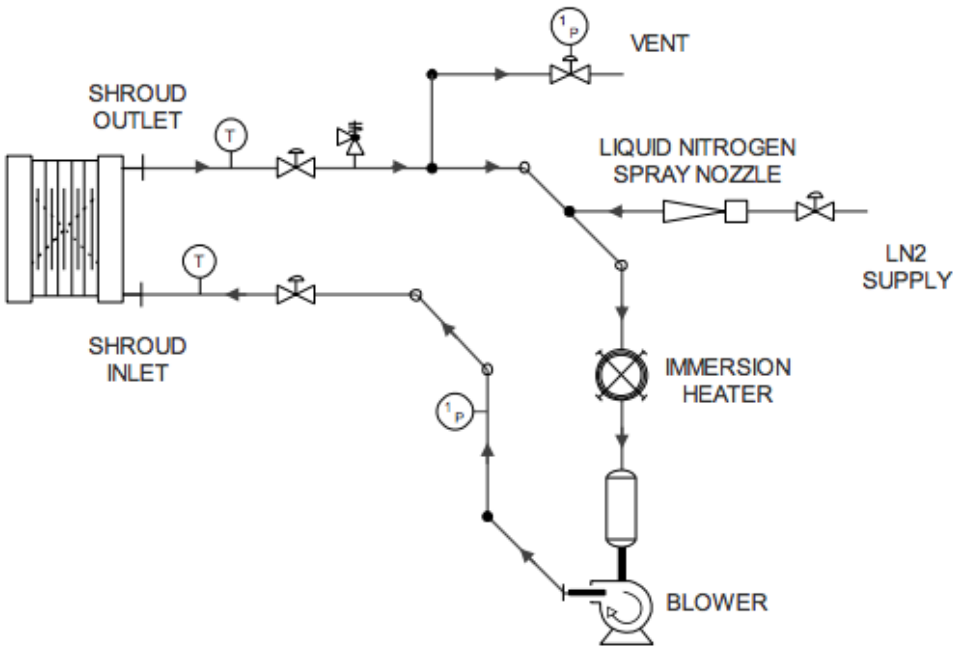

Figure 17- GN2 circulating system [5]

3.5.3 Liquid Nitrogen (LN2)

For lower temperature than -180 °C liquid nitrogen, LN2, is commonly used. It is used to fill the tubes and allow for a uniform temperature in the heat exchanger. In some systems a pump may be used to increase the flow to aid the heat exchange [21].

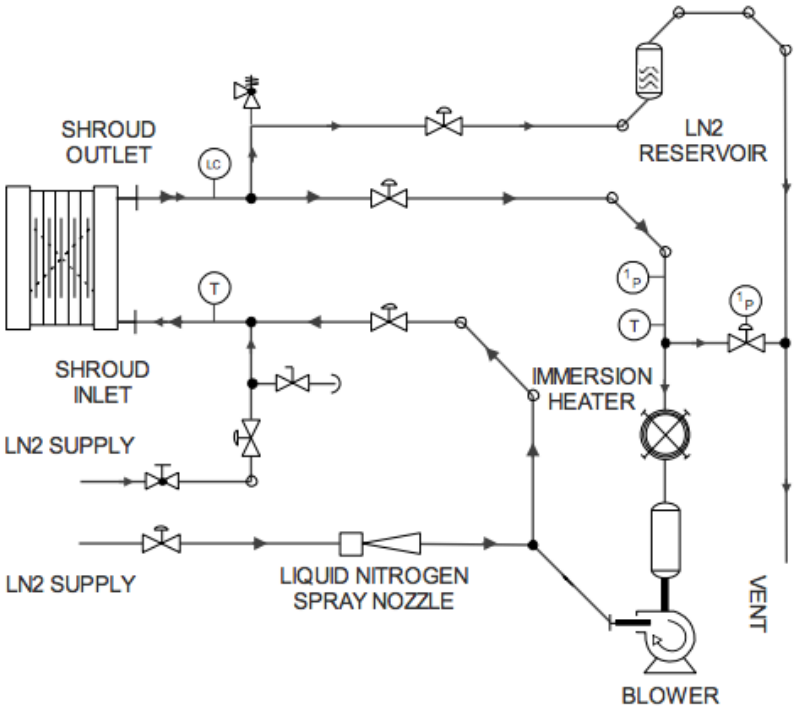

Figure 18- LN2 and GN2 circulating system [5]

3.5.4 Gaseous Helium

When even lower temperatures are needed, gaseous helium (GHe) is capable of achieving temperatures lower than 77 K (-196 °C) by going through a special refrigeration plant, which also functions as a pump to circulate the fluid. Special needs to be taken for exterior lines, which must be vacuum jacketed in order to minimize heat loses [21].

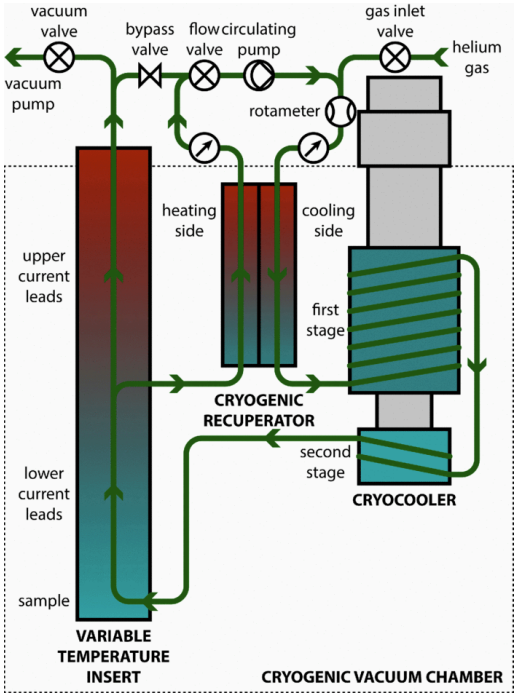

Figure 19- GHe circulating system [22]

3.6 Heat exchange systems available on the market

As stated earlier, the main problem to address in this project is the temperature control in the vacuum chamber. Therefore, there is the need to identify solutions capable of operating under such circumstances and determine which is more adequate.

There are several methods used for heating and cooling under vacuum environments, depending on the target temperature, some systems are capable of achieving the target temperatures using one fluid only, other solutions use multiple fluids or systems, usually to achieve more extreme temperatures.

Therefore, there was the need to find and analyse the systems available on the market and find the best approach to our problem.

Some of the systems offered by Dynavac, allow for the following temperature ranges:

Flooded Liquid Nitrogen	-190C
Circulating Gaseous Nitrogen	-180C to 150C
Mechanical Refrigeration	-50C to 125C
Gaseous Helium	As low as 20K
Radiant heating options	Up to 200C

Figure 20- Temperature range capabilities of different systems [23]

Other solutions, such as the Thermal Conditioning Units (TCU) for space simulation available from Telstar, allow for temperatures in the following ranges:

- Fluid recirculation for optimum performance:
  - Silicone Fluid, with a temperature range from -90ºC to +150ºC
  - Dense GN2, with a temperature Range from -180ºC to + 180ºC

Figure 21- Telstar's systems temperature range [24]

Bemco in their space simulation line-up also has some systems, that are presented in the following table:

Bemco Model	Fluid In Shroud	Cooling Method	Heating Method	Live Load Maximum	Temperature Maximum
Direct	LN2	Flooded LN2	None	Medium	-185 C Only
PCLN	LN2	Circulated LN2	None	High	-185 C Only
HPG_LD	GN2	LN2 Injection	Electric	Medium	-185 C to +150 C
HPG_LH	GN2	LN2 Exchanger	Electric	Medium	-170 C to +150 C
HPG_MF	GN2	Mechanical Cooling	Electric	Medium	-35 C to +150 C
HPG_MN	GN2	Mechanical Cooling	Electric	Medium	-70 C to +150 C
PCL-III	Fluid	LN2 Exchanger	Electric	High	-85 C to +150 C
PCL-III	Fluid	Mechanical Cooling	Electric	High	-65 C to +150 C

Figure 22- Bemco space simulation solutions [25]

There are also products available on the market that can replace and execute the same function as liquid nitrogen, this equipment is called cryocoolers and are available form brands such as Brooks.

Figure 23- Brooks P-102 Cryocooler [26]

One more example of available systems is, a custom solution, the vacuum chamber presented by Laco technologies, which is a vacuum chamber cooled by LN2 and heated using heating elements. This chamber has a range of -130ºC to 200ºC.

Figure 24- Laco's Space Simulation System for Satellite Component Testing [27]

From a control stand point, a system with only one fluid that allows the heating and cooling of the chamber is the ideal solution, being that its cost may be a prohibitive factor.

Another solution, presented by NASA in a report entitled "An alternate method for achieving temperature control in the -130°C to 75°C range" consists in the use of gaseous and liquid nitrogen to lower and increase the temperature, respectively, using a mixer to absorb thermal shock and to better control the temperature.

As seen in the commercially available solutions, to control the chamber heating, infrared lamps or heating elements can be used to help the process, although lamps are not the best solutions due to the possible contamination of the testing environment due to breakage under vacuum. Another solution that can be used to improve thermal behaviour is the use of shrouds and reflective materials around the test subject and the chamber, to reduce wall energy losses. The use of an encasing around the part allows for better concentration of radiation and faster heating, and in the case of use of heating elements aids for a uniform distribution of the incident radiation reducing the hot spots in the part. The systems that allow temperature in the -100 °C range need to use liquid nitrogen to achieve such values.

3.7 Vacuum chamber insulation

Testing of small components and subsystems may be done in very small vacuum chambers. Even at reduced scale, it is still possible to have a controlled thermal environment as well as high vacuum. Platens cooled by liquid or gaseous nitrogen or by closed-loop chillers offer way to create a variable temperature condition; typical of a small lab system are the LN2-cooled platen cooling the chamber. In order to better control the inside temperature of the chamber, there is the need to insulate it, this is done using shrouds which play an important role in

obtaining precise test conditions for space simulation. These shrouds may also be used as heat exchangers, as it is explained in another sub-chapter [21].

3.7.1 Insulation functions

Heat loses by radiation play a big role during the tests, since it is the main source of heat transfer during the whole process. The solution is the use of shrouds to control said losses.

Control ingress of room temperature radiation

One of the functions of the shroud is to control the influence of external radiation, isolating the test article from the outside environment. Vacuum chamber walls usually are at room temperature, and there is the need to control their influence on the part. The solution for this, usually is the use of an insulation that reflects infrared radiation and doesn't absorb the heat from the chamber exterior walls [21].

Vacuum flow

The insulation must isolate the part from the external thermal radiation but should also be able to allow for the outgassing of the test article to be removed by the vacuum pumps, avoiding any blocking of the progression of the vacuum achieving process [21].

High emissivity (ε) and absorptivity (α)

The internal surfaces of shrouds are usually coated in black paint, to allow for the shroud to have high absorptivity and at the same time high emissivity of radiation, to allow for a better heat transfer. Depending on the temperature of the test articles and trial to be executed, different paint and its properties need to be taken into account in order to control its behaviour at certain wavelengths [21].

3.8 Control system and instrumentation

Instrumentation and Control systems are the means by which the operator can monitor and exercise some type of control over the thermal vacuum process. These systems allow the control and monitoring of the test subject, as well as control, monitoring and adjustments over the thermal cycle process and each of the steps of the vacuum achieving process.

The most recent control systems "for space simulation chambers are computing platforms powered by the use of Programmable Logic Controller (PLC), which enables automation for some stages of operation and safe manual control of vacuum processes acquisition and thermocycling inside the chamber. The PLCs control units of main and auxiliary pumping, as well as vacuum valves, safety valves, thermal devices and other components that are part of chamber systems. Such controllers are connected to a central processor where their operating status is displayed on a Supervisory Control and Data Acquisition Program (SCADA)" [5].

The operator has the ability to control the chamber and their systems through a computer and a graphical interface. Real time data, from systems status to chamber environmental conditions and alarms are also displayed.

A common control method for the thermal system is the use of a PID controller, that receives a setpoint value.

3.9 Limitations

The main limitation under vacuum is the heat transfer. Since only radiation and conduction occur, the time taken to balance any temperature differential is increased. Not only that, but also the need to concentrate all the exchange around a part and avoid any type of losses that may increase the process time is crucial. This difficulties in heat exchange will also be a challenge in the domain of the control of the process.

4 VACCUM CHAMBER AND SUPPORTING SYSTEMS

This chapter describes the original system and its components; the proposed solutions for the heat exchange system are also described and commented. Lastly, the final solutions to be used in the TVC are shown.

4.1 Pre-existent solution

The vacuum chamber used on this project is a round chamber, with horizontal axis with a top loading hatch, with approximately 910 mm in length and 650 mm in diameter. Inside the chamber, and for support of the parts being tested there is a copper plate that also works as a heat exchanger, supported by rails that slide in and out of the chamber.

Figure 25- Vacuum chamber

4.1.1 Vacuum system

Throughout this project, the system used for achieving vacuum is a multistage setup, with two pumps connected in series and continuously working, to counteract any vacuum leaks.

The vacuum is achieved by the use of two pumps. The primary one also known as a roughing pump, is a positive displacement Trivac D30A dual stage rotary vane mechanical vacuum pump and gets the chamber to up to approximately 10^{-3} mbar of pressure.

The secondary one is an Alcatel ATP 400 turbomolecular pump, that allows the chamber to achieve the high vacuum state of 10^{-6} mbar although rated for as low as 10^{-10} mbar. As explained in previous chapters, this is a turbine style pump that pushes the gas molecules from the inside of the chamber to the roughing pump.

4.1.2 Heat transfer systems

The temperature on the inside of the chamber was being controlled resorting to two systems. One allowed for the heating of the chamber and another allowed its cooling.

4.1.2.1 Thermal fluid

The fluid utilized in the thermal bath is a Julabo supplied silicon oil, denominated H20S, that has an operating temperature range of 0ºC to 220ºC.

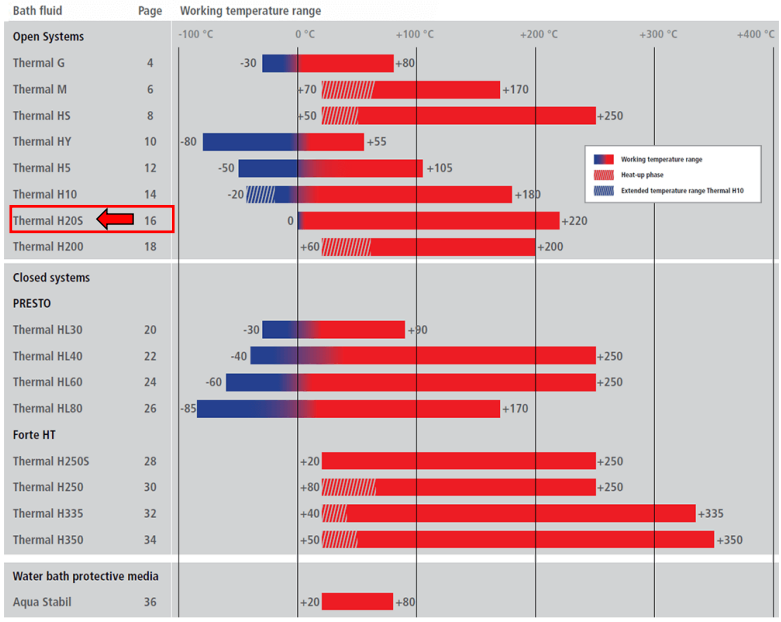

Figure 26- Julabo's fluid working temperature range [28]

4.1.2.2 Heating system

The heating system consists of a silicon oil-based recirculating system, the Julabo F12-MC, which it is controlled by its own PID controller installed on the main unit, and the temperature that is used for the control is acquired from a sensor inside the oil bath. This system is capable of working from 0 to 200 ºC, allowing a smooth transition between the positive temperatures. It has a heating system and a cooling system integrated in the lower part of the unit to allow for the cooling from 200 ºC to 0 ºC.

Figure 27- Julabo F12-MC

4.1.2.3 Cooling system

For the cooling of the system, the lower part of the Julabo, the F12 unit, is capable of reducing the temperature up to 0 °C. For lower temperatures, the method used is liquid nitrogen, running in the same copper serpentine as the previous system. It is comprised of one 60 litre self-pressurizing vessel, TP60 from Air Liquide, equipped with two safety release valves, one pressure gauge, one liquid level indicator, two manual release valves and two solenoid-controlled valves, with one of them connected to a flow regulator. The control of this system is an on-off type of control, meaning that the only adjustments done are resorting to a state machine that controls the two solenoid valves, allowing for the use of either the regulated or unregulated branch of the liquid nitrogen bottle. Shown in Figure 28 is the valve setup and Nitrogen routing, with the insulation removed.

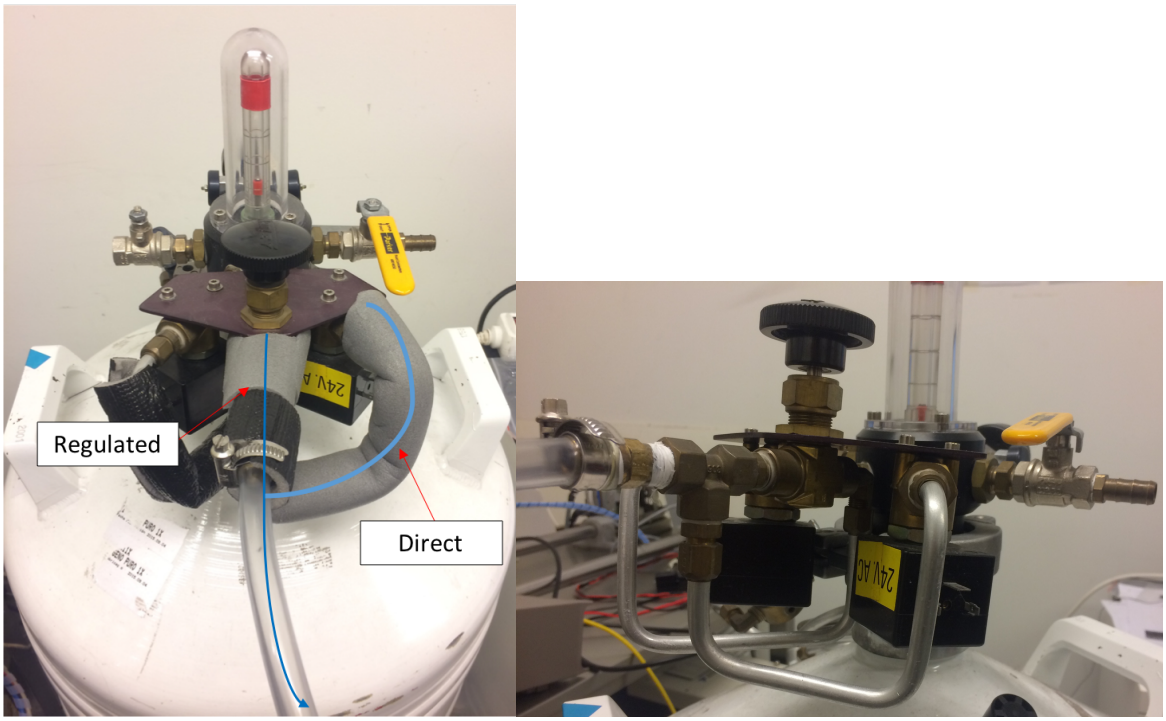

Figure 28- Liquid nitrogen bottle outlets

Working Principle of the liquid Nitrogen bottle

The liquid nitrogen container used in this project is a self-pressurizing vessel (Figure 29), that holds the nitrogen at low pressure (maximum working pressure of 0,5 bar). The self-pressurizing system works on the simple principle of nitrogen evaporation. The liquid nitrogen is picked off the bottom of the vessel (assuring it is liquid) and is heated by going through a serpentine that is at a higher temperature than the liquid. When it reaches the gaseous state, the nitrogen goes to a pressure regulating valve, that controls the pressure in the upper part (gaseous state nitrogen) of the interior of the bottle. With the control of the "gaseous atmosphere" above the liquid, the pressure at which the liquid flows is controlled. So, in order to control the pressure, there is the need to consume liquid nitrogen.

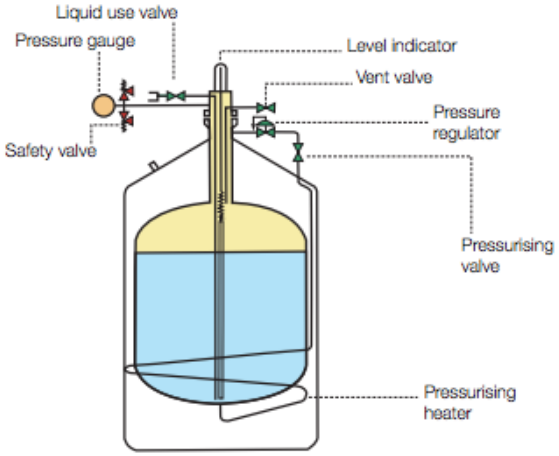

Figure 29- Liquid Nitrogen bottler (Air Liquide TP60) [29]

More systems attached to this bottle include safety systems, such as two safety release valves, that have a release pressure of 0.5 bar, and a pressure gauge to control the pressure inside the vessel. There is also the liquid dispensing system, which consist of a cut-off valve attached to a pickup line that goes to the bottom of the vessel in order to extract nitrogen in its liquid form. Lastly there is a liquid level indicator, which consists of a float that follows the liquid level and has a scale to evaluate the level inside the bottle.

Nitrogen conditions

The nitrogen is in its liquid state inside of the vessel since it is at under -192.3ºC @ 1.5bar. When it starts exiting the bottle it is in gaseous states due to the hotter tubes and ways it goes through, but after these parts lower their temperature the N2 flows as liquid.

4.1.2.4 Heat Exchanger

The copper plate, that works both as a heat exchanger and a support plate, has on its base two copper serpentines that allow for the conduction of heat from the circulating fluid to the rest of the plate (Figure 30).

Figure 30- Copper plate tubing

The system uses both serpentines connected (Figure 31) which means that only one fluid can be used at a time.

Figure 31- Copper tubing arrangement

On top of the copper plate there is a fixture (Figure 32) to hold the part being tested, that also plays a role in the heat exchange process, allowing for an increase in heat transfer to the part, due to conduction.

Figure 32- Part support

4.1.2.5 Control system

The control system of the chamber is composed of four controllers (Figure 33). The main controller, is programmed into the computer does the control of the overall system, that is, it selects the system to be used during cooling or heating in a certain temperature range. The second one sends a setpoint reference to the silicon oil bath main unit, while the third sends an on-off signal to the solenoid valves connected to the LN2 bottle, while choosing which, the regulated or direct, branch is used. The other controller is the internal controller of the silicon oil main unit, whose function is to keep its temperature at the desired setpoint. The monitoring of the temperatures is done through PT1000 sensors and a data acquisition interface that allows the connection between the computer and sensors. The setpoint reference is sent through RS232 communication.

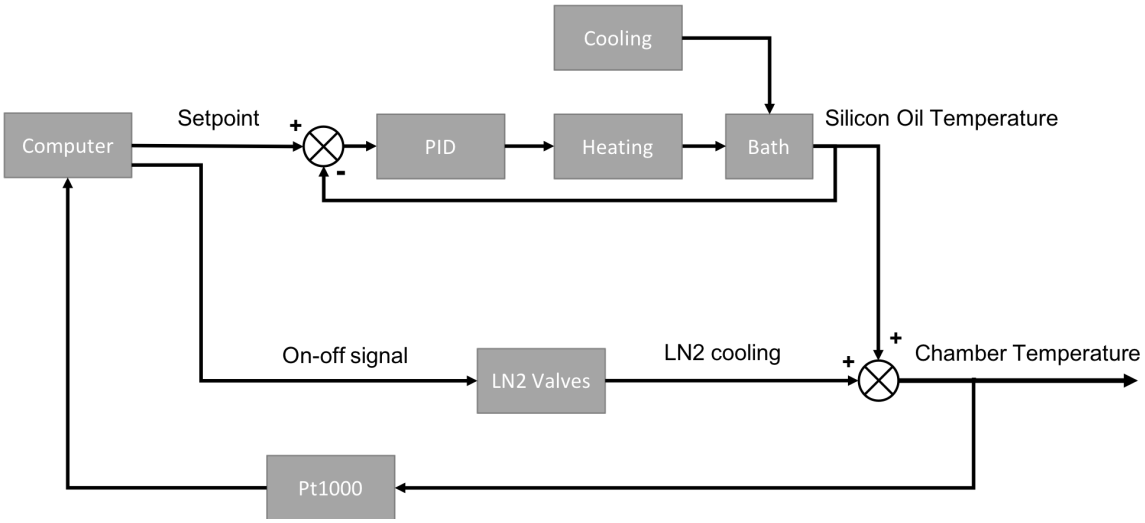

Figure 33- Vacuum chamber control system

4.2 Problem description

The problem to be solved is the control of the temperature, allowing for thermal cycles that are performed as fast as possible but in the most controlled manner possible. The transitions between high and low temperatures also needs to be taken into consideration. The main problem will be the control of cooling, primarily for temperature in the sub-zero range, since the liquid nitrogen cooling has dynamics that may present a control challenge.

4.3 Requirements

From a control standpoint, the thermal cycles must be carried out as fast as possible while maintaining the required temperature under the maximum defined error.

From an equipment stand point, there are some requirements to be met. All the solenoid valves must be able to withstand the cryogenic temperatures, as well as the higher temperatures. The temperature sensors must also be able to work within the working temperature range.

Lastly, the thermal fluid must be changed in order to have a wider working temperature range.

4.4 Possible solutions

4.4.1 Temperature sensors

- **Negative Temperature Coefficient (NTC) – Thermistor**

A thermistor is a thermally sensitive resistor that exhibits large, precise and predictable changes in resistance according to temperature. Because the resistance characteristic falls off with increasing temperature they are called negative temperature coefficient (NTC) sensors. On one hand, this type of sensors experiences large changes in resistance per increase of degree in temperature, which allows for a fast and high accuracy response (0.05 °C to 1.5 °C). On the other, due to its exponential behaviour it need linearization in order to get a correct reading out of the sensor. This type of sensors can be used in the -50 °C to 250 °C range [30].

- **Resistive Temperature Detector (RTD)**

As the name suggests, RTD are sensors where the resistance also varies with the temperature. This type of sensors consists of a wire wrapped in film or, for better accuracy, a glass or ceramic core. Their resistance to temperature curve is fairly linear in the -200 °C to 600 °C range, where they offer a highly accurate (0.1 to 1 °C) output [30].

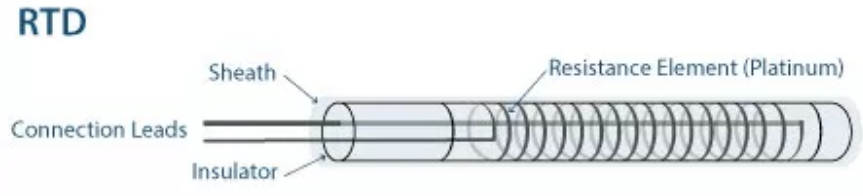

Figure 34- RTD components [31]

- **Thermocouples**

Thermocouples are sensors that consist of two wires of different materials connected at two different points. The tension measured across these two connections varies with the change in temperature. Due to its non-linearity, thermocouples require conversion of the reading, which can be accomplished using a lookup table. Their accuracy is low (0.5 °C to 5 °C) but the working range is the widest of the sensors (-200 °C to 1750 °C) [30].

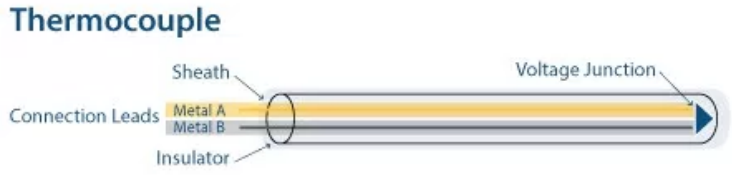

Figure 35- Thermocouple components [31]

4.4.1.1 Advantages and disadvantages

Table 3- Pros and Cons of the various types of thermal sensors

	Pros	Cons
NTC	• High accuracy • Can be produced in very small designs with a fast response and low thermal mass.	• Temperature range • Pronounced output non-linearity
RTD	• High accuracy • Fairly Linear Output (without linearization)	• Cost
Thermocouples	• Temperature range • Cost • Size	• Lowest accuracy • Output non-linearity • Long-term stability (increase in few °C in one year)

With this, we can conclude that both RTD or thermocouples are a viable solution for the project. Since Pt1000 (RTD) are already available this will be the chosen type of sensor to be used.

4.4.2 Thermal fluid

In order to have a better control solution, there was the need to change the thermal fluid. After some search, three fluids were selected (Table 4).

Table 4- Selected thermal fluids

	Min Temp (°C)	Max Temp (°C)
Therminol VLT	-115	175
Dow Syltherm XLT	-100	260
Lauda Cryo 95	-95	160

The selected fluid was the Syltherm XLT, due to the best fit to the working temperatures and better characteristics for the application.

4.5 Discussed solutions

After identifying the problem, there was the need to find solutions in order to improve the system. This consisted in finding available components to suit the needs of the different iterations of the system, checking compatibility with the desired solution and timeframe of the project.

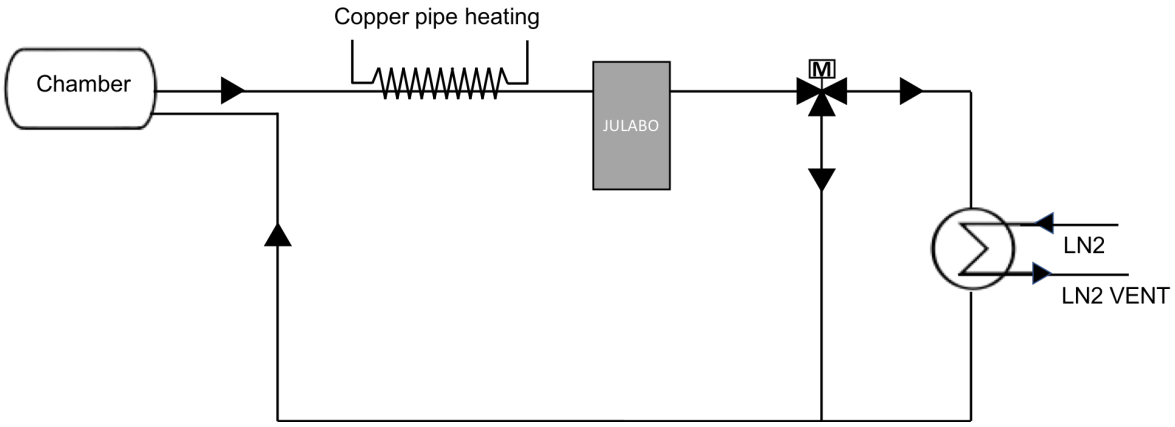

Figure 36- First proposed solution

The first iteration of the system consisted in running the heating and cooling circuit in parallel. This solution had the advantage of keeping the thermostatic bath, which has good dynamics when heating, while allowing the improvement of the cooling, a field where it struggles the most. The systems used a motorized three way mixing valve to control the mixing of two flows. There was the need to insert the Julabo before the junction in order to utilize its pumping power for circulating the fluid. When heating, the stream coming from the Julabo would be all redirected to the not cooled branch, which meant that the circuit would only be

the output of the Julabo. When cooling, since the Julabo is capable of reducing the fluid temperature up to -20ºC, the fluid would then be cooled in a LN2 heat exchanger to allow the reach of temperatures in the -100ºC range. This difference of temperatures also meant that, the motorized mixing valve could be used to control the temperature of the outputting fluid from the two branches.

The main limitation of this system is Julabo's working temperature range, which meant that the fluid would need to be heated before entering the device. For this, there could be used either a heat exchanger or heating elements, in the form of heating sleeves, around the pipes.

This system was excluded due to the sheer amount of energy that would need to be transferred to fluid in order to, for example, heat it from -100ºC at the exit of the chamber to the -20ºC tolerable by the Julabo system. Also, although not a determining factor, the heating and subsequent cooling would mean a big waste of energy.

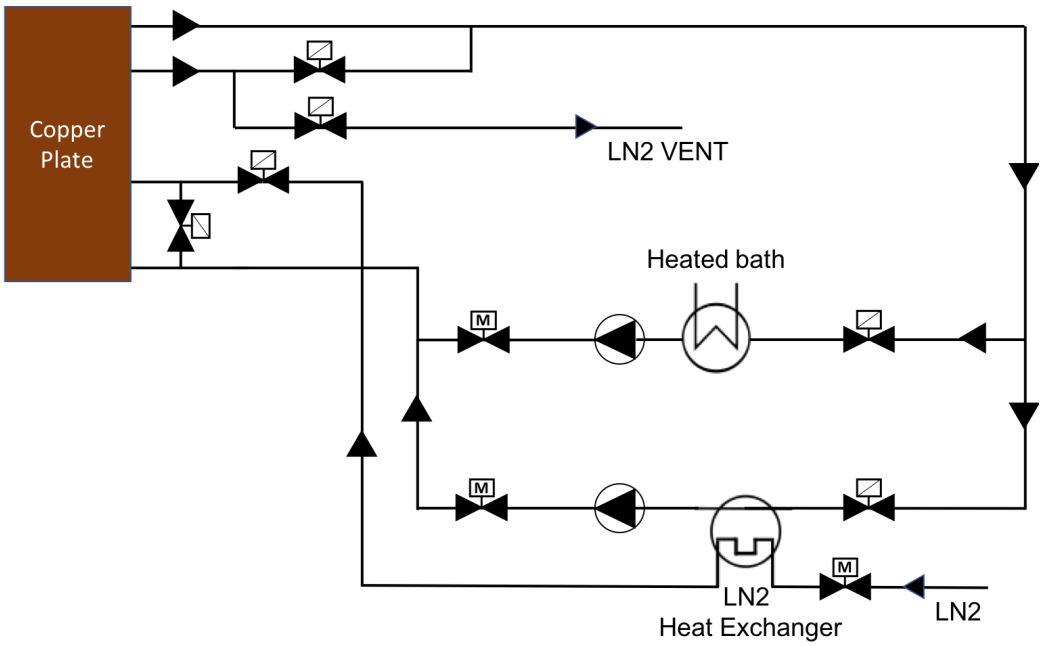

Figure 37- Second proposed solution

The second iteration of the system, presented in Figure 37, is an improvement to the first setup. In this system, the Julabo's bath is replaced with a heated bath, based on a heating element submerged in a tank of fluid, and its pump is replaced by two pumps prepared to work in the full range of temperature. Also having the heating and cooling systems in parallel, the main improvement is having all the components, including pumps, in the corresponding branches. This means that, although with a limited working temperature range, both pumps will only be subjected to temperatures to which they were designed for since all the cooling and heating will occur in the corresponding branch to which each pump is associated with. The nitrogen resulting from the cooling in the heat exchanger could also be inserted into one of the serpentines, and for that, while cooling, only one serpentine would have thermal fluid in it allowing for less flow to be cooled, hence faster cooling.

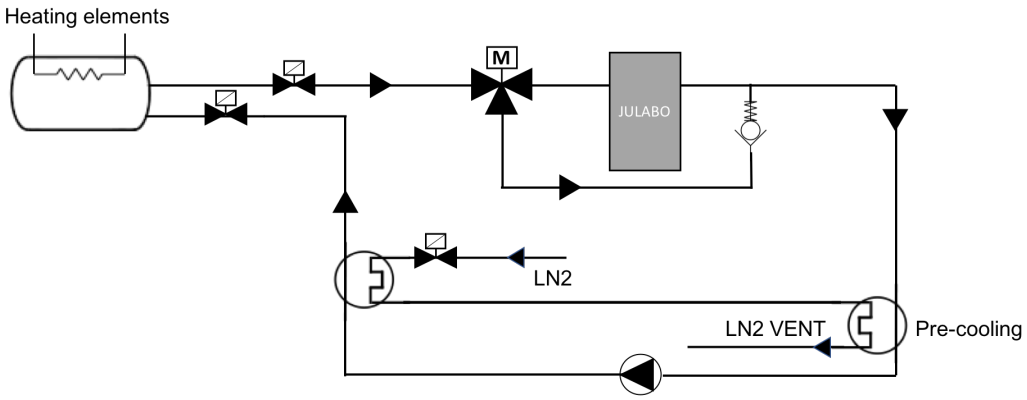

Figure 38- Third proposed solution

The third iterations tried an approach similar to the liquid nitrogen, by, in this case, heating the chamber directly from the inside, instead of using a transfer fluid. This would be accomplished by heating elements inside of the chamber. This would also allow for a better dynamic while heating, while reducing the number of components in the system. This system would be able to continuously control the temperature, due to a mixing valve that could be used to mix fluid exiting the thermal bath and the cooler fluid exiting the chamber, or completely bypass the thermal bath for temperatures lower than its working range ones.

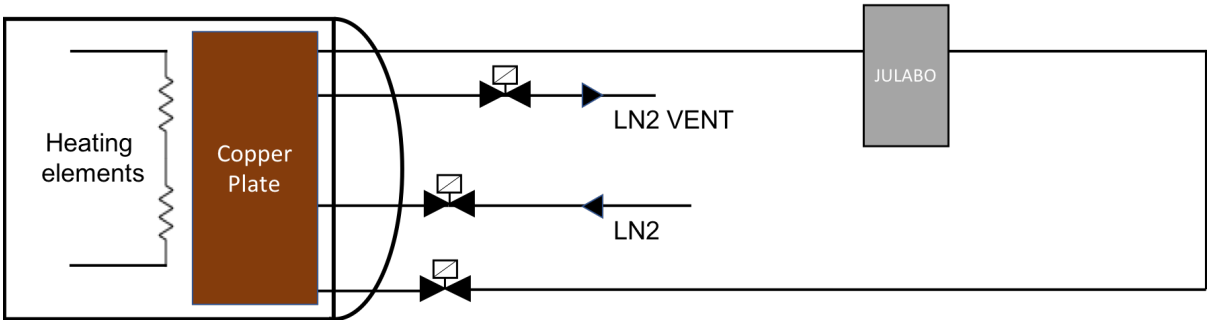

Figure 39- Fourth proposed solution

Lastly, although some of the other iterations would be possible, the selected solution, due to the timeframe of the project, is the use of the two serpentines separately, with one being used directly with liquid nitrogen and the other circulating thermal fluid. Theoretically, this will cause a better dynamic in the cooling domain, in comparison to the use of a transfer fluid, while disrupting the heating domain. In order to compensate for this, the use of heating elements inside the chamber is recommended. These assumptions will later be tested and validated in experimental tests.

4.6 Selection of the solution to implement

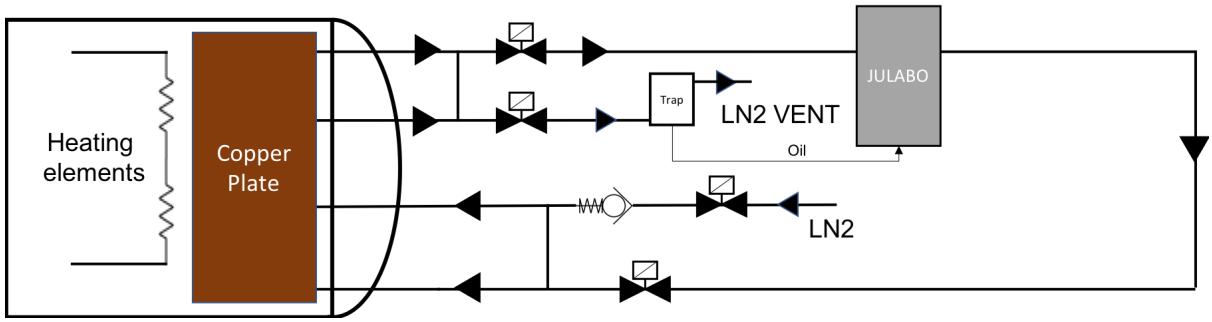

Figure 40- Solution to implement

A common modification to all the system iterations was the use of a thermal fluid with a wider working temperature range that would allow below zero temperature.

Furthermore, after testing the dynamics associated with the use of only one serpentine or both, it was determined that it would be advantageous the use of both ways. After, it was tested if the liquid nitrogen, as it starts flowing in a gaseous form, would be able to purge the tubing. Since the gas was able to do it, there is no need to introduce an external purge system. A trap will be added to the system in order to collect the oil resulting from the purge.

5 SYSTEM IDENTIFICATION

This chapter describes all the information regarding the systems identification. First, a brief review of the identification methods is presented, then the data acquisition equipment and test setup are shown. Afterwards, the approximated models of each system are deducted and the results validated with real data from experimental tests.

5.1 Identification methods

The design of a control systems requires a mathematical model of the system to be controlled. The procedure to build a model of a system from measured data is called system identification. Sometimes, the models are too complex to obtain because of the complexity of the process, due to unknown or partially know dynamics.

After obtaining the mathematical model, its complexity may make it not suitable for designing a controller out of it. In that case, the solution is to find a model with a behaviour similar to the one of the system, for the parameters considered, but with less complexity [32].

There are three different types system identification:

White box- the model structure is based on known principles (ex: newton's law), the model parameters are estimated from measured data.

Grey box- In this case, some of the model is known from first principles, but the rest and parameters are reconstructed from measured data.

Black box- System behaviour is difficult to be obtained from known principles, so model structure and parameters are estimated from I/O data.

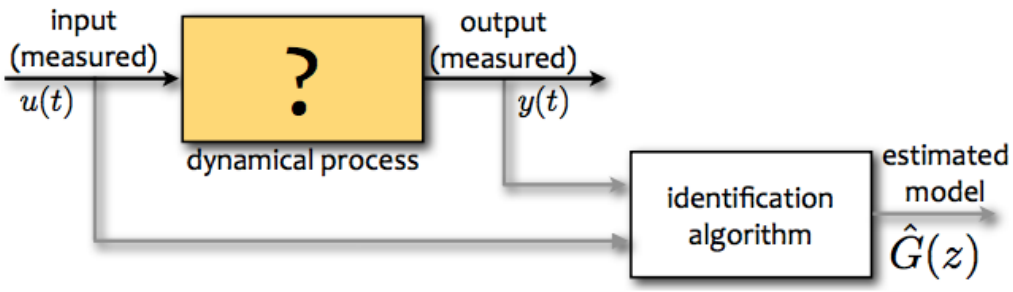

Figure 41- Model identification process [32]

Blackbox identification method

The Blackbox identification method is the method suited for the application of this project and has four crucial steps, starting with choosing what type of input to apply to the system to observe its behaviour, followed by choosing the class of the model structure that fits the collected data. Then, the selection of parameters that best match the model to the real response. Lastly, the validation of the system, by verifying if the model found reproduces the dynamics of the system [32].

5.2 Data acquisition equipment

To acquire all the data needed from the trials, there was the need to use several equipment to read, convert and store said data.

The main equipment was a computer running LabVIEW, that was responsible for all the data acquisition from the other system elements, as well as the storage and display of the acquired values.

The data from the temperature sensor was acquired by a National Instruments NI USB-6229 DAQ board, that was connected to the computer via USB.

Figure 42- National Instruments USB-6229 DAQ

Initially, all of the data read from Julabo's system was acquired from the internal system, with the extracted information being transmitted via a RS232 communication protocol. But, due to low sampling frequency, there was the need to utilize other equipment, in order to better analyse the control action and determine how it was done. For this, a Keithley 2701 multimeter was connected to the computer via ethernet, and control data measured by connecting it directly to the heating element terminals and thus acquiring the control action imposed by the internal PID of the F12 unit.

Figure 43- Keithley 2701 multimeter

5.3 Tests

The dynamics analysis of the silicon oil thermostatic bath was carried out, simulating the working conditions of this bath. For this, a sequence of steps was imposed to the systems in order to acquire the response curve. After cooling the system to a stable 10ºC, for the initial conditions, the first test consisted of an increase of temperature from 10ºC to 50ºC, letting the system become stable and then increasing the temperature to the next step, to 100ºC. The second test consisted of a cooling test. After stabilizing at the maximum temperature, a new setpoint was set in order to test the cooling of the bath, also done in steps. The first was to 50ºC and the last to 10ºC bringing the system to its initial conditions.

While monitoring the bath temperatures, there was the need to also acquire information from the control system. The data acquisition was done using a LabVIEW written program and interface to save all the needed data to a text file for later post processing.

The data recorded during the trial is as follows:

- Elapsed time- In order to control time duration of every phase of the test
- Bath temperature- The main data to be recorded from these tests, acquired directly from the F12 internal system.
- Power being delivered to the fluid- Data acquired that correspond to the control action from the internal PID. This data corresponds only to the heating power, since the cooling power is always on, and therefore is a constant, and is acquired directly from the Julabo's internal system.
- Setpoint- Acquired to verify that there is no change in the set temperature during the test, also registered from the F12 internal system.
- PID parameters- Allows to check the parameters and make sure they do not change during the trial, acquired from Julabo's internal system.
- Control action recorded with a high sampling rate multimeter – In order to more closely evaluate the shape of the control action, data acquired directly from the connection point of the heating elements using the multimeter.

The post treated data can be seen in the following graphics:

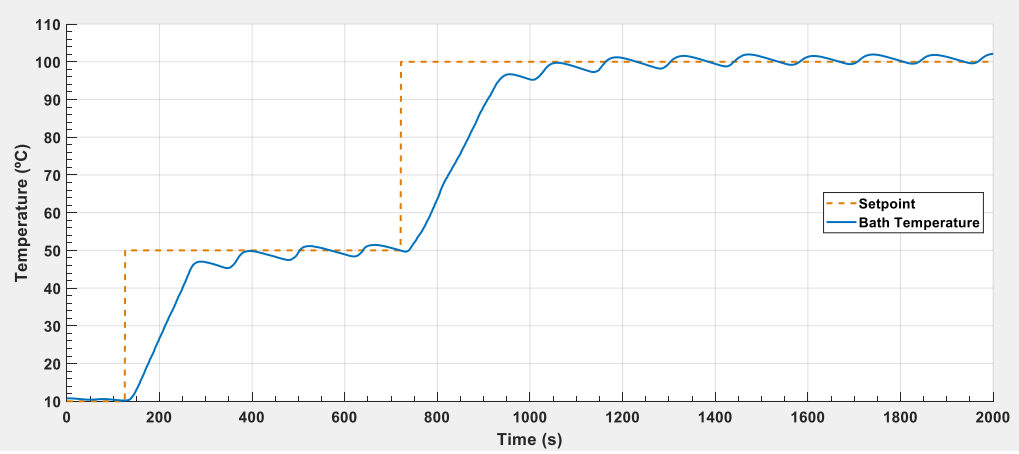

Figure 44- Julabo heating

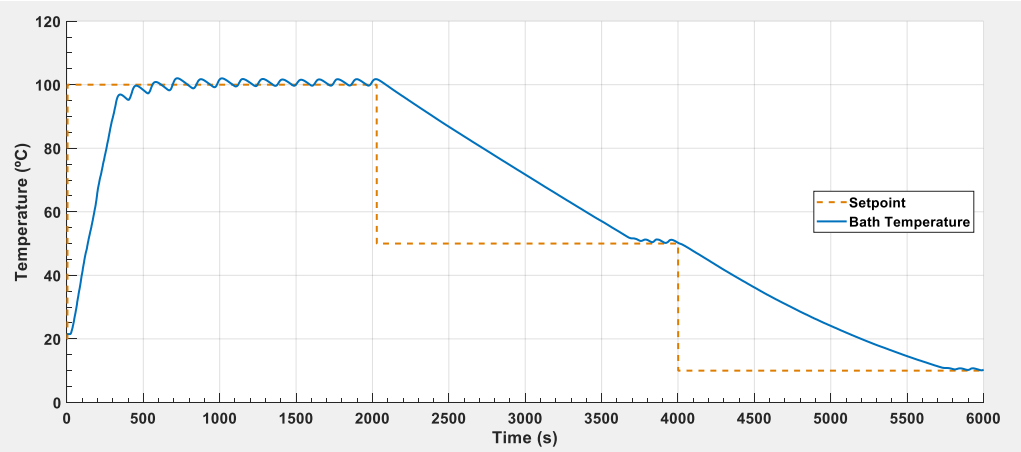

Figure 45- Julabo cooling

5.4 Julabo F12-MC

The first system to be studied is the thermostatic bath. This is composed by two separate systems, a refrigeration circuit that is responsible for cooling the fluid and a heating head that heats the fluid. The cooling system is always doing work, which means that while heating part of the energy is being driven out of the system by the refrigeration circuit.

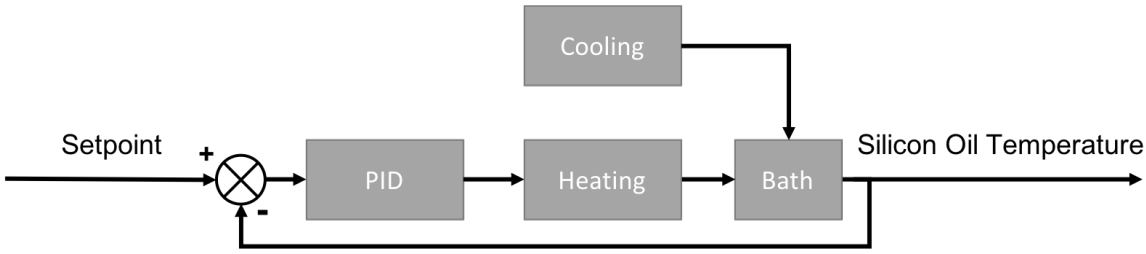

Figure 46- Julabo control scheme

5.4.1 First order system

The main function that describes a first order system in the frequency domain relates a steady state gain with a time constant of the system.

$$\frac{Y(s)}{U(s)} = \frac{K}{Ts + 1} \tag{3}$$

This relates the input (U(s)) with the output of the system (Y(s)). In the case of a unit step, the input of the system is represented by the function

$$U(s) = \frac{1}{s} \tag{4}$$

Which replaced as the input of the system allows us to relate it to the output:

$$Y(s) = \frac{1}{Ts+1}\frac{1}{s} \tag{5}$$

It can be converted into the time domain by applying the inverse Laplace transform:

$$\mathcal{L}\{Y(s)\} = y(t) = 1 - e^{-t/T} \tag{6}$$

The output of a system that starts at zero and finally becomes unity is now established. Although, this is not always the case, such as in the following system dynamics identification. Therefore, in the case of a non-zero start of the system and a non-unity step the output function is as follows:

$$Y(s) = \frac{K}{Ts+1}\frac{P}{s} \tag{7}$$

The response to a step of P amplitude in the time domain can be obtained by doing it's inverse Laplace transform, thereby obtaining:

$$\mathcal{L}^{-1}\{Y(s)\} = y(t) = K \cdot P - e^{C1} \cdot e^{-\frac{t}{T}} \tag{8}$$

Now, by applying boundary conditions we can obtain the missing constant:

$$\begin{cases} t = t_0 \\ y = y_0 \end{cases} \Longrightarrow y_0 = K \cdot P - e^{C1}.e^{-\frac{t_0}{T}} \Leftrightarrow c1 = \ln\left(K \cdot P - y_0\right) + \frac{t_0}{T} \tag{9}$$

And lastly, the final equation that translates the system output to a step input with initial conditions different from zero:

$$y(t) = K \cdot P \cdot \left(1 - e^{\frac{t_0 - t}{T}}\right) - y_0 \cdot e^{\frac{t_0 - t}{T}} \tag{10}$$

Where the variables represent:

$y(t)$- system output
K-Steady state gain of the system
T-Time constant of the system
P-Amplitude of the input step
t_0- time delay of the output in relation to the input

5.4.2 Identification

For the identification process, there is the need to do some trials of the system by inserting an input into it and evaluating its response. In the case of the thermostatic bath, the input into the system is a setpoint, based on which the system controls the heating element by turning it on or off.

For the dynamics study of the cooling, the system was set at a high temperature and then a low setpoint defined, in order to evaluate the cooling rate. Different initial and end points were selected in order to better verify the found solution.

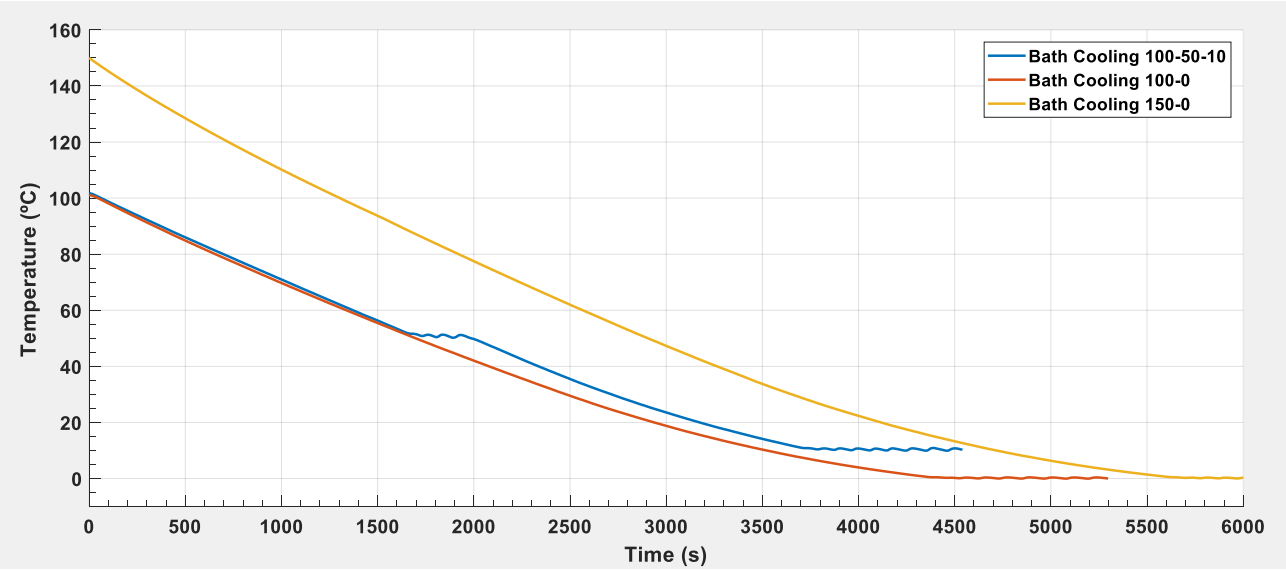

Figure 47- Cooling measured data

The system is controlled by a PID controller near the defined setpoint and, in the case of the stepped trial, the controller uses the heating elements to control the bath temperature. Which means that the values close to the setpoint are controlled values and influenced by the controller. In order to remove the influence of this, the data considered for the estimation was outside of the controlled values.

From the acquired data this system behaviour can be approximated by a first order one, in order to simplify further simulations and calculations. As explained on point 5.4.1 this type of system can be expressed in the form of a transfer function and, since the input corresponds to a step in the setpoint value, we can also consider the step response input.

$$T_{bath}(s) = \frac{K}{Ts+1} \cdot \frac{1}{s} \tag{11}$$

Using the experimental data, the equation that describes the behaviour of the system is:

$$T_{bath} = 5{,}672 * -20 * \left(1 - e^{-\frac{t}{6115}}\right) + T_0 * e^{-\frac{t}{6115}} \tag{12}$$

The fitting to the real observed behaviour can be seen in Figure 48.

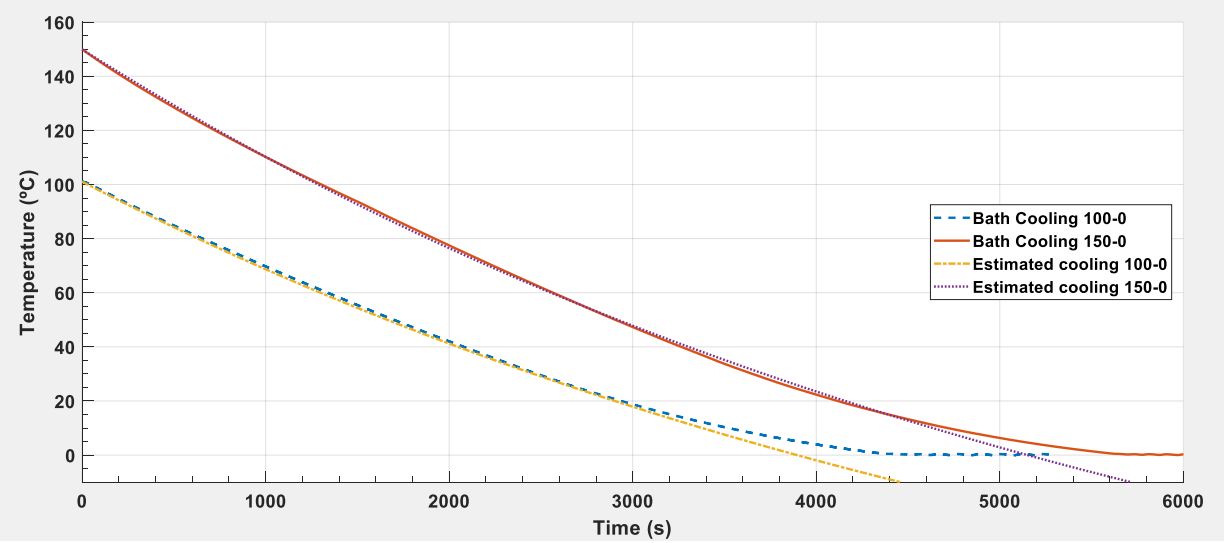

Figure 48- Cooling estimated vs measured data

Equation 12 was then calculated for different time instants using Matlab and the graphics in Figure 49 were obtained.

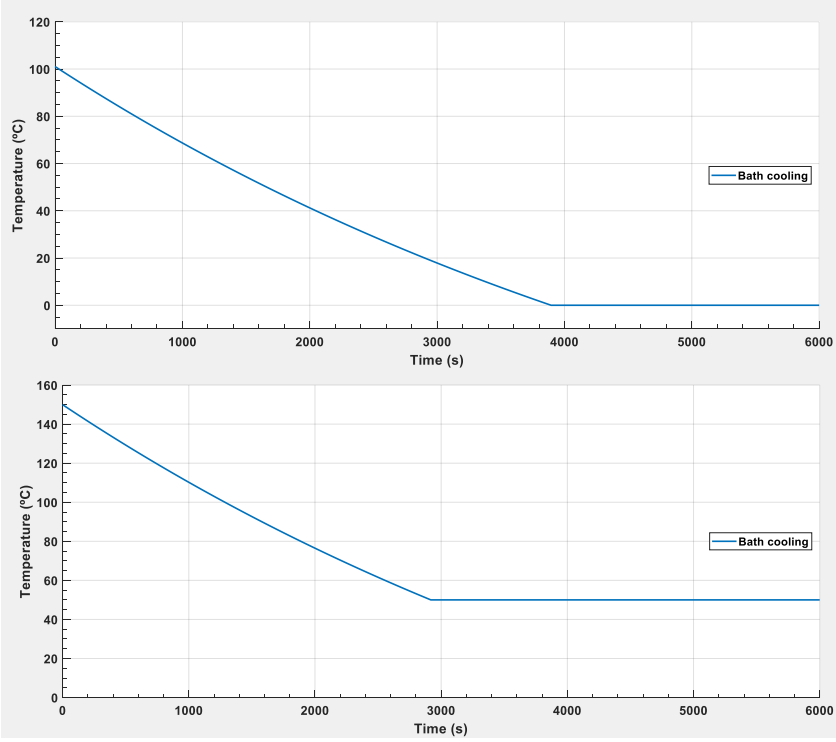

Figure 49- Controlled cooling simulated for 100-0 (Top) and 150-50 (Bottom)

Although when connected to the chamber the behaviour varies slightly, that is still very similar to the behaviour without load and the model is a good approximation to the real dynamics of the thermal bath (Figure 50).

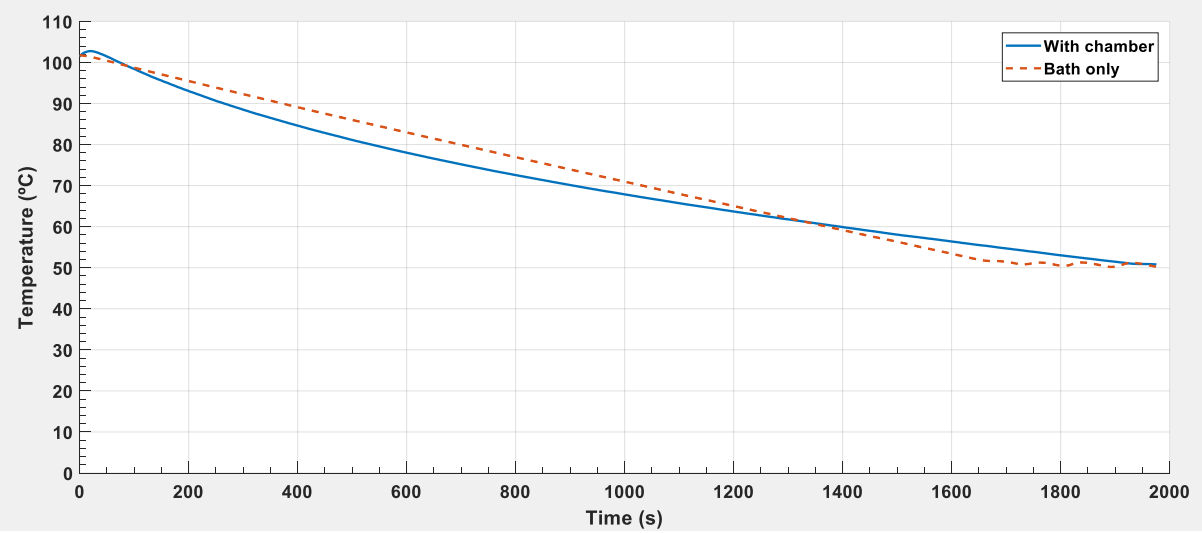

Figure 50- Comparison between cooling with load and no load

The second part of this system is the heating module. To determine its dynamics, a similar strategy was followed. First, there was also the need to understand the type of control being applied to the heating element. The data extracted from the heating head can be seen in Figure 51.

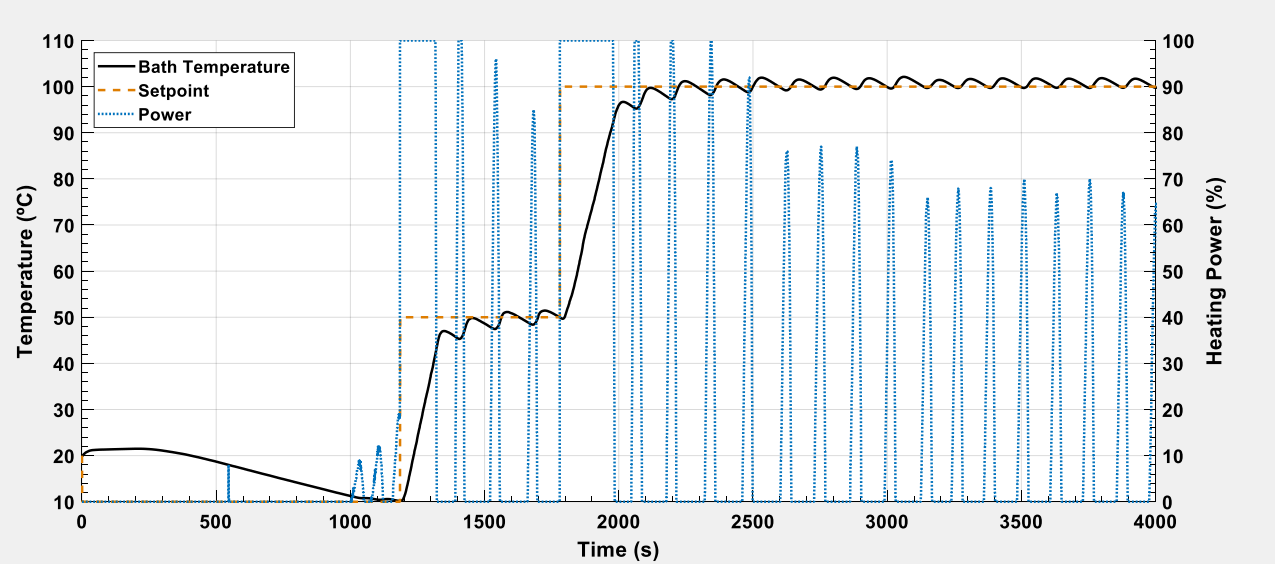

Figure 51- Data extracted from Julabo

As described in section 5.1.3, there was the need to connect a multimeter for an increase in sampling rate and better data acquisition. That way, as seen in figure, it was possible to verify that what in the Julabo data seemed to be a smooth power input was in fact a series of pulses, allowing to conclude that the heating is controlled by an on-off controller.

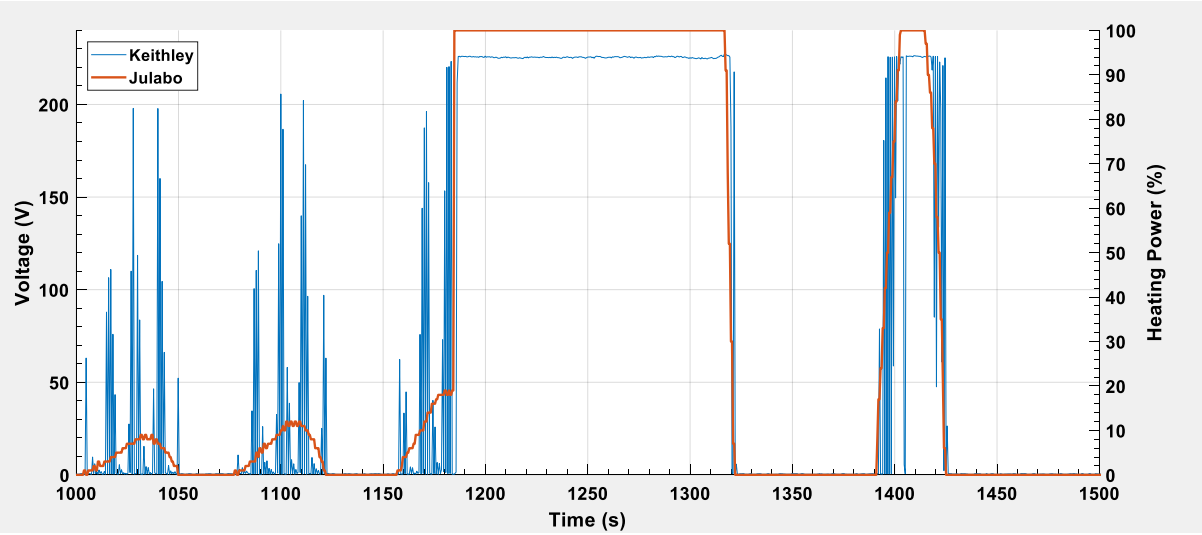

Figure 52- Julabo power data vs measured Keithley data

The test performed for the heating can be seen in Figure 53.

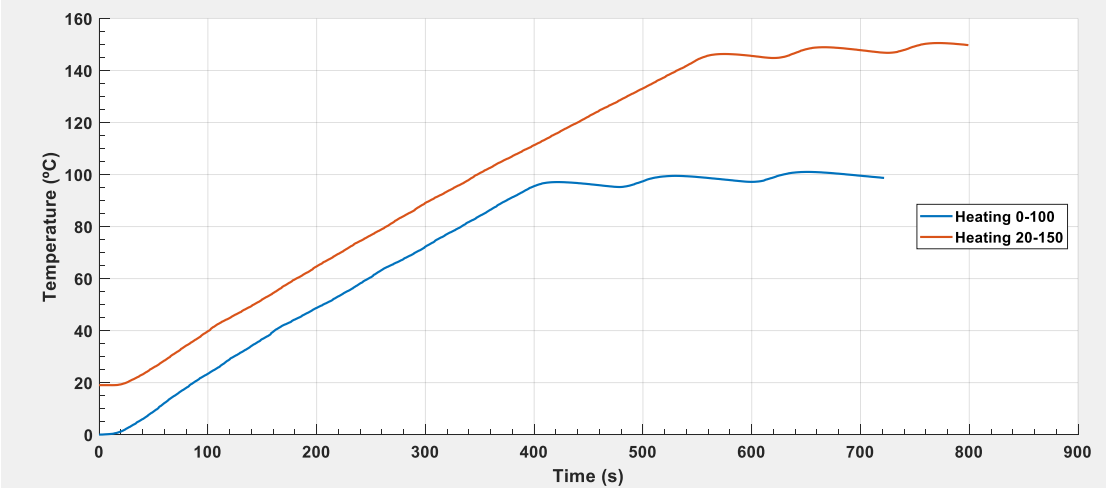

Figure 53- Heating measured data

These were performed from various lower temperature to various upper temperatures in order to get various possible behaviours from the system. Since it works in parallel with the cooling system, the heating response is influenced by it. The PID controller, as it happens in the cooling system, has an influence in the values near the desired setpoint. Because of this, the values chosen and used for the estimation are the ones where the system behaves in its natural form, without influence of the PID.

From de acquired data the behaviour of this system can be approximated by a first order system with delay, that is represented in the following form:

$$T_{bath}(s) = \frac{K}{Ts+1} \cdot e^{-t_d \cdot s} \cdot \frac{1}{s} \tag{13}$$

Using the experimental data, the equation that describes the heating of the system is:

$$T_{bath} = 2{,}928 * 200 * \left(1 - e^{\frac{18{,}7-t}{2183}}\right) + T_0 * e^{\frac{18{,}7-t}{2183}} \quad (14)$$

The fitting to the real observed behaviour can be seen in the following figure.

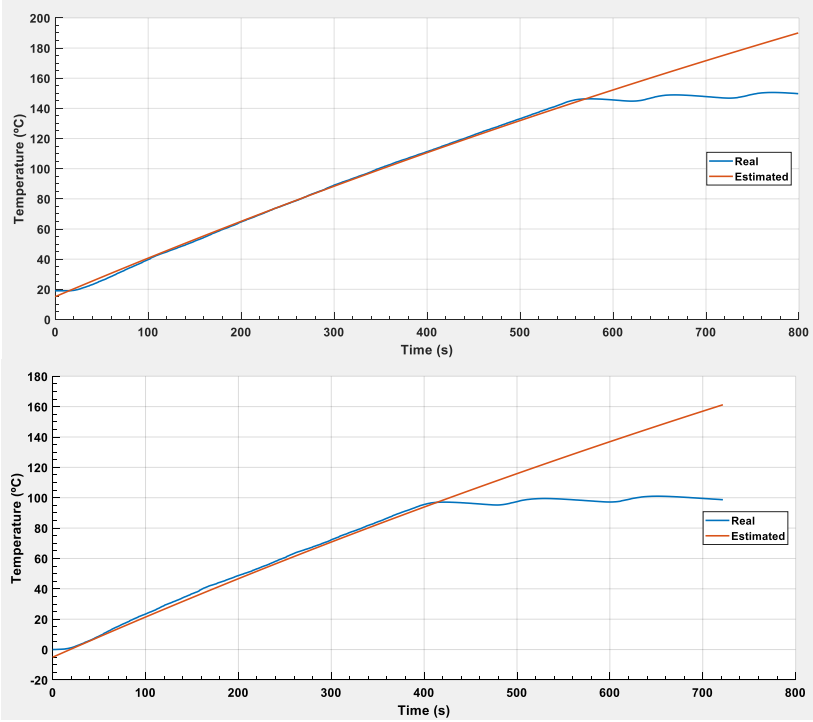

Figure 54- Heating measured vs estimated data

As with the cooling, the equation for the heating was solved for various time instants and the result can be seen in Figure 55.

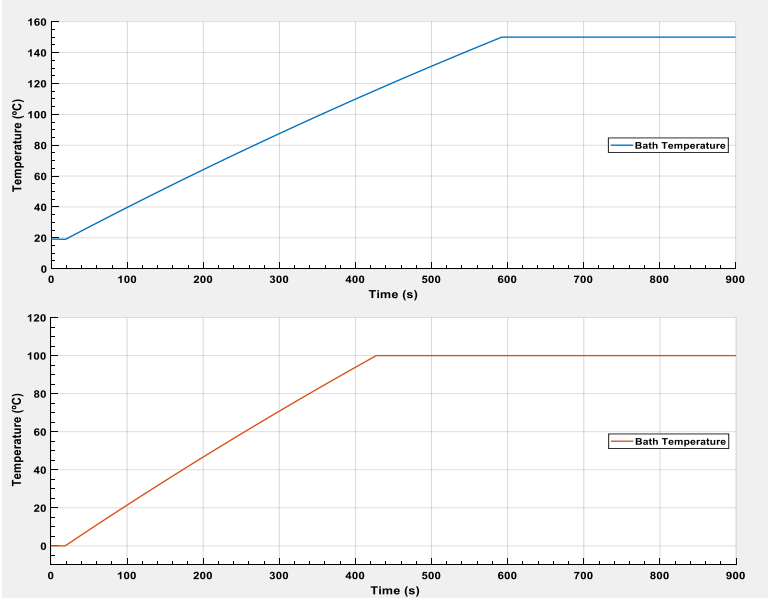

Figure 55- Controlled heating simulated for 20-150 (Top) and 0-100 (Bottom)

5.5 Chamber system

The chamber system is a second order system, taking into account the heat transfer from the thermal fluid to the copper plate and the subsequent heat transfer from the plate to the support and part. Due to the thermal capacities of the components, there is energy stored in each one with its influence on the process dynamics. This system can be represented by an analog electric diagram, as shown in Figure 56.

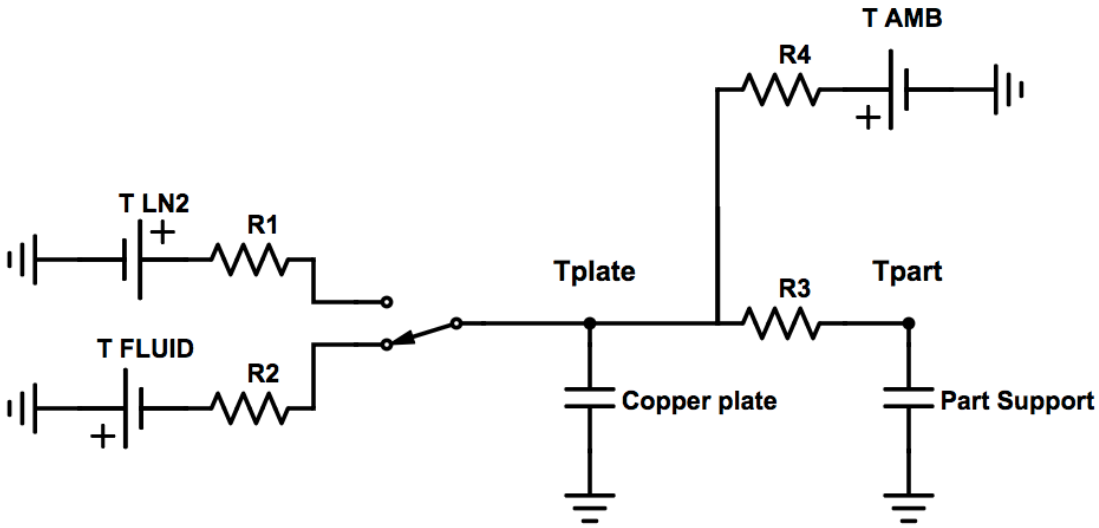

Figure 56- Analog electric diagram of the chamber

This diagram represents the energy transfer between the multiple components of the fluid-plate-part system. Since there are two ways of cooling the chamber, there was the need to introduce those as different temperature sources in the system.

The different branches represent different dynamics. The first one, represents the cooling when LN2 is used, which can be considered at a constant temperature of -195 °C, and the thermal resistance associated with said heat transfer to the plate. The second one, represents the same cooling or heating of the plate but with the thermal fluid as the source of temperature. Lastly, there is a switch that represents the use of one of the systems at a time.

In the system, there are also two capacitors that represent the energy stored in both the copper plate and part support, that recreate the increase in part temperature even after, for example, turning the liquid nitrogen off.

The ambient temperature also represents a role in removing or adding some energy to the system. This contribution is represented in the form of a temperature source and a resistance that represents the contact between the exterior air and the chamber, where the plate is connected.

Lastly, the node where all these perturbations interact represents the plate temperature, since it is dependent on all of them. The part temperature, which is directly connected to the plate temperature is only dependent on the resistance of the energy transfer between the plate and support, also being influenced by the energy previously stored.

The relation between the chamber heating and bath heating can be seen in Figure 57. As shown, the bath dynamics are much faster than the chamber one.

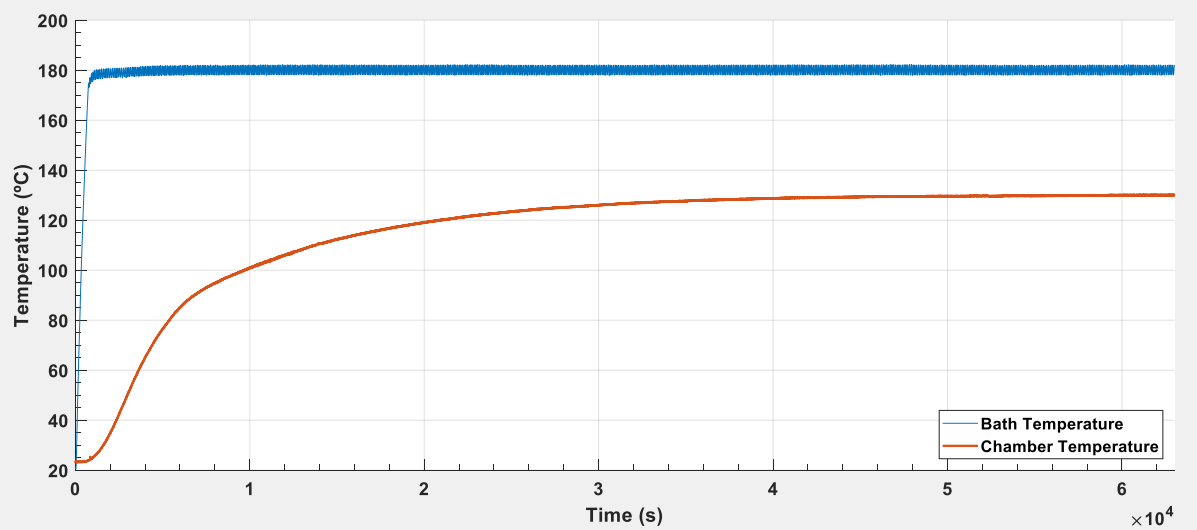

Figure 57- Chamber and bath heating

5.5.1 Approximation by a first order system

Since this model will be used to estimate control parameters, in order to reduce complexity, it was approximated by a first order system. This is done using the least squares method, based on experimental data acquired during the tests and allows for future estimation of the PI controller parameters. The model was determined for positive temperatures since the chosen method for sub-zero cooling control does not require a model of the system.

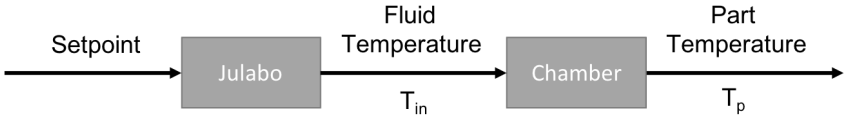

Figure 58- Simplified chamber block diagram

$$\frac{T_p}{T_{in}} = \frac{k}{Ts+1} \Leftrightarrow T_p(\mathrm{T}s+1) = K.T_{in} \tag{15}$$

$$\frac{dT_c}{dt} = \frac{K.T_{in} - T_c}{T} \tag{16}$$

The data from the test allowed for the computation of the unknown constants, describing the system with the following differential equation:

$$\frac{dT_c}{dt} = \frac{0.71446.T_{in} - T_c}{7102} \tag{17}$$

In the simulation environment, this model is represented as shown in Figure 59.

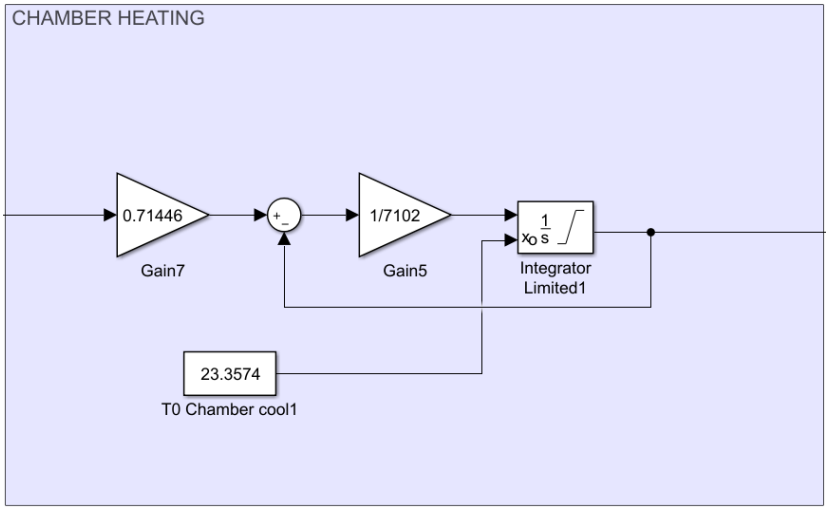

Figure 59- Chamber model

The estimated chamber behaviour, in comparison to the real one is shown in Figure 60.

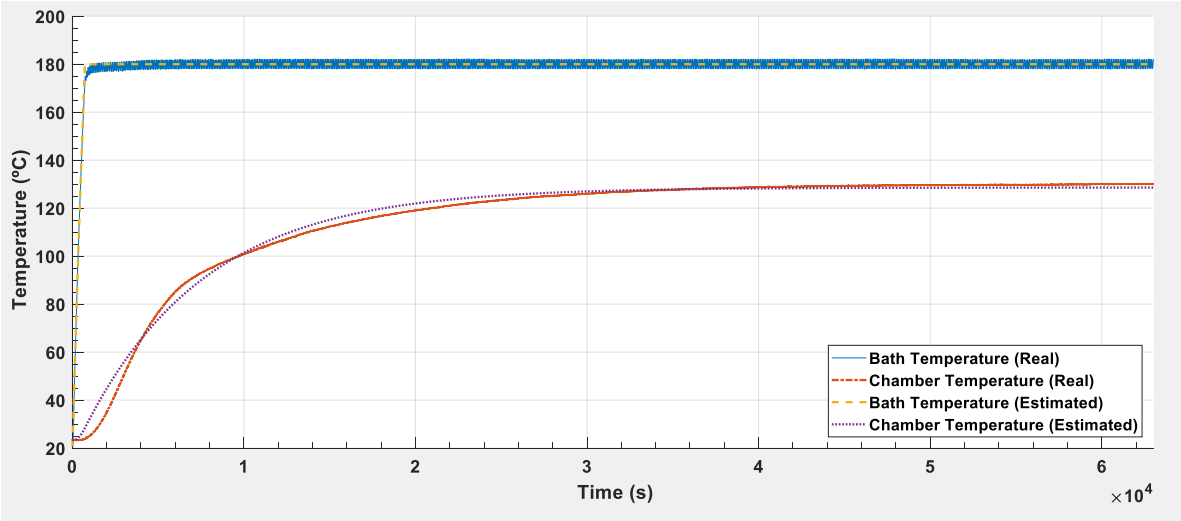

Figure 60- Real vs Estimated chamber dynamics

6 CONTROL STRATEGY

The various controllers of the system are described in this chapter. Initially an overview of the system control tree is described, followed by the analysis of each individual controller. The control logic and the tuning steps for each controller are also explained.

6.1 Overview

The chosen control strategy is based on a cascade controller, which can be seen in Figure 61. The main controller is responsible for doing the thermal cycling, and thus select which heat exchange system to use and its parameters. The specific controller for each sub-system will the do the corresponding tasks, with the data transmitted from the high-level controller.

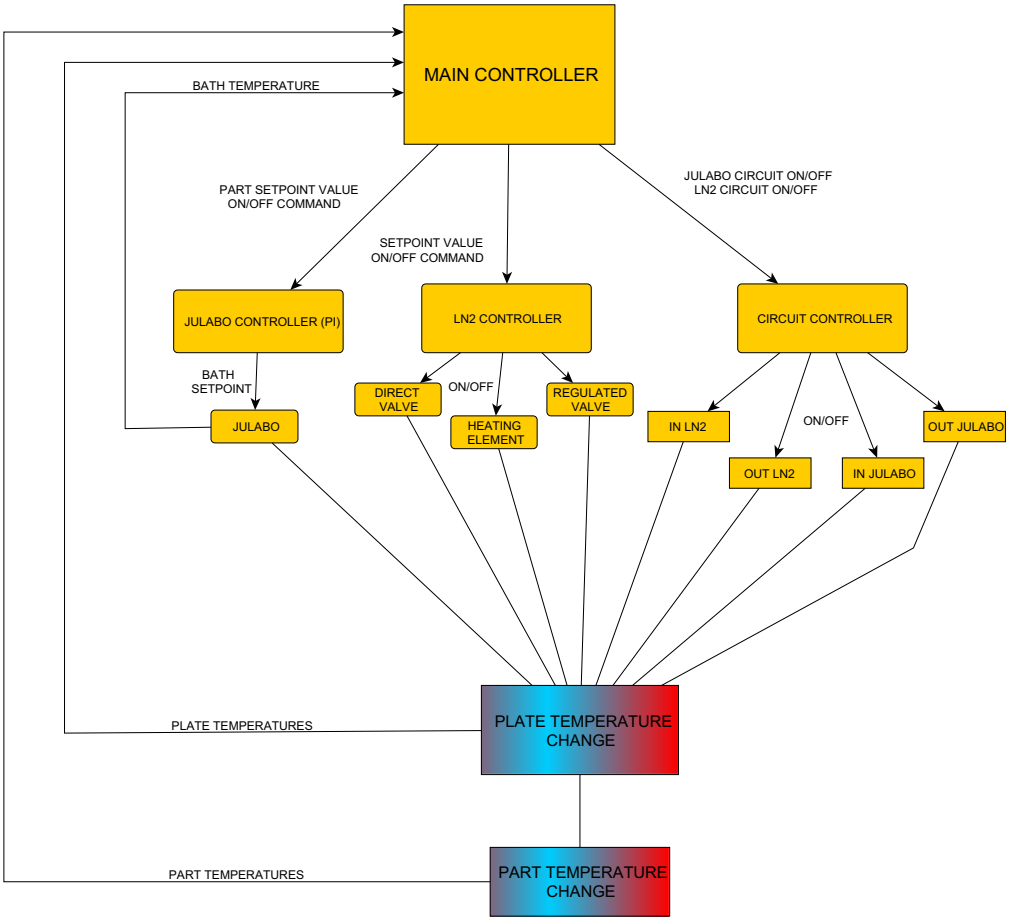

Figure 61- Main control scheme of the chamber

The two heat transferring systems are controlled separately. The control action of each system determines and limits the type of control used in each case. The above zero system, is able to accept a continuous input and therefore is able to use a PID controller tuned for its function. On the other hand, the sub-zero cooling is done using solenoid valves, which mean it

is a digital control, the valve is either closed or open, there is no in between. With that said, the following sub-chapters explain the followed method for tune and selection of each controller.

6.2 Main controller

The main controller is responsible for the cycling action. It controls which system is tuned on, and corresponding setpoint. This action is described in the Grafcet shown in Figure 62.

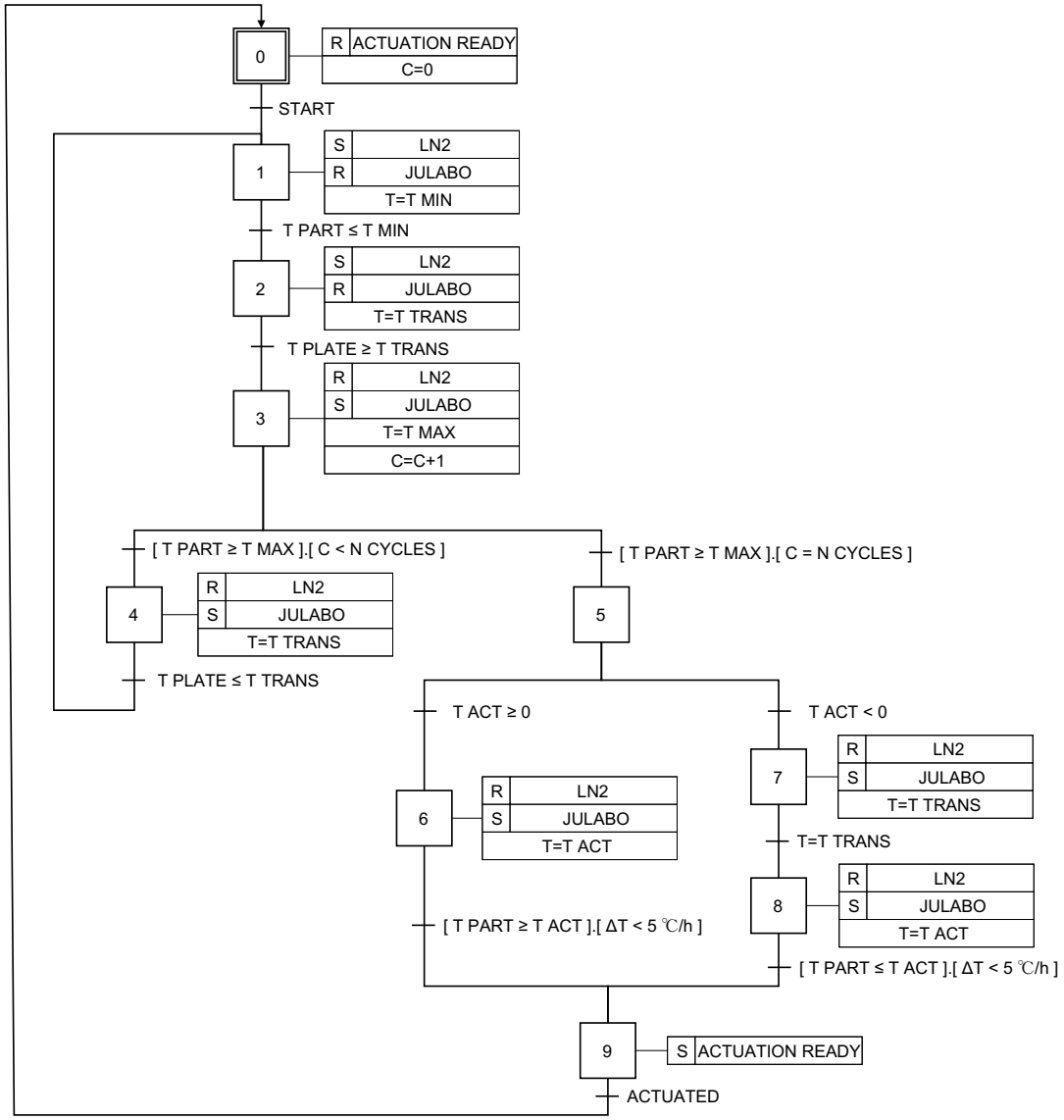

Figure 62- Grafcet describing the working of the main controller

As described in the testing procedure, the cycles start with the minimum temperature. After which, in order to complete one cycle, it is changed to the maximum one. The change between systems, LN2 to Julabo and vice versa, is done by defining a transition temperature, to which both systems are sent to for a smooth exchange, avoiding thermal shock of the parts. Also to

note, is the transition for the actuation, based on the temperature stability criteria, that cannot exceed the 5ºC/h.

6.3 Positive temperatures controller

6.3.1 PID Controller

A PID control algorithm is one of the most common in the industry. Its popularity is due to its robustness and wide range of operating conditions.

This controller is based on, as the name suggests, proportional, integrative and derivative actions. The control is done in a closed loop with the feedback of a variable of the system.

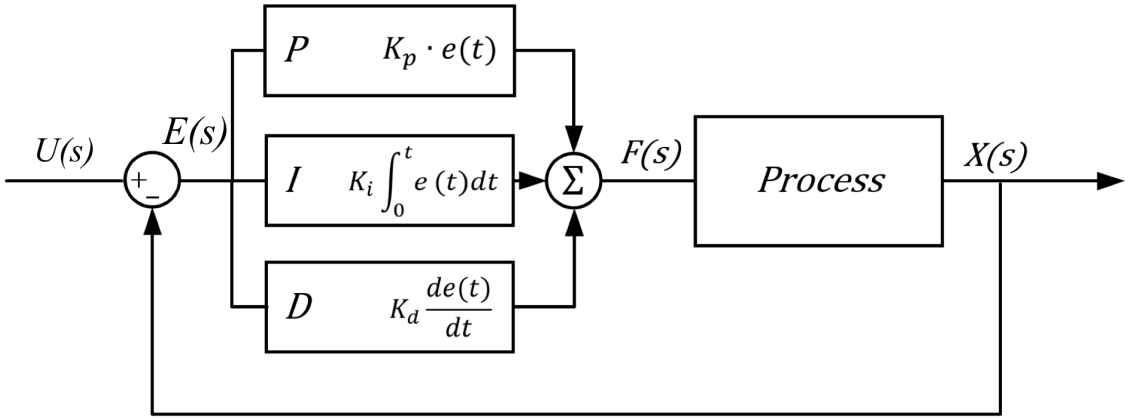

Figure 63- PID controller block diagram [33]

The controller uses the proportional gain to reduce the response time of the system, the integral gain allows for the estimation of the control action based on previous behaviour of the system and allows for zero steady state error. Lastly, the derivative gain tries to predict the future values based on the trend from the last measured values, allowing for the reduction of the overshoot. The control action outputted by the controller is represented by Equation 18.

$$u(t) = K_p e(t) + \frac{K_p}{T_i}\int_0^t e\, d\tau + K_p T_d \dot{e}_f(t) \tag{18}$$

6.3.1.1 Discrete-time PID controller

The previous form of PID is valid for continuous time systems. Since in a real system, there is no infinite sampling frequency, any measured values are separated by a sampling period.

The PID formula for discrete time is then given by:

$$u(t_k) = u(t_{k-1}) + K_p[e(t_k) - e(t_{k-1})] + \frac{K_p h}{T_i} e(t_k) + \frac{K_p T_d}{h}\left[e_f(t_k) - 2e_f(t_{k-1}) + e_f(t_{k-2})\right] \quad (19)$$

It relates the PID current output with the previous one and the error. Since it is a discrete-time controller, the sampling time (h) and PID parameters also affect the control action.

6.3.2 Selection of the controller

The first problem to address is the type of controller that is going to be used. There are several options from P, PI or PID to more specific types.

The Julabo-chamber system is the case of a temperature system, that is inherently a slow dynamic system, which relates to the selected components of a PID controller.

As explained above, the proportional gain allows for a faster response of the system, desirable in the case of this system. The integral gain, responsible for the zero steady state error, is also necessary in order to define the temperature difference between bath setpoint and part temperature that allows for the desired part setpoint. On the other hand, the derivative component of the PID, responsible for reduction of overshoot makes more sense in faster systems, since it is very sensitive to sensor noise and would be compensating the control action based not in the real slow changing temperature change but in this fast-changing noise, generating an erratic control of the setpoint.

Therefore, the selected solution was a PI controller.

6.3.3 Tuning

In order to estimate the PI parameters, the previous model of the chamber was used, coupled to the Julabo heating model. The selected model was the heating one, since it is where there is better control, and the cooling is performed continuously and at full power, being the temperature controlled with heating of the bath. The system control diagram is represented in Figure 64.

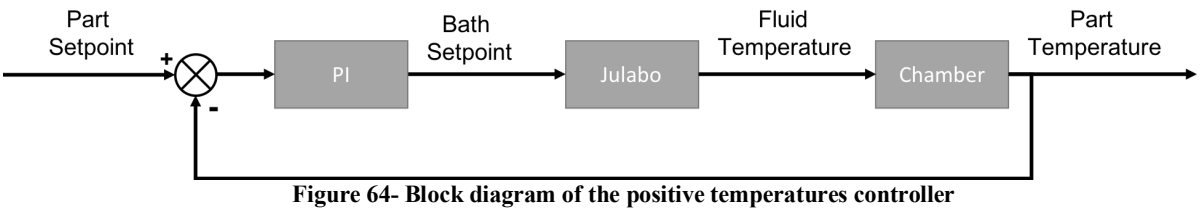

Figure 64- Block diagram of the positive temperatures controller

The system and response in simulation environment, without any type of controller can be seen in Figure 65 and Figure 66.

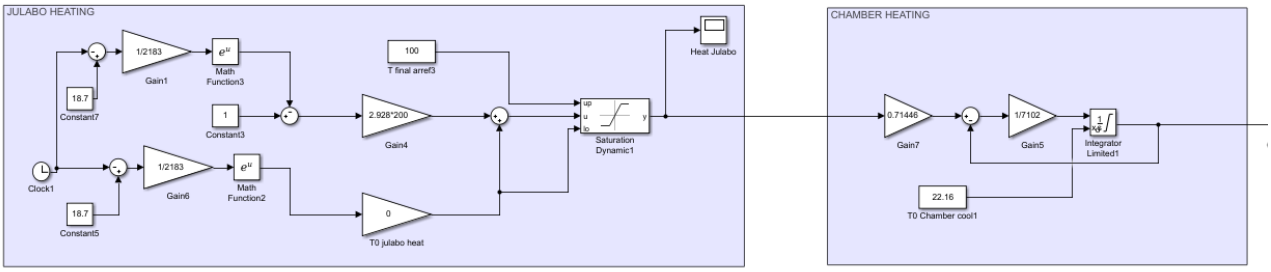

Figure 65- Chamber heating in simulation environment

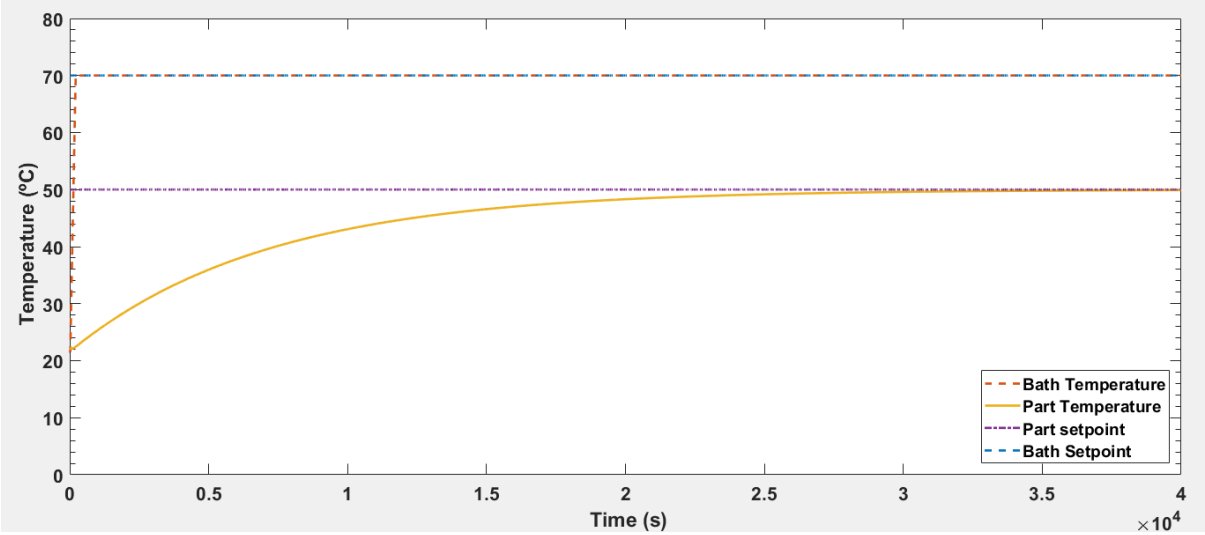

Figure 66- System response with manual set setpoint

Note that, even in the simulation, there was the need to try different values of the bath setpoint in order to achieve the desired part setpoint. This is the equivalent to what would need to be done in the control system implemented at the beginning of this project.

After estimating the controller parameters, the values shown in Table 5 were found to be optimal.

Table 5- Estimated PI parameters

Kp	4,1913
Ki	0,00097903

The difference in response time of the system, with the controller implemented and in simulation environment, is shown in Figure 67.

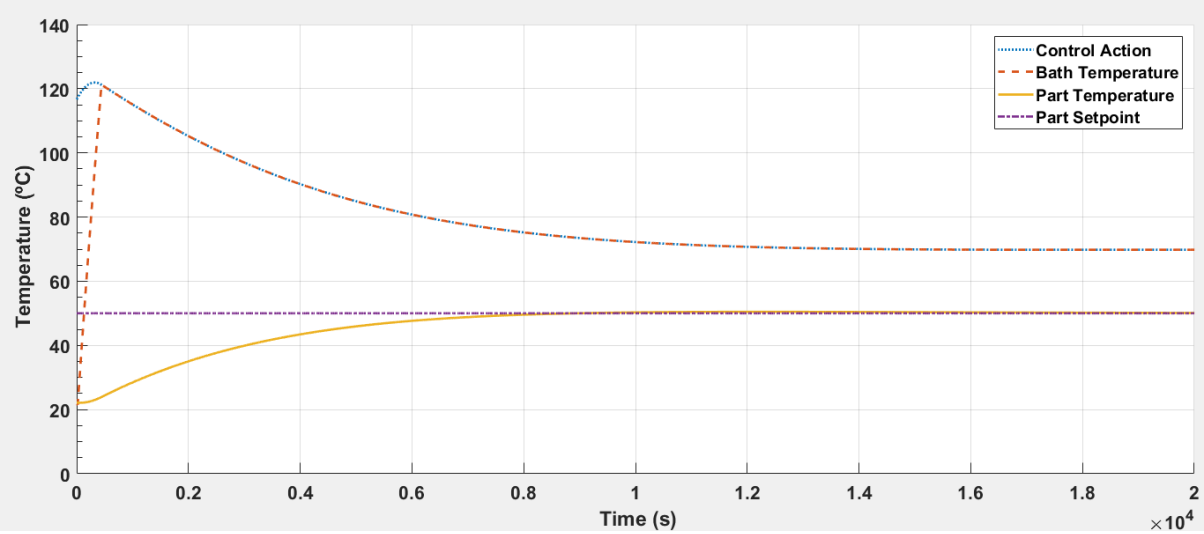

Figure 67- Simulated system's response with the PI setpoint controller

The system is estimated to have approximately 1/3 of the response time, compared to the manually controlled setpoint, as well as a much better response to any outside changes that may occur during the test.

After verifying the correct working of the PI controller in the simulation, it was implemented in the real system and its function assessed. The results are shown in Figure 68.

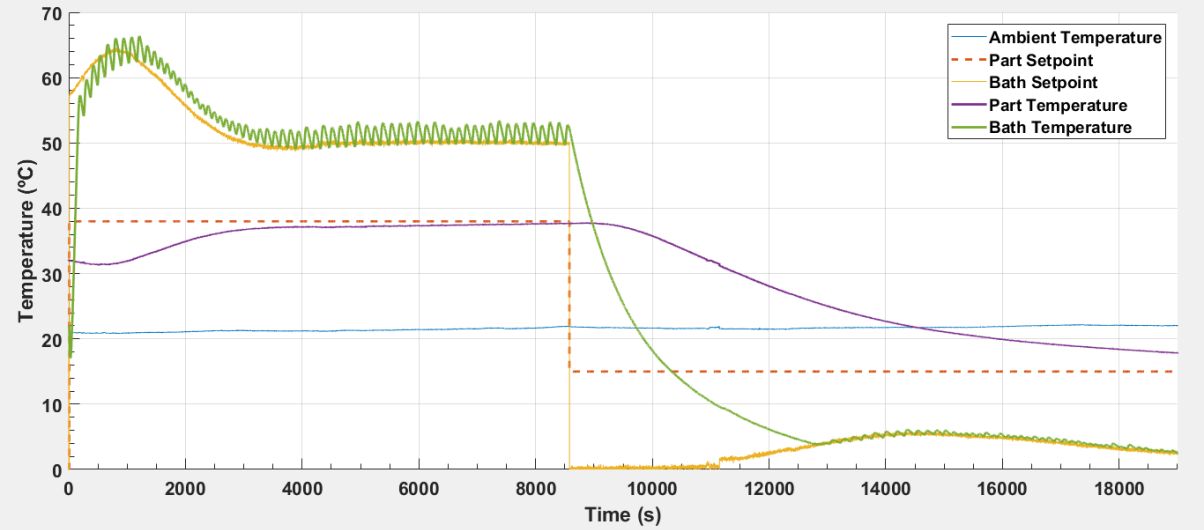

Figure 68- PI controller implemented in the real system

In order to compare to the simulated behaviour shown in Figure 67, a test was conducted with the same conditions in the real system. The results are shown in Figure 69. In this test the part temperature was set to 50 °C and after reaching the desired temperature, the setpoint was

changed to verify the minimum temperature that the system was able to achieve with the 0ºC lower limit.

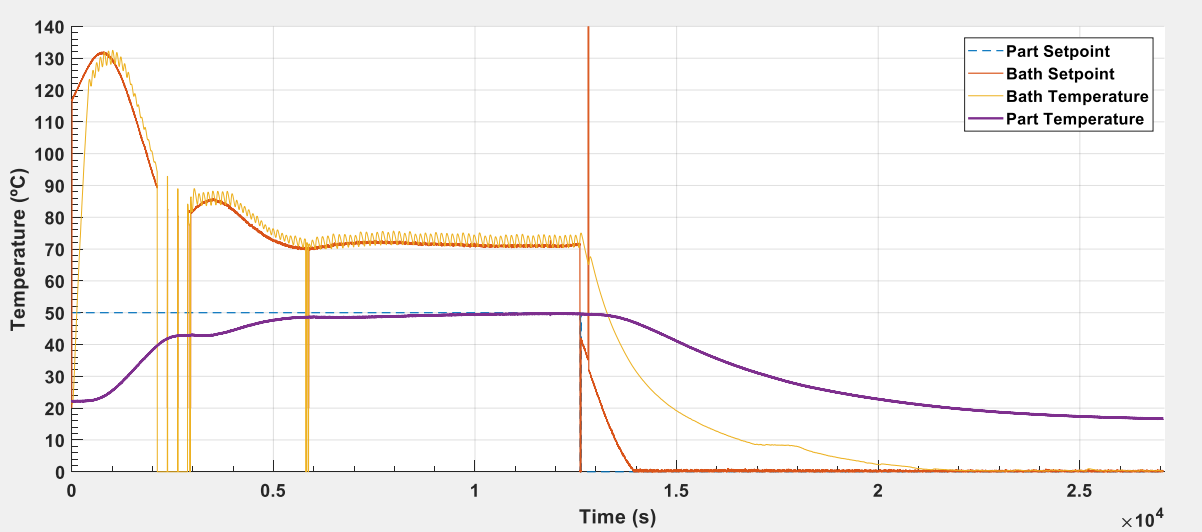

Figure 69- Real test with the same conditions as the simulated

Something to note, is the capability of the controller to respond to the system errors, namely the communication errors between Julabo and the computer, and continue working after the system is auto-reconnected, operation programmed in the main controller to be done automatically in case of failure.

6.4 Sub-zero Cooling

In order to control the liquid nitrogen cooling, due to its nature, the chosen solution was the control of its flow based on the setpoint and a control window, where the main control occurs, using two valves, one regulated (R) and another direct (D) from the bottle.

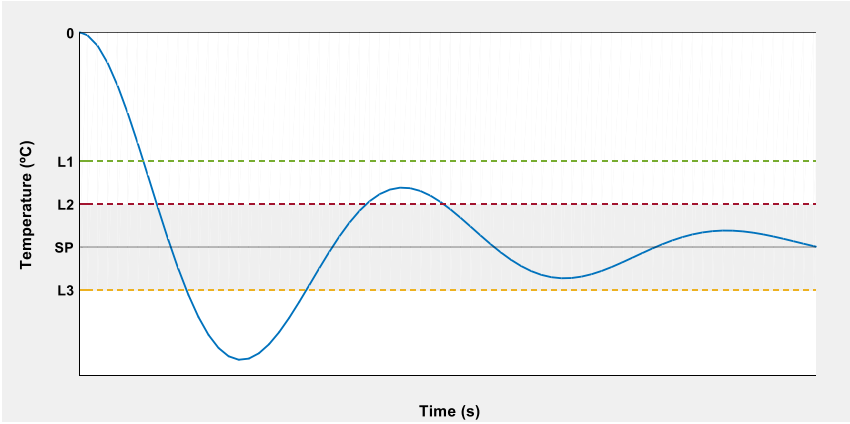

Figure 70- Liquid nitrogen control limits

The controller is based on three limits and the setpoint, all shown in Figure 70, that allow for the switch between control actions.

The first limit (L1) is a variable limit, that is set having in mind the Nitrogen cooling behaviour.

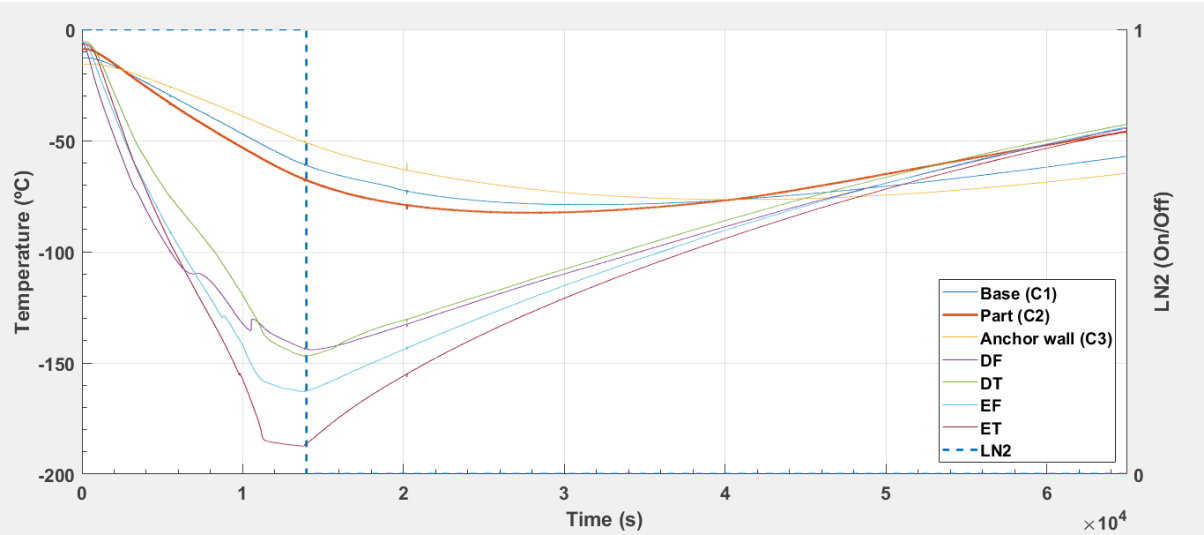

Figure 71- Liquid Nitrogen cooling response

Based on the studied dynamics of the Nitrogen, after switching off the supply the part continues to cool due to the stored energy in the baseplate (Figure 71), which leads to an overshoot of the part temperature. This overshoot was calculated with the data acquired from the test, shown in Figure 72. The values are shown in Table 6 and equation 20.

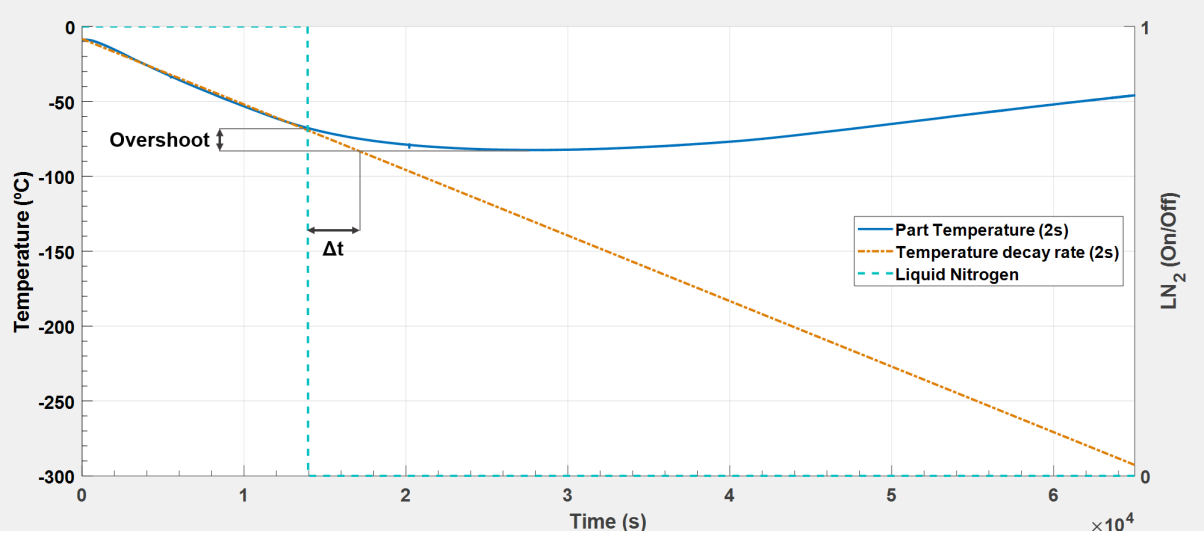

Figure 72- Cooling overshoot and Δt

Table 6- Data acquired from the Nitrogen cooling test

Δt (s)	LN2 OFF (°C)	MIN TEMP (°C)
3010	-67,8237	-82,5348

$$Overshoot = \frac{-82{,}5348 - (-67{,}8237)}{-67{,}8237} = 0{,}2169 \quad (20)$$

This overshoot, in percentage, allows for the placement of the L1 limit on the scale.

$$L1 = T_{off} = (1 - 0{,}2169) * SP = 0{,}7831 \quad (21)$$

Another strategy that could have been followed, is based on the cooling rate found in these tests and the Δt shown in Table 6. A constant verification of the estimated part temperature based on the time difference and decay rate, using the equation from Table 9, would allow for an estimation of how much ahead of time the liquid Nitrogen supply should be turned off.

With the equation for L1 set, the controller for the Nitrogen when in approach to the control band can be set and is shown in the form of a GRAFCET in Figure 73.

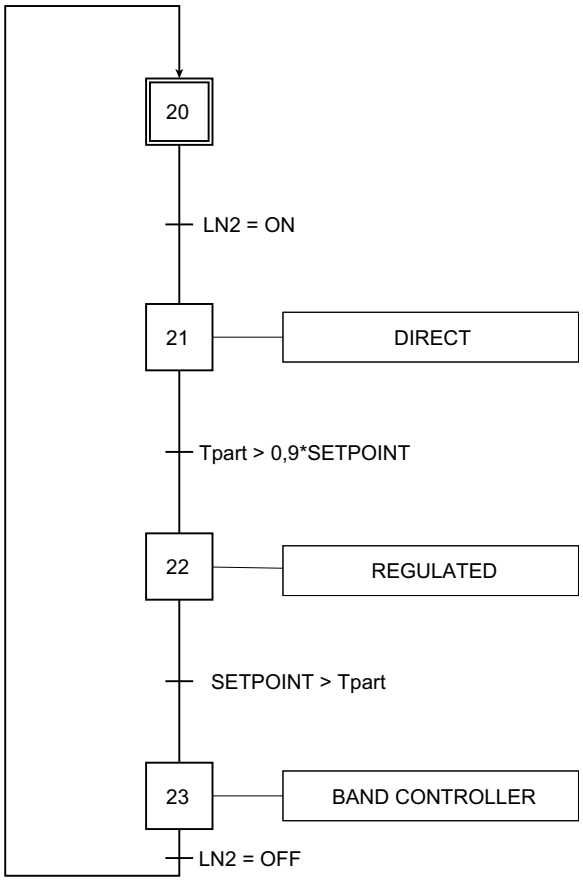

Figure 73- Liquid Nitrogen main controller

When the system is turned on, the Nitrogen is set at maximum flow, achieving the maximum cooling power. Based on the resulting delay when turning off, the cooling is reduced to the regulated state when the part temperature is at the estimated temperature where the overshoot is reduced, defined at 90% of the setpoint. This will lead to a decrease in temperature but at a

smaller rate and more controlled. Instead of turning the regulated valve on, other solution was tested, namely the complete cut off of the Nitrogen supply, but was found to be too slow.

After, when the system achieves the desired setpoint (SP) the controller is changed to a more refined band controller.

6.4.1 Band controller

Inside the control window, there is the need to choose when to turn on or off the nitrogen. The logic behind this is explained in the following relations.

In order to define conditions for the switch of the system, the behaviour of the error (Figure 74) was studied and analysed, since it will be the variable used to determine where the system is in its response curve and subsequent control action to impose.

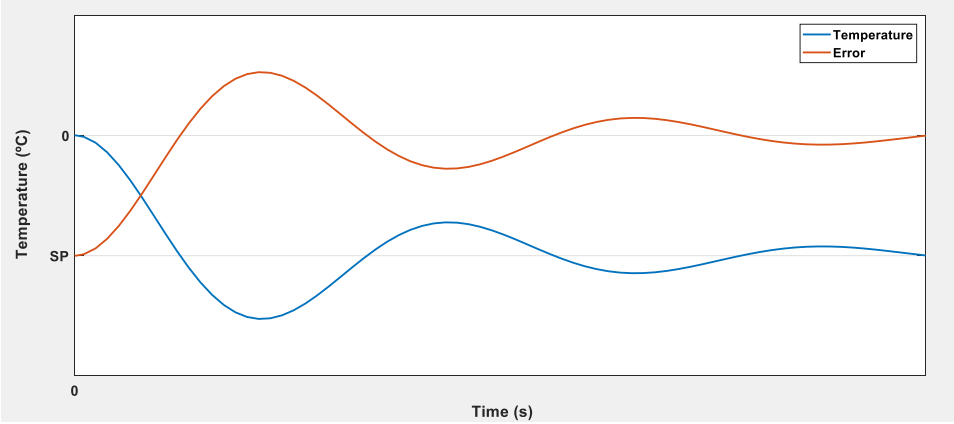

Figure 74- Error behaviour

The current error of the system is measured as shown in Equation 22.

$$e = SP - Measured \tag{22}$$

This relation allows to determine whether the current measured value is above or below the setpoint, as shown in Figure 75.

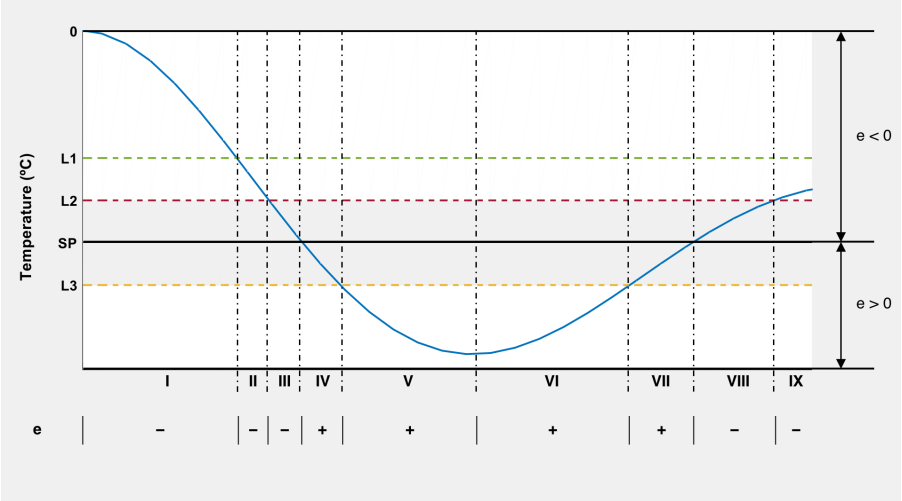

Figure 75- Error signal variation along the system response

The second expression used to determine the tendency of the curve is the variation of the error, seen in Equation 23.

$$\Delta e = e_t - e_{t-1} \tag{23}$$

This parameter, in conjunction with the previous one, can determine if the value is trending to the setpoint or diverting from it, this is illustrated in Figure 76.

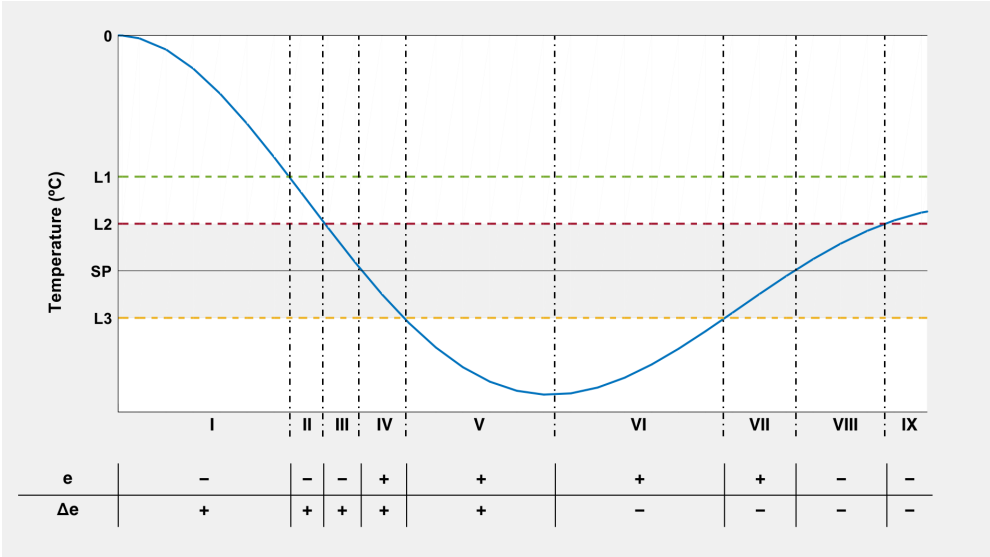

Figure 76- Variation of the error and error difference

The rules for determining which of the systems (regulated valve, direct valve or heating element) is turned on are then determined by these factors in conjunction with the band limits.

Based on the previous information, inside the band controller, the sub-systems control based on the limits is the following:

Table 7- Relation between limits and control element

Element / Condition	Direct Valve	Regulated Valve	Heating element (50% Power)	Heating element (Full Power)
T > L2	ON	OFF	OFF	OFF
L3 ≤ T ≤ L2	OFF	CAN BE USED	CAN BE USED	OFF
T < L3	OFF	OFF	OFF	ON

In between the L2 and L3 limits, the control is ruled by the previously shown error and error variation. The resulting control action is shown in Table 8.

Table 8- Control action based on error and error variation

Δe / e	< 0	≥ 0
< 0	R=1 $H_{50\%}$=0	R=0 $H_{50\%}$=0
≥ 0	R=0 $H_{50\%}$=0	R=0 $H_{50\%}$=1

6.4.2 Heating element control

With the objective of achieving a power delivery to the system as smooth as possible, during the control near the setpoint, a controller for the heating elements was developed.

The chosen strategy was a PWM modulation of the control signal. This modulation allows for the control of the mean power by switching on the signal for a certain time (duty cycle) within a base period (Figure 77). Since the heating element is actuated via a mechanical relay, it was taken into account the amount of actuation needed and the limits of the device. Therefore, a base time period of 5 seconds was chosen as the base interval.

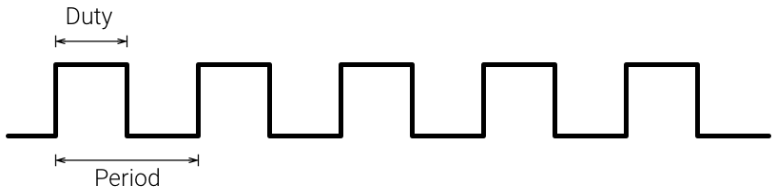

Figure 77- PWM signal [34]

By changing the duty cycle, the mean power being supplied to the system can be controlled (Figure 78).

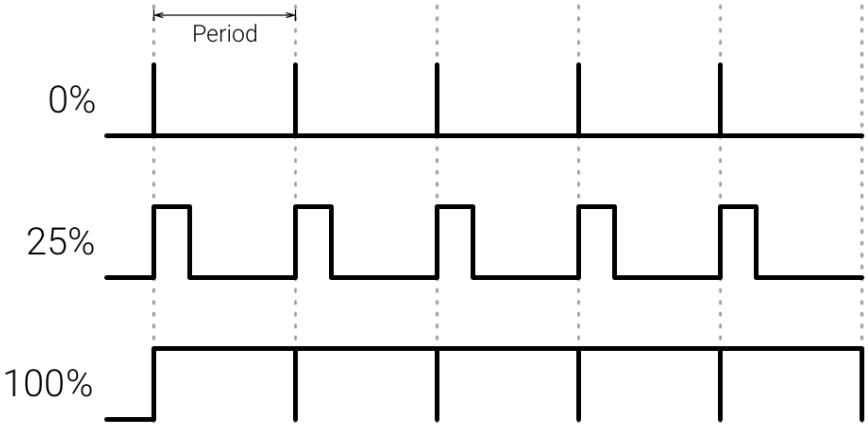

Figure 78- Mean power resulting from PWM [34]

6.5 Circuit controller

The circuit controller is responsible for switching the circuits automatically. The two available circuits are shown in Figure 79.

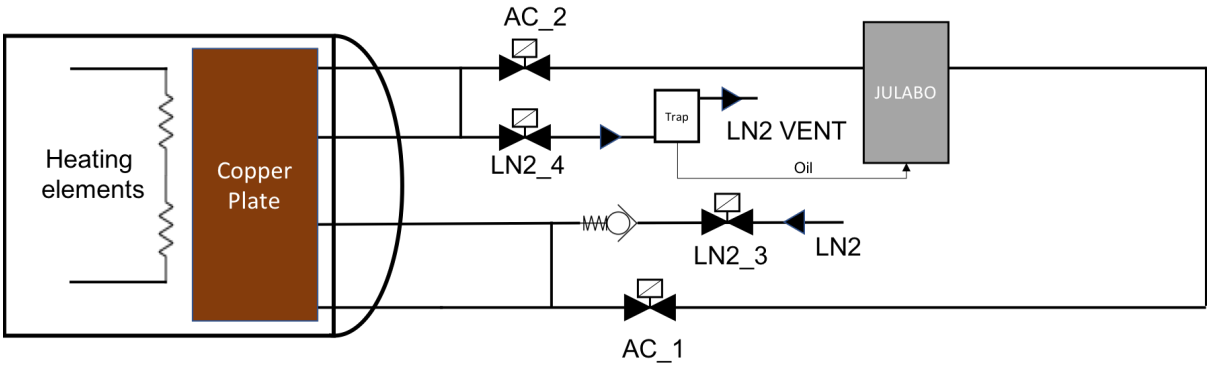

Figure 79- Controlled valves

There are four valves to control, being LN2_3 and LN2_4 the in and out, respectively, of the liquid nitrogen system and the AC_1 and AC_2 the in and out of the thermal bath circuit.

The operation of this controller is expressed under the form of a Grafcet in Figure 80.

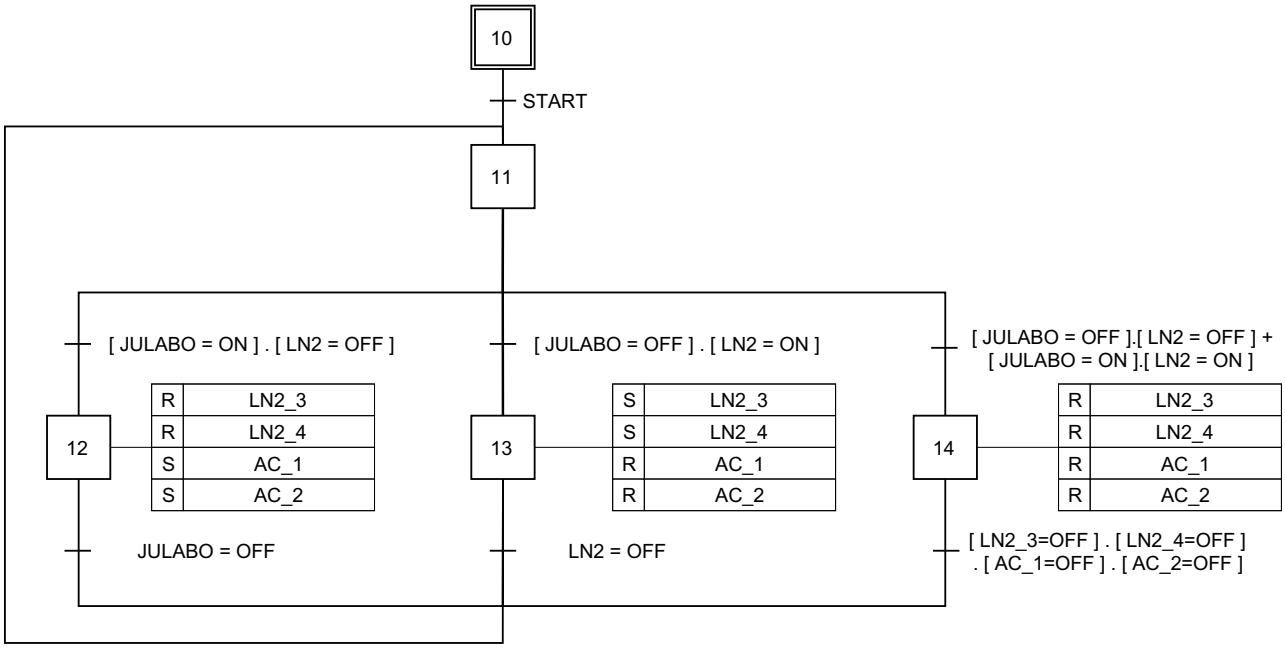

Figure 80- Grafcet of the circuit controller

As a matter of safety, the valves are shut-off either if both are not requested or if both are requested at the same times, in order to prevent conflict between the two systems. Also to note, in the final controller, the reset of the valves is always done previous to the set of the others, in order to also prevent conflict between the systems.

7 EXPERIMENTAL PROCEDURE

The necessary steps for completion of the system, as well as test performed to evaluate the possible strategies to follow are presented in this chapter. Firstly, the leak test performed to access the chamber condition is described, followed by the upgrades done to the control and heat exchange system. Secondly, the tests for accessing different control possibilities are shown and the results examined. Lastly, the implementation strategies of the controllers to the system are described and the system user interface presented.

7.1 Leak test

In order to access the chamber condition and to develop the control for the best possible situation, there was the need to do a leak test in order to identify any possible vacuum leak that would further along not only affect the test requirements but also the temperature control of the chamber. As explained in section 3.2 the leak test was conducted using helium gas and a helium spectrometer, shown in Figure 81.

The spectrometer was attached to one of the available flanges of the chamber, as it is possible to verify in Figure 81.

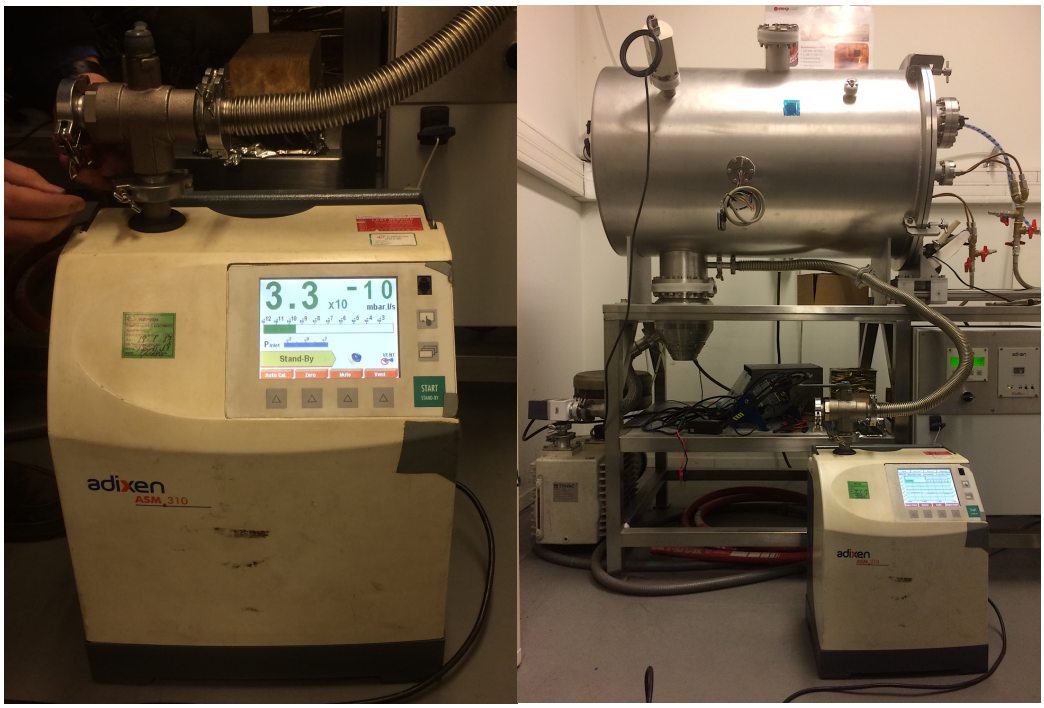

Figure 81- Helium spectrometer (Left) and Leak testing setup (Right)

The test was then started by getting the chamber to working pressure, in this case 10^{-5} mbar and then the leak test was conducted. For this, a helium gun, as shown in Figure 82, was used

to deploy helium near every seam of the chamber, including welds, in order to verify its air tightness.

Figure 82- Helium gun

Regarding the results of the test, all the welds of the camber and small flanges showed to be sealing correctly. On the other hand, the main seal, that is responsible for sealing the chamber door to its body, showed a small leak where the O-ring seam was located. This leak presented itself as a spike in the meter (Figure 83).

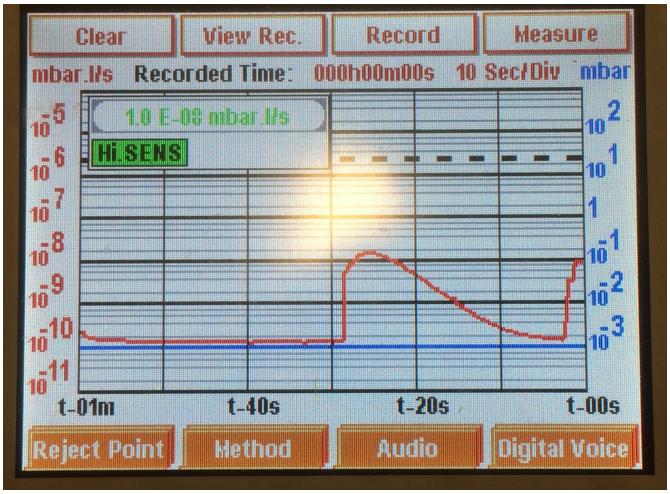

Figure 83- Graphical representation of the leak

In order to solve this problem and based on the search done at the beginning of this work, it was replaced with a seamless O-ring.

7.2 Utilized components

7.2.1 Thermal fluid

As stated in section 4.4.2, the old fluid was changed and the Syltherm XLT is now the employed fluid due to its better suitability to the working temperatures and future uses of the chamber.

7.2.2 Temperature sensors

The Pt1000 temperature sensors were distributed in the chamber in key locations, in order to better understand the chamber dynamics. Four sensors were placed in the copper plate, one at each corner, in order to understand the temperature distribution on the plate. Other three sensors were placed in the support. The three chosen locations were, one in the base plate, one in the top of the support, which best represents the phenomena that the part will be exposed to, and, lastly, one sensor was placed on that face that the part attaches to.

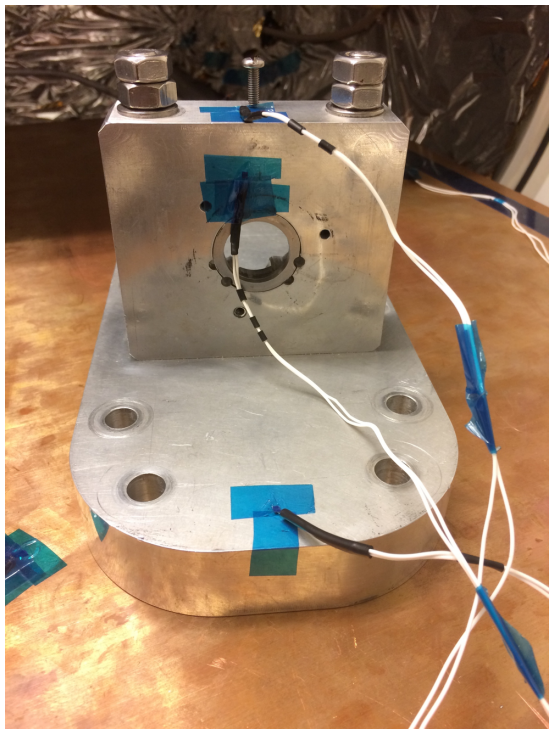

Figure 84- Location of the temperature sensors on the part support

7.2.3 NI USB-6229 DAQ

The DAQ is not only used as a data acquisition interface, but also as a control interface, using its output ports to control the valves and heating elements. The digital output ports send a 5V signal, signals that will be used to control the chamber peripherals.

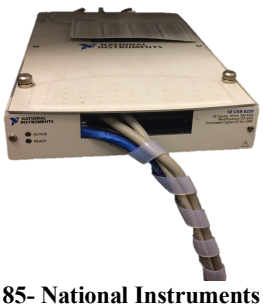

Figure 85- National Instruments USB-6229 DAQ

7.2.4 Interface boards

The 5V control signals from de digital outputs of the DAQ board are used to control both the valves and the heating elements. Therefore, it is necessary to amplify this signal in order to supply the needed 24V DC, to power each LN2 valve, and 230V AC, for the heating element.

The previously installed board (Figure 86), already used to control the two 24 AC solenoid valves and was upgraded with two more boards needed for the control of the newly added components (Figure 87).

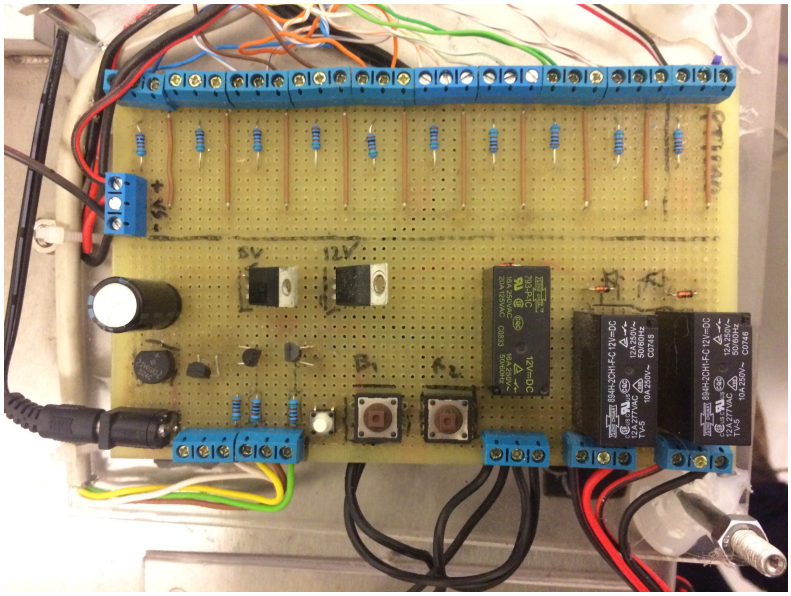

Figure 86- Original board

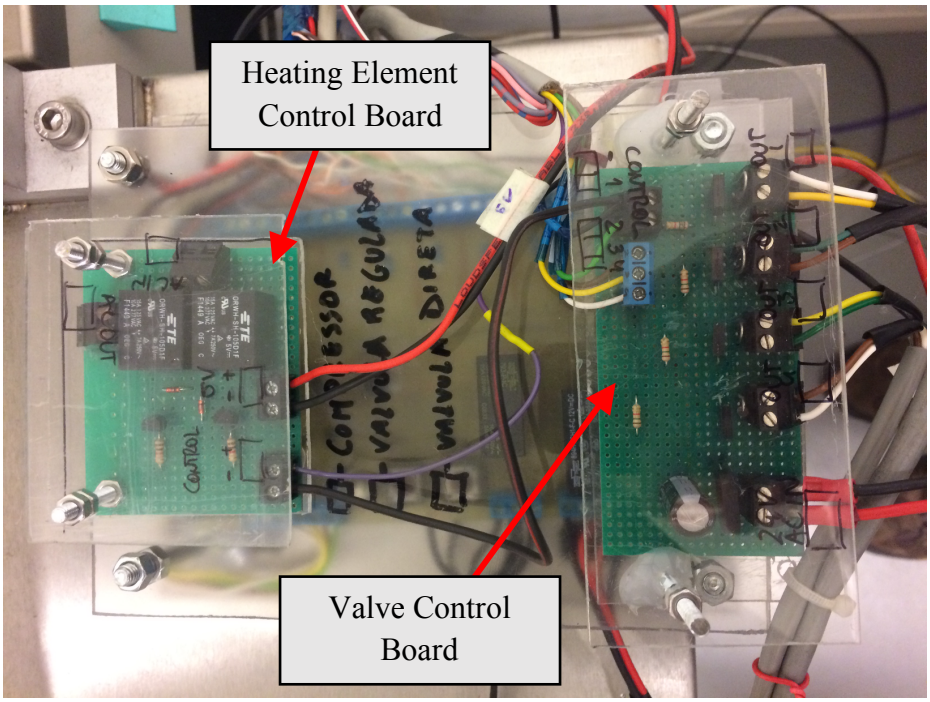

Figure 87- Upgraded board

7.2.4.1 Valve control board

For the solenoid valve control, it is necessary to convert four control signals, into the actuation of the corresponding valve. The chosen method was the use of transistors to actuate the 24 DC with a 5V signal. The pre-existent system had available a 24V AC supply, which was used to actuate the two LN2 solenoid valves. This is used to supply the needed voltage to the new board. Hence, the voltage needs to be rectified to transform the AC supply into the DC used by the new valves.

This is done using a diode bridge attached to a capacitor (Figure 88), to filter the output and remove the ripple resulting from the diode rectification.

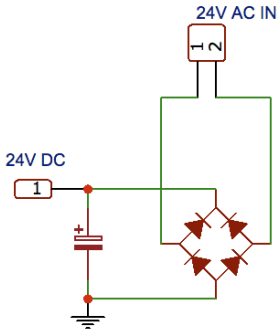

Figure 88- Rectification circuit

Initially, the valve actuation was done using single transistors. Although working, to ensure a more robust system they were replaced with Darlington Transistors, which are able to better withstand the load imposed by the inductive elements of the solenoid valves. The final configuration of the system is shown in Figure 89.

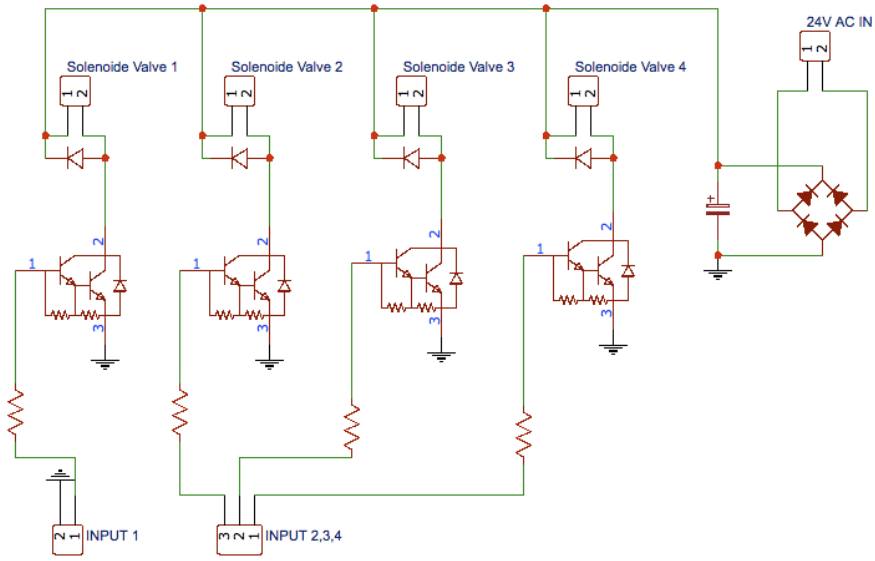

Figure 89- Valve control circuit

7.2.4.2 Heating element control board

Similarly, the actuation of the heating element needs to actuate 230V AC from a 5V DC input. So, the use of relays was the chosen solution. Two relays ensure the control of the Live and Neutral leads of the AC current, while two transistors are responsible for applying the 12V DC voltage, used to actuate the relays. As in the previous board, the control signal from the board is what controls the transistors, and ultimately permits the actuation of the relays. The schematic of the circuit is shown in Figure 90.

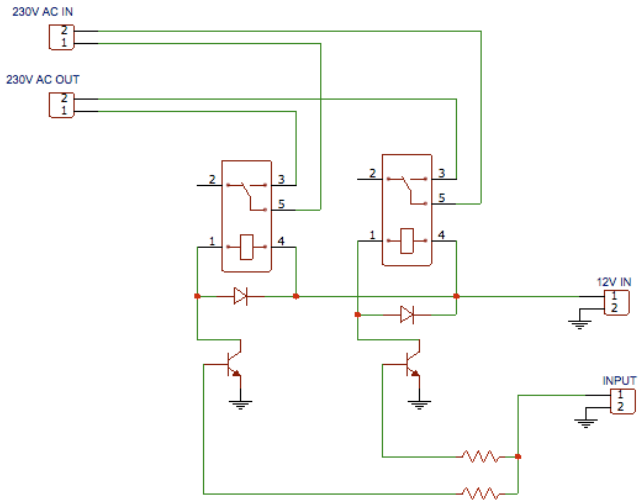

Figure 90- Heating element control board

7.2.5 Solenoid valves upgrade

To control the Nitrogen flux, the previous solenoid valves were replaced with ones better suited for this specific job, in order to prevent the valves getting stuck open or closed. The chosen valves are Gems sensor's D2017-LN2-C204 solenoid valves, which are designed to withstand the conditions imposed by liquid nitrogen and use a DC coil, that aids the valve not getting stuck due the hotter working temperatures, compared to the AC current used in the previous flow control valves.

The original circuit switch solution was the manually controlled circuit shown in Figure 91.

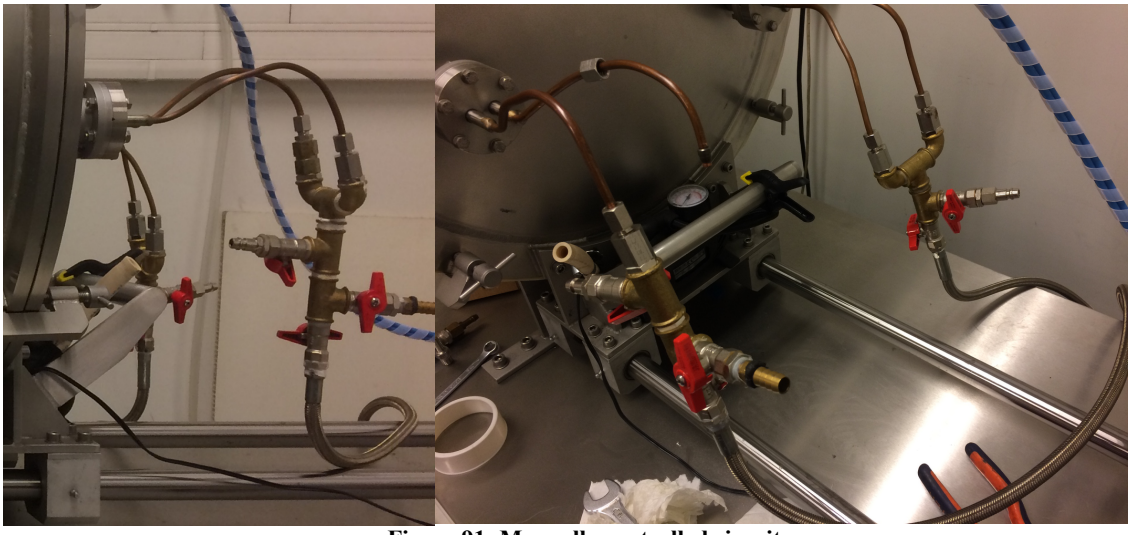

Figure 91- Manually controlled circuit

The upgraded circuit, shown in Figure 92, consists in the addition of the solenoid valves.

The old solenoid valves were changed to the thermal fluid circuit and two new Nitrogen suitable valves added for the Nitrogen circuit.

The maximum temperature the new solenoid valves can work at is 80ºC. With that in mind, a separation using a copper serpentine was used to create a temperature differential for when the oil is at temperature higher than the valves maximum temperature they are not affected. In the future, depending on the tests temperatures, a fan can be added to increase heat transfer in case of the temperature being close to the maximum value.

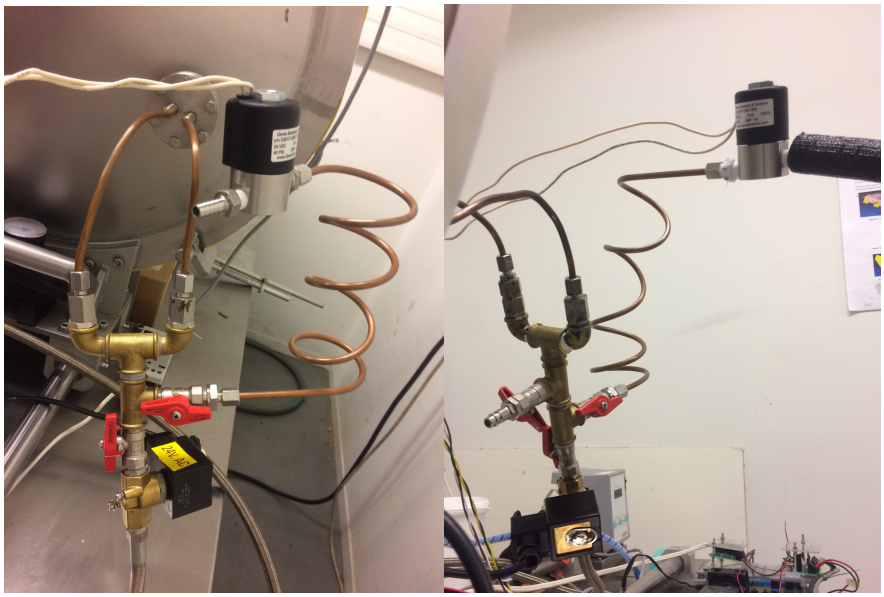

Figure 92- Upgraded circuit

The direct and regulated valves in the bottle were then replaced with the liquid Nitrogen suited ones, shown in Figure 93 without the insulation. In total, the system has 6 solenoids valves.

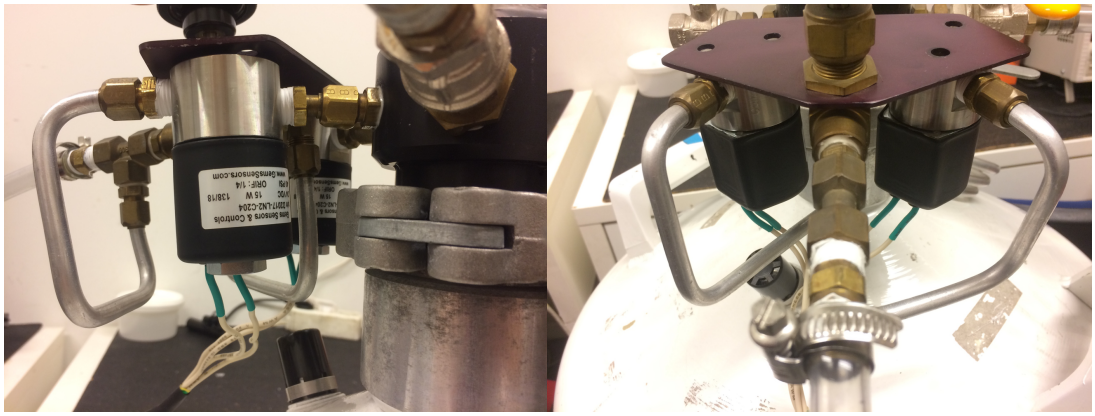

Figure 93- Nitrogen bottle upgraded valves

7.2.6 Catch can/Oil trap

Since the liquid Nitrogen purges the two serpentines, the oil that is removed from the system needs to be stored in a container, so as to not be wasted. The solution used is a catch can (Figure 94), that traps the oil on the bottom and only allows the gaseous Nitrogen to escape from the vessel.

Figure 94- Oil trap

Inside the trap the incoming fluid is directed to the wall, to work as a baffle and avoid the oil escaping through the exhaust. There is also a physic separation between the oil reservoir and the outlet, where a filtering medium is added to trap any suspended oil particles.

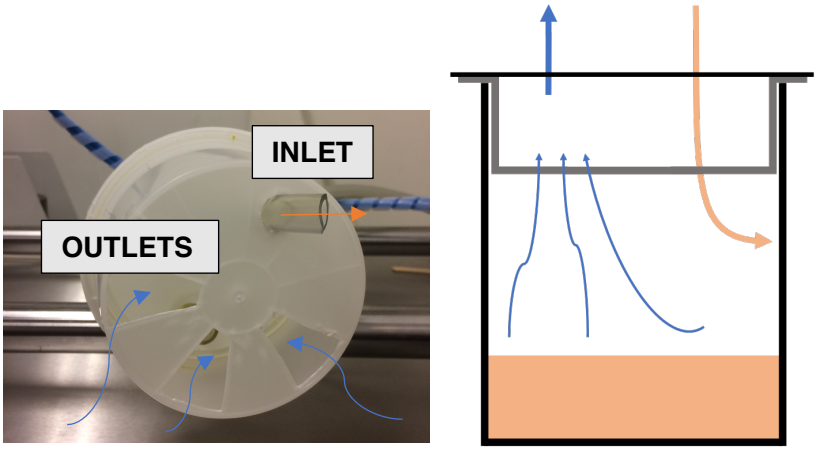

Figure 95- Separation solution

This way the purged oil can be reused, and the waste is reduced.

7.3 Heat Exchange systems experiments and implementation

7.3.1 1 serpentine vs 2 serpentines

In order to select a heat exchanging setup, there was the need to perform some tests in order to understand if the reduction in complexity of the system would outweigh its performance decrease.

The main goal of this tests was to verify if the use of one serpentine would greatly influence the cooling time of the chamber when using the liquid nitrogen, since it would be benefic to use only one serpentine to reduce LN2 consumption, and consequent number of bottle exchanges.

7.3.1.1 Above zero

To evaluate the influence of the second serpentine in the above-zero range a test was conducted with different setpoints, which allows to study the part temperature behaviour not only when heating or cooling, but also when the starting and end temperatures are in the lower or upper part of the scale. The full test with one serpentine can be seen in Figure 96.

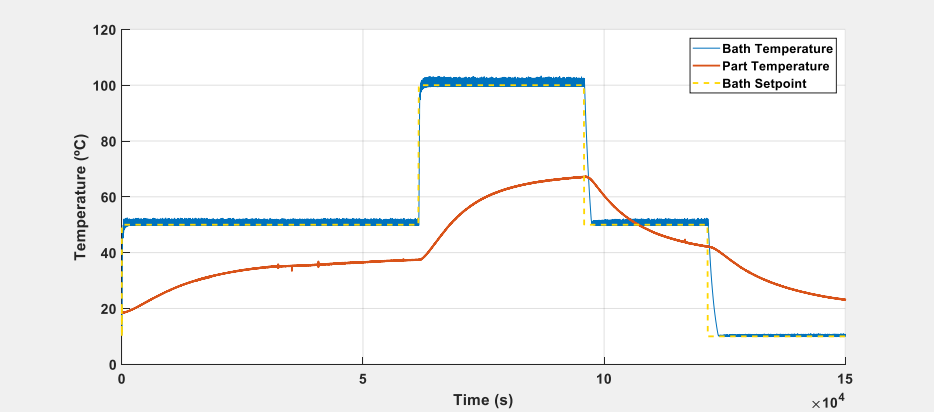

Figure 96- One serpentine Julabo test

The same test was conducted for with the two serpentines connected to the thermal fluid circuit, the comparison between tests can be seen in Figure 97.

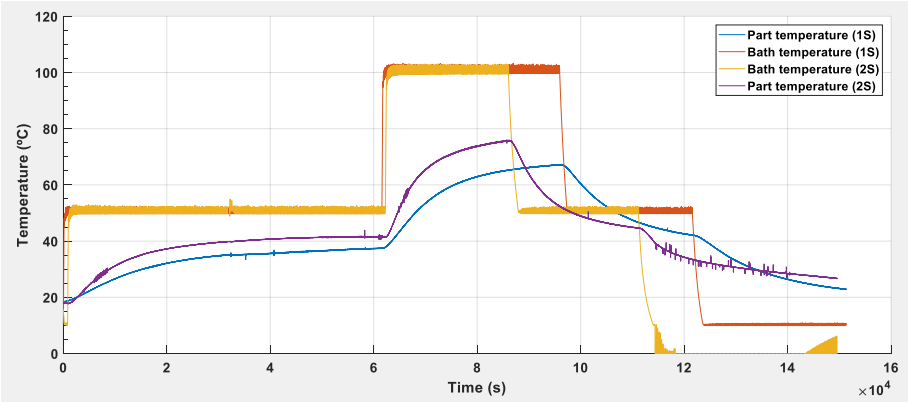

Figure 97- 1 vs 2 serpentines Julabo test

The various setpoints response of both tests can be seen in Figure 98, with starting times corrected to analyse the temperature change rate and verify which solution is more advantageous.

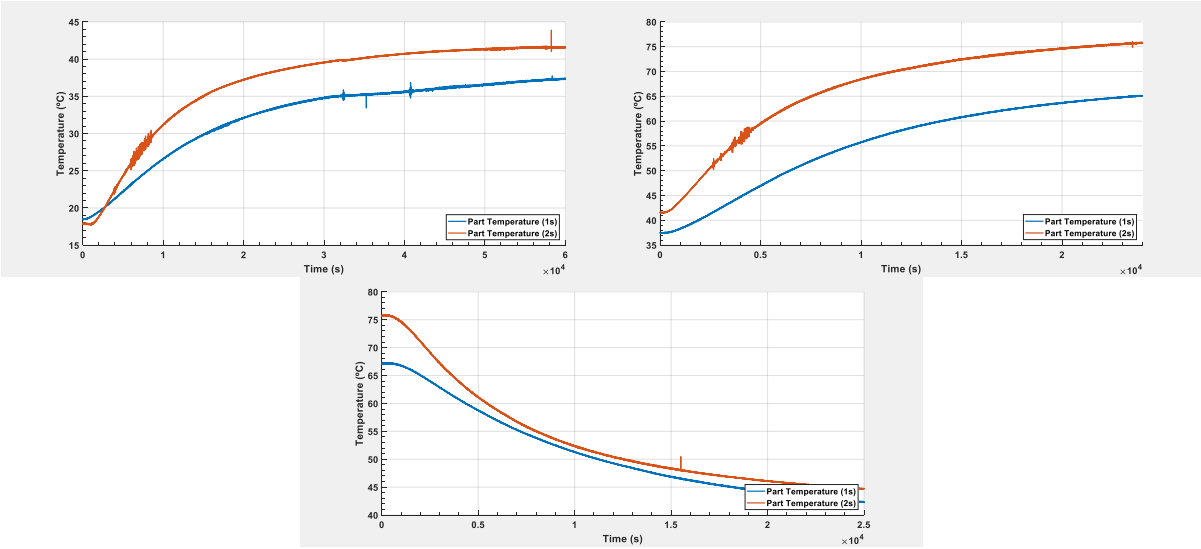

Figure 98- 1 vs 2 serpentines (Top left - 10-50; Top right 50-100; Bottom 100-50)

From the extracted data, we can verify that the use of two serpentine produces an increase in the temperature change rate. The maximum temperature achieved with only one serpentine is always lower than in the other case. For the thermal bath this may not present such complication, since the use of a PI controller can induce an increase in the bath temperature and therefore increase not only the temperature change rate, but also control the final temperature of the part, this is valid not only to increase the maximum temperature in a heating scenario with one serpentine, but also to lower the minimum temperature in a cooling situation with two serpentines.

Consequently, for the above-zero heat exchange scenario the use of one or two serpentines can be compensated by the controller and thus is not critical.

7.3.1.2 Sub-zero

With the influence in the upper part of the range analysed, it was essential analyse the part temperature behaviour in the lower part of said range. The test performed consisted in opening the LN2 direct valve, that being the more advantageous case for both systems, a similar amount of time and verify the part temperature dynamics in each case.

The first test was carried for one serpentine, and the results are shown in Figure 99.

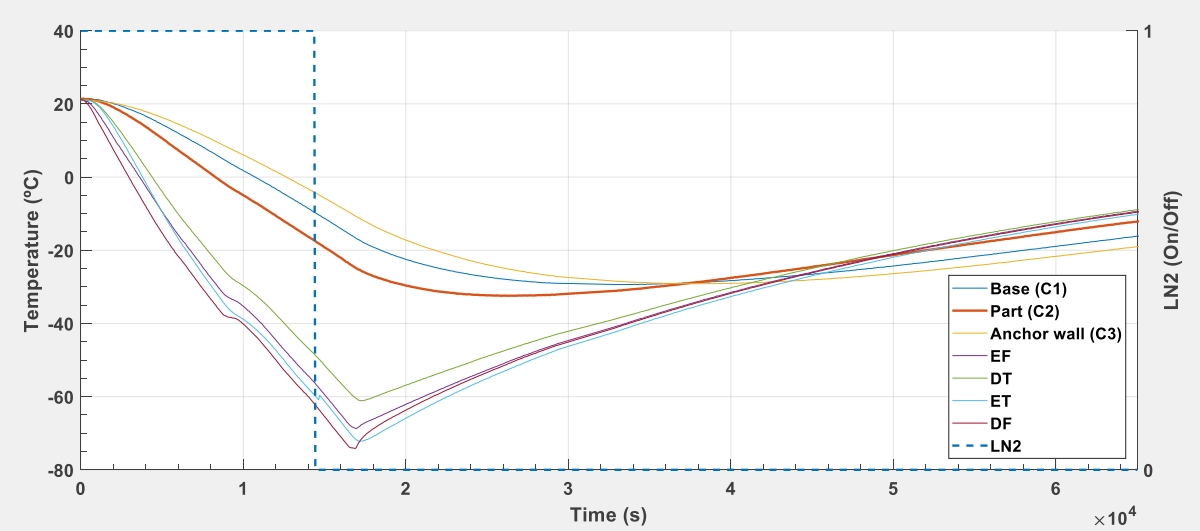

Figure 99- Liquid nitrogen cooling with one serpentine

As it is possible to assess, the liquid nitrogen was turned on for approximately 4 hours, after which was tuned off and the temperature left to evolve naturally within the part.

The second test, with two serpentines, followed a similar procedure and the results can be seen in Figure 100.

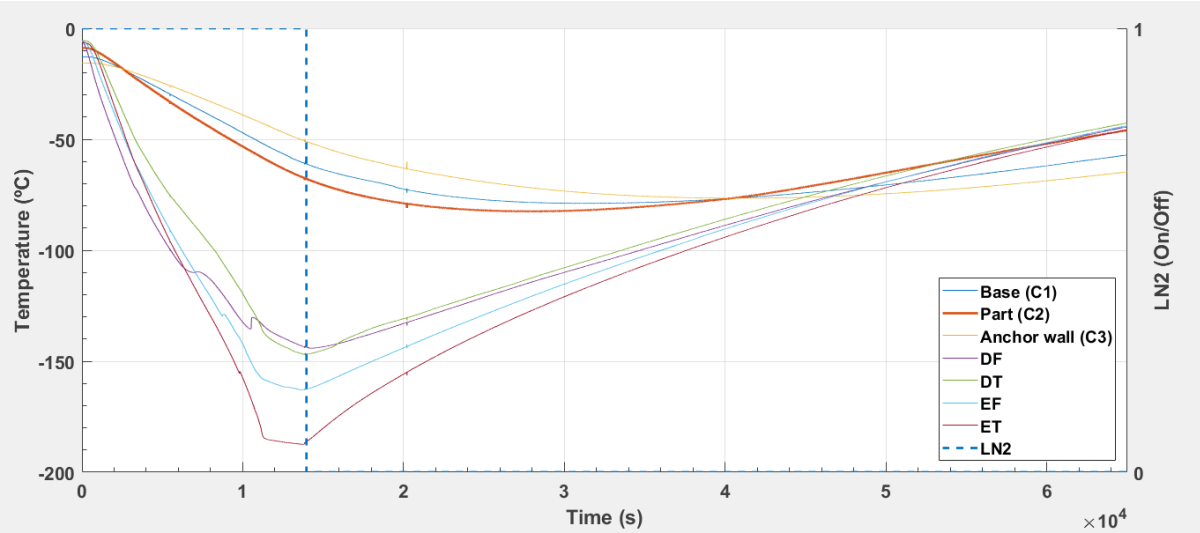

Figure 100- Liquid nitrogen cooling with two serpentines

Comparing both responses (Figure 101), as expected the use of two serpentines ensured a higher heat exchange and therefore a faster cooling. Not only it was faster, but also achieved a higher temperatures differential form the starting point.

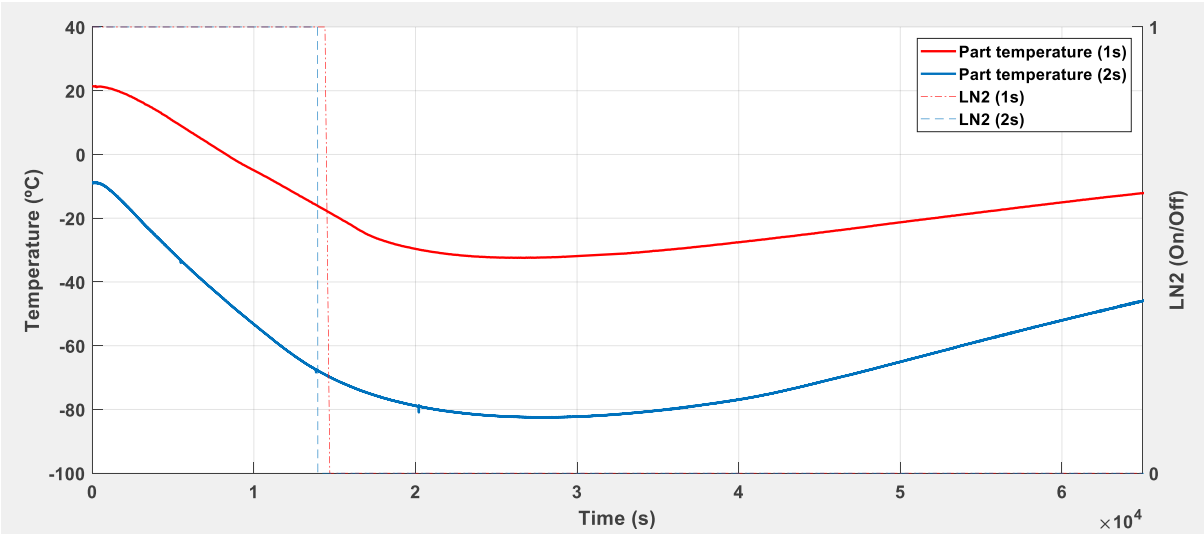

Figure 101- LN2 cooling - 1 vs 2 serpentines

Although starting at different temperatures, and in a more thermodynamically beneficial scenario for the single serpentine, since the cooling occurs at higher temperatures, the two serpentines still achieved better performance.

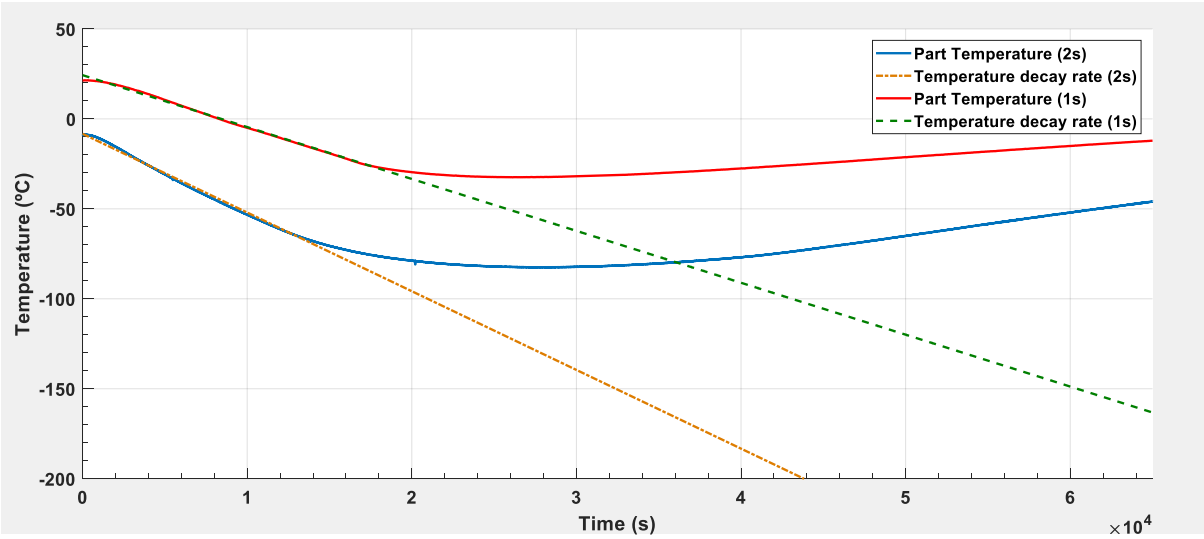

Figure 102- Temperature decay rate - 1 vs 2 serpentines

From the analysis of the decaying rate of temperature in each case, represented by the lines shown in Figure 102 and quantified in Table 9, the situation with two serpentines achieved a 33% better performance, which in a cooling from room temperature to -100ºC may represent a gain of almost 4 hours, a significant amount of time for the long duration tests carried out.

Table 9- Temperature decay rate values

Case	Decay rate equation	Hourly cooling capacity (°C/h)
1S	$T = -0.002885 * t - 24{,}31$	10,39
2S	$T = -0.004375 * t - 8.29$	15,75

Hence, from the tests we can confirm that the use of two serpentines, although requiring a higher consumption of LN2, is the most advantageous situation and is the chosen solution.

7.3.2 Serpentine purge with Nitrogen

After verifying that the use of two serpentines was the best option, there was the need to select the method used to purge the oil that was in the serpentines, to allow for the free flow of the Nitrogen. The solutions were the use of a small compressor or the direct use of the liquid Nitrogen to flush the system. To test this, the Nitrogen hose was connected to the serpentines full of oil and the fluid purged to the oil trap. It was therefore verified that the pressure at which the Nitrogen exits the bottle is enough to clean the serpentines, even if any remains stay inside de serpentines. The oil was selected based on this possibility and can withstand the conditions without degrading.

7.3.3 Cryogenic cooling and natural heating

To evaluate the dynamics of the chamber for the cryogenic cooling, a test with two serpentines was conducted (Figure 103) cooling the chamber for 4 hours and turning the LN2 off letting the chamber heating naturally.

The limitation in heat exchange both due to high vacuum conditions and also cryogenic temperatures, are two key points when heating the part from cryogenic temperature up to the transition temperature, that allows for the heating of the part externally with the thermal fluid.

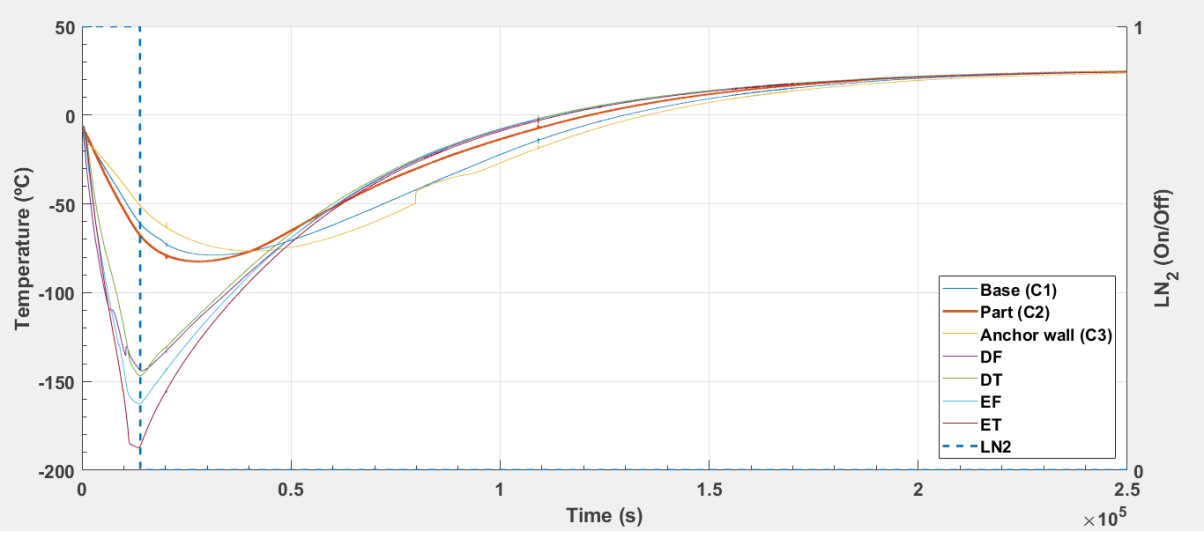

Figure 103- Complete LN2 cooling cycle

From the data acquired with the test, it can be verified that after turning the cooling off, the part temperature continues to decrease due to stored energy, mainly in the copper plate.

To counteract this, and to increase the heating rate of the part, a heating element was added to the inside of the chamber. This ensures a faster temperature increase response in the cryogenic temperatures.

7.3.4 Heating element

The heating element was mounted on the outside of the shroud (Figure 104), to get a more homogeneous radiation distribution irradiating on the part.

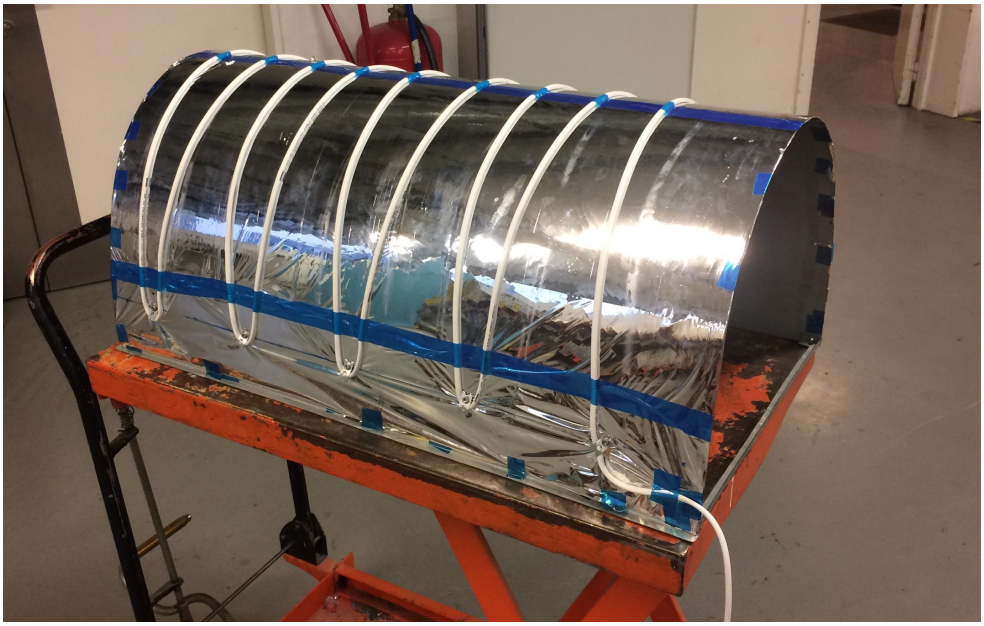

Figure 104- Heating element installed in the shroud

After installing the heating element, and to better understand its influence on the system, tests were performed with the heating element at full power and half power, to determine the temperature change rates and delays.

Based on these values, the heating delay may be determined as significant and thus included in the liquid Nitrogen controller.

The results from the tests are shown in Figure 105.

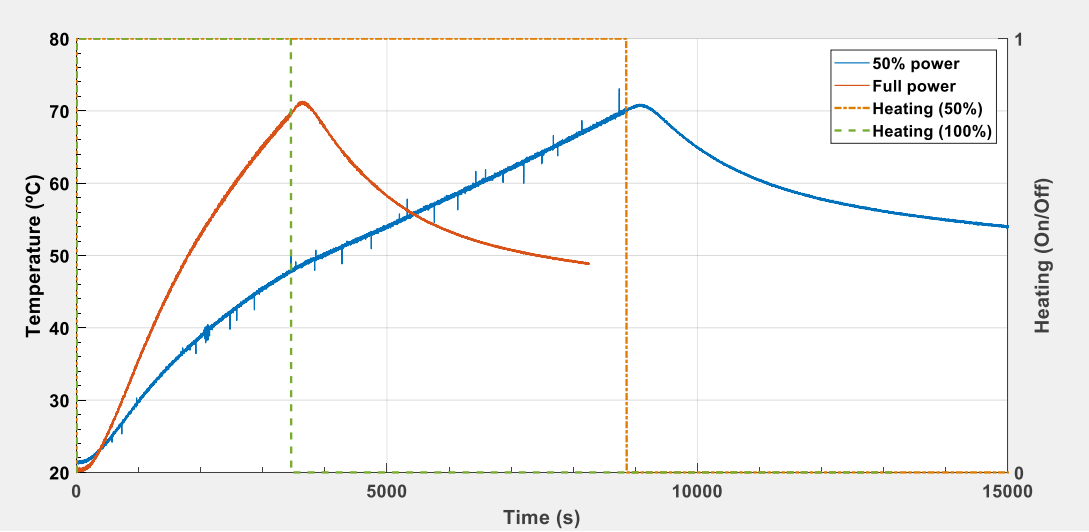

Figure 105- Heating at full and 50% power

The approximate temperature change rates are shown in Table 10.

Table 10- Data from the heating element test

Case	Hourly heating capacity (°C/h)	ON Delay (s)	OFF Delay (s)
50% Power	19,88	219	178
Full power	51,35	129	209

The delays, both when turning on and off, based on the dynamics of the nitrogen cooling can be overlooked in the controller. Also to note, is that the heating capacity is much higher than the cooling of the Nitrogen.

7.4 Controllers implementation

7.4.1 Control action filtering

As already discussed regarding the Derivative action of a PID controller, the control system may be susceptible to erratic behaviour due to sensor or input data noise. The same applies for the Nitrogen controller developed, since it is a type of controller that uses real time data from the temperature sensors, to determine the error and its variations. This means, that any small change originated by sensor noise may lead to a fast variation in the control signal that may prove harmful for the system. Therefore, a filtering was imposed to the output of the controller.

The chosen strategy was defining a frequency at which the signal can change. Due to the slow dynamics of the system, a 30 seconds interval was enforced where the control signal would remain unchanged and therefore avoid erratic behaviour of the valves. Therefore, the control signal is set every 30 seconds and the last control action retained in that period.

7.4.2 Maximum cooling

When the PI controller of the thermal bath system receives a lower setpoint, it changes its reference accordingly. But, due to the characteristics of this system, where a PI controller is controlling another PID controller, this leads to an inconvenience in the event of cooling.

The control action given by the PI in conjunction with the control order of the PID can lead to a situation where the setpoint is being lowered by the PI but the PID is heating, foreseeing the cooling of the bath and trying to control the temperature to that reference when it may immediately change to lower one.

So, given that the cooling is much slower than the heating, any small amount of heat will increase bath cooling time. Therefore, a solution was implemented in the main controller, where the PI works for the heating of the bath, being tuned off when cooling until near the setpoint, with a value defined by a percentage. In this situation, the reference is set to the lowest possible value since any correction by the PID is to be avoided. The temperature is then precisely controlled when the PI is activated before reaching the setpoint.

This same control doesn't need to be applied to the heating, because the PI control action is above the bath temperature in the interval where this control would be applied, resulting in the correct behaviour.

7.5 Graphical User interface (GUI)

National Instruments' LabVIEW was the chosen program for the development of the data acquisition system and the final control system. For post processing, all of the data is recorded to a text file setup at the beginning of the test.

The main program is responsible for setting up this file and has the user interface to display and control all the data required (Figure 106).

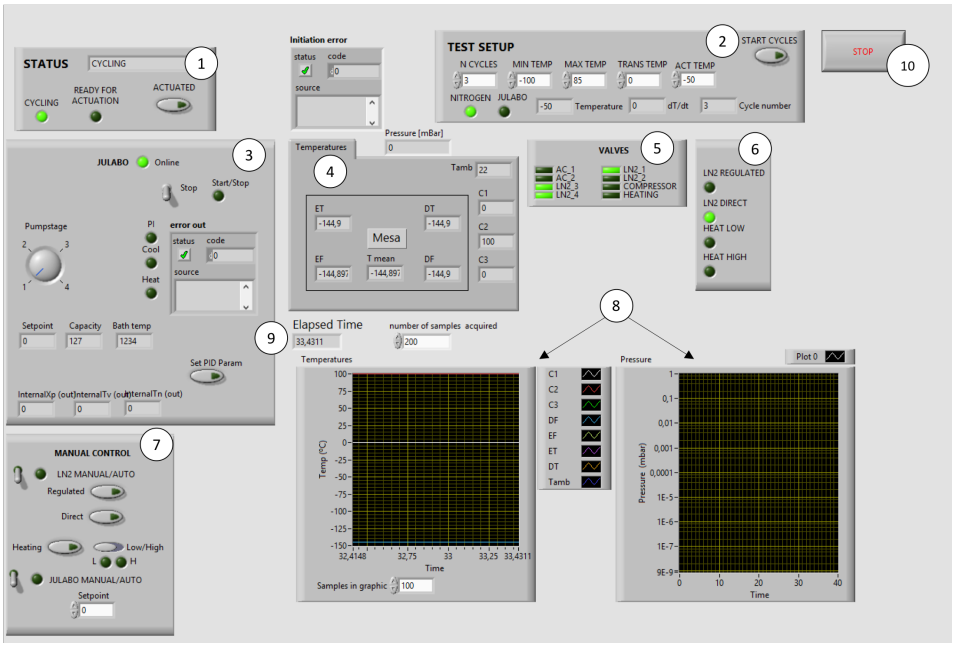

Figure 106- Graphical User Interface

The graphical user interface has the following controls:

Table 11- GUI description

1	Status	Block where the status of the cycle is shown, and actuation is confirmed to start a new cycle
2	Test setup	Where the test is set up. The temperatures and number of cycles are set and the start order is given.
3	Julabo setup	Block for the setup of the thermal bath, writing and reading of internal variables and control action being sent.
4	Sensors	Data acquired from the temperature and pressure sensors is shown numerically.
5	Valves	Displays the current status of all the valves of the system.
6	Control LN2	Shows the control signals being sent to the LN2 sub-system.
7	Manual control	Allows the override of the system, and manual control of the sub-systems.
8	Graphic display	Graphically shows the sensor values. One graphic for the pressure and another for the temperatures.
9	Elapsed time	Shows the time elapsed since the beginning of the data acquisition.
10	Stop button	Button that stops the program and end the writing of the data file.

8 RESULTS AND SOLUTION VALIDATION

The last step of this work was the validation of the control system. For this, a full cycle was performed, where the key points of the control system were tested.

8.1 Systems transition

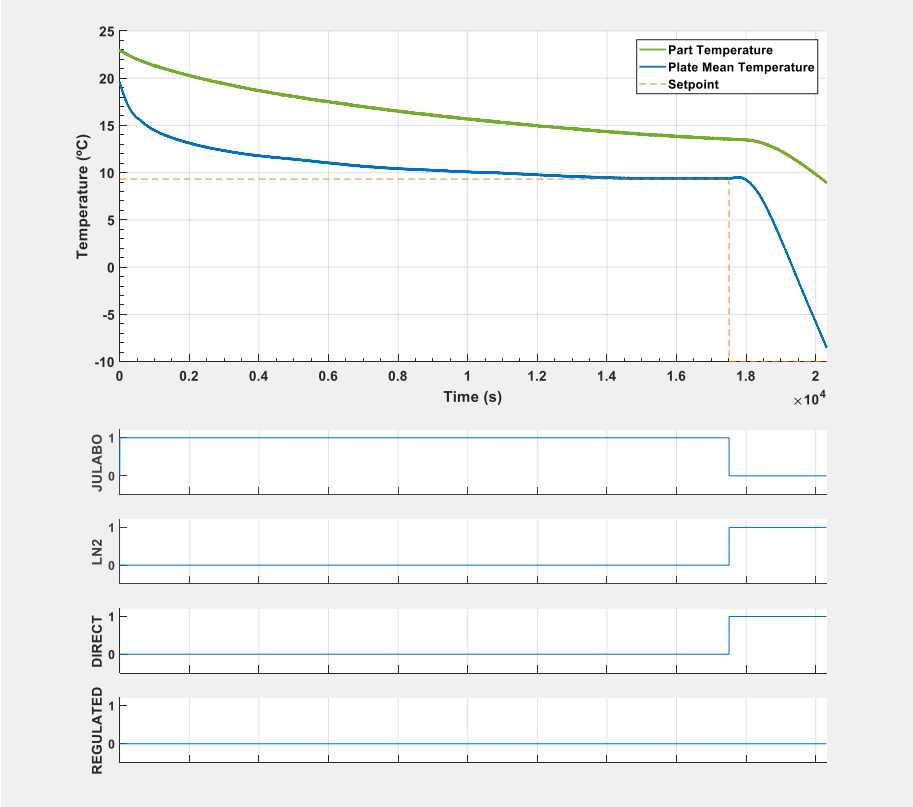

Figure 107- Thermal bath to LN2 transition

Shown in Figure 107 is the transition between the above zero and sub-zero systems. The system starts by being cooled by the thermal bath, and when the plate achieves the desired transition temperature, in this case set at 9 °C, the systems are switched. As it is possible to see in the control signals, the Julabo signal is turned off and the liquid nitrogen turned on. As soon as this occurs, the LN2 controller receives the new setpoint, this time referring to the part, and generates a control signal accordingly. As defined in this controller, the Direct valve is turned on and the system achieves higher cooling rates.

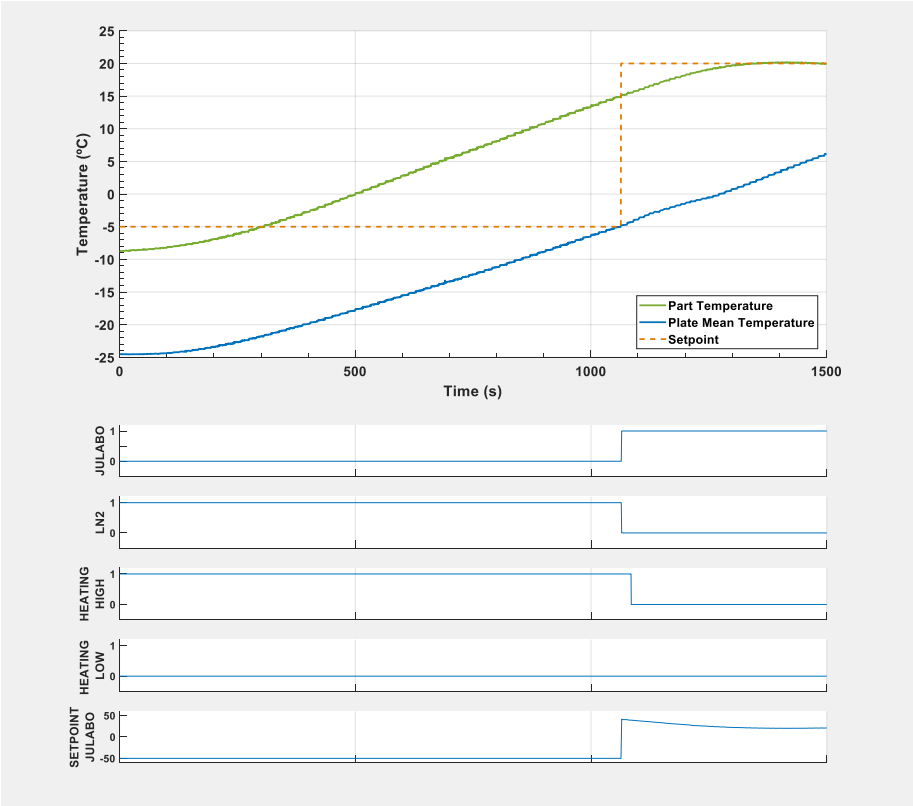

Figure 108- LN2 to thermal bath transition

Similarly, Figure 108, shows the transition between the liquid nitrogen and the thermal bath. When the LN2 controller is given the transition setpoint, -5 ºC for this case, the heating elements is turned on until there is a switch of systems. This occurs when the mean temperature of the plate achieves the defined transition temperature. After this, the thermal bath is turned on and the PI controller takes over the setpoint of the thermal bath, controlling the part temperature with the new setpoint.

8.2 Sub-zero control

After switching from the thermal bath system to the liquid Nitrogen, as shown earlier the Nitrogen direct valve is turned on and the temperature part starts decreasing (Figure 109). This condition is maintained until crossing the defined setpoint.

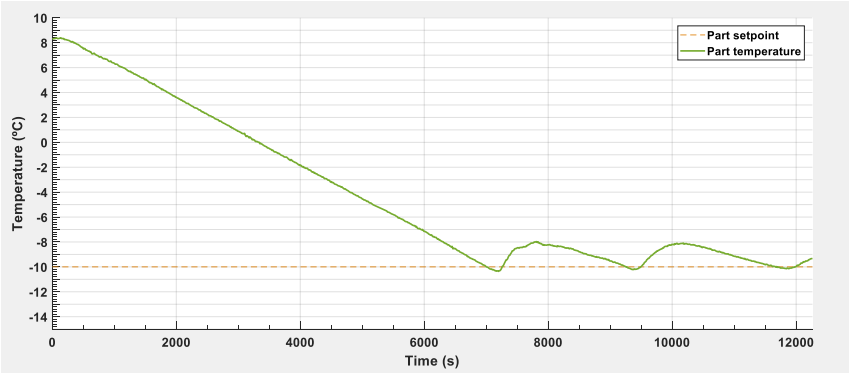

Figure 109- Sub-zero cooling and control

When the first limit (L1), defined in the controller as 90% of the setpoint, is crossed (Figure 110) it is possible to verify that there is a programmed switch from the direct to the regulated valve. From the moment the setpoint is crossed on, the system starts being controlled by the band controller. Its control actions can mainly be seen in the regulated valve and low power heating element.

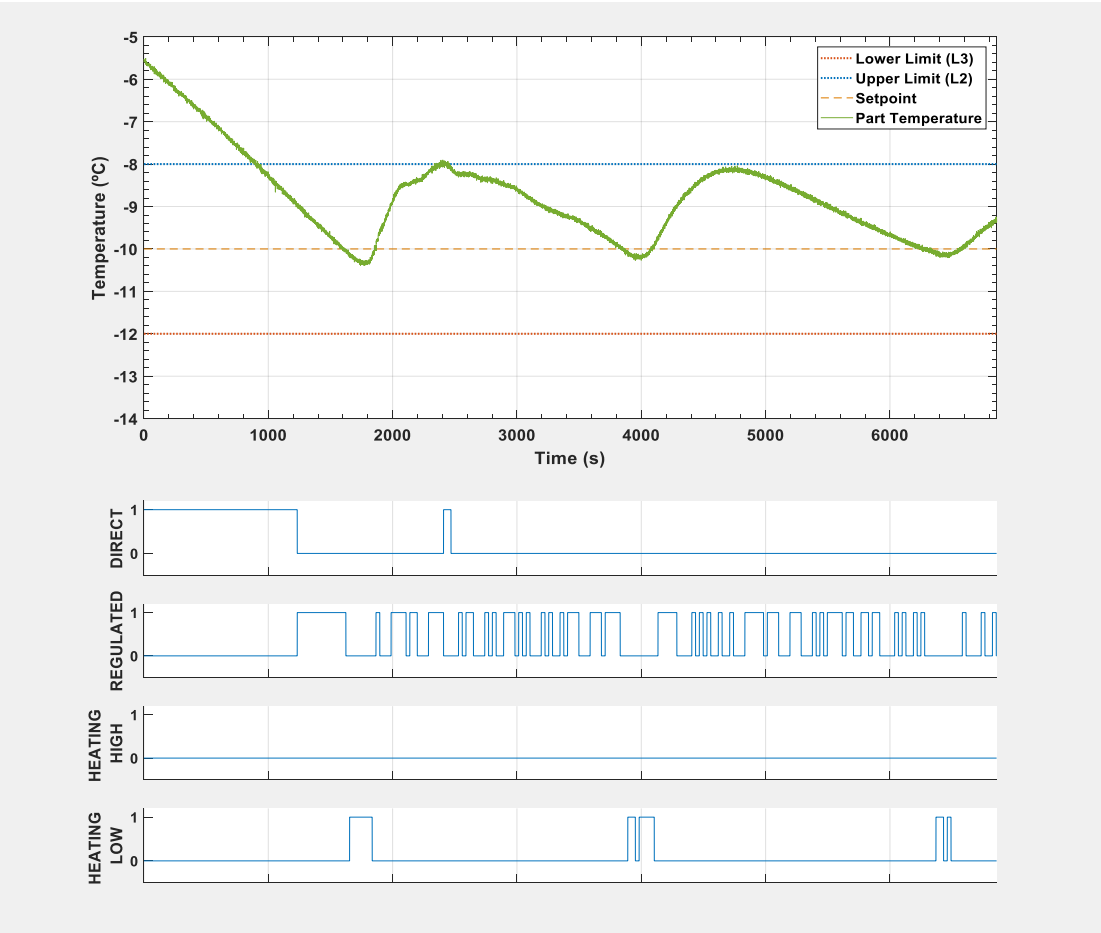

Figure 110- Nitrogen cooling band control

The limit crossing conditions are also attested, as shown by the direct valve turning on as soon as the temperature is higher than the upper limit.

The temperature is kept within 2 °C of the setpoint which is within acceptable margin of error. Given the mean value of the part is approximately 1ºC above the setpoint, in future improvements of the controller, the output setpoint must be internally corrected to meet the input setpoint.

Regarding the increase in temperature after setpoint crossing, the filtering done to the control action, ensuring that it stays on for at least 30 seconds, combined with the 50% power of the heating element and system response delay, leads to a significant energy storage and consequent increase of the part temperature. The reduction of the heating power and of the filtering frequency for the heating are possible corrections to be done.

Nevertheless, the controller works, and the stabilization criteria and temperature tolerances specification are met.

8.3 PI controller

After cycling and sub-zero temperature controlling, the PI controller was put to the test. A complete cycle can be seen in Figure 111 and shows the controller responding to system variations.

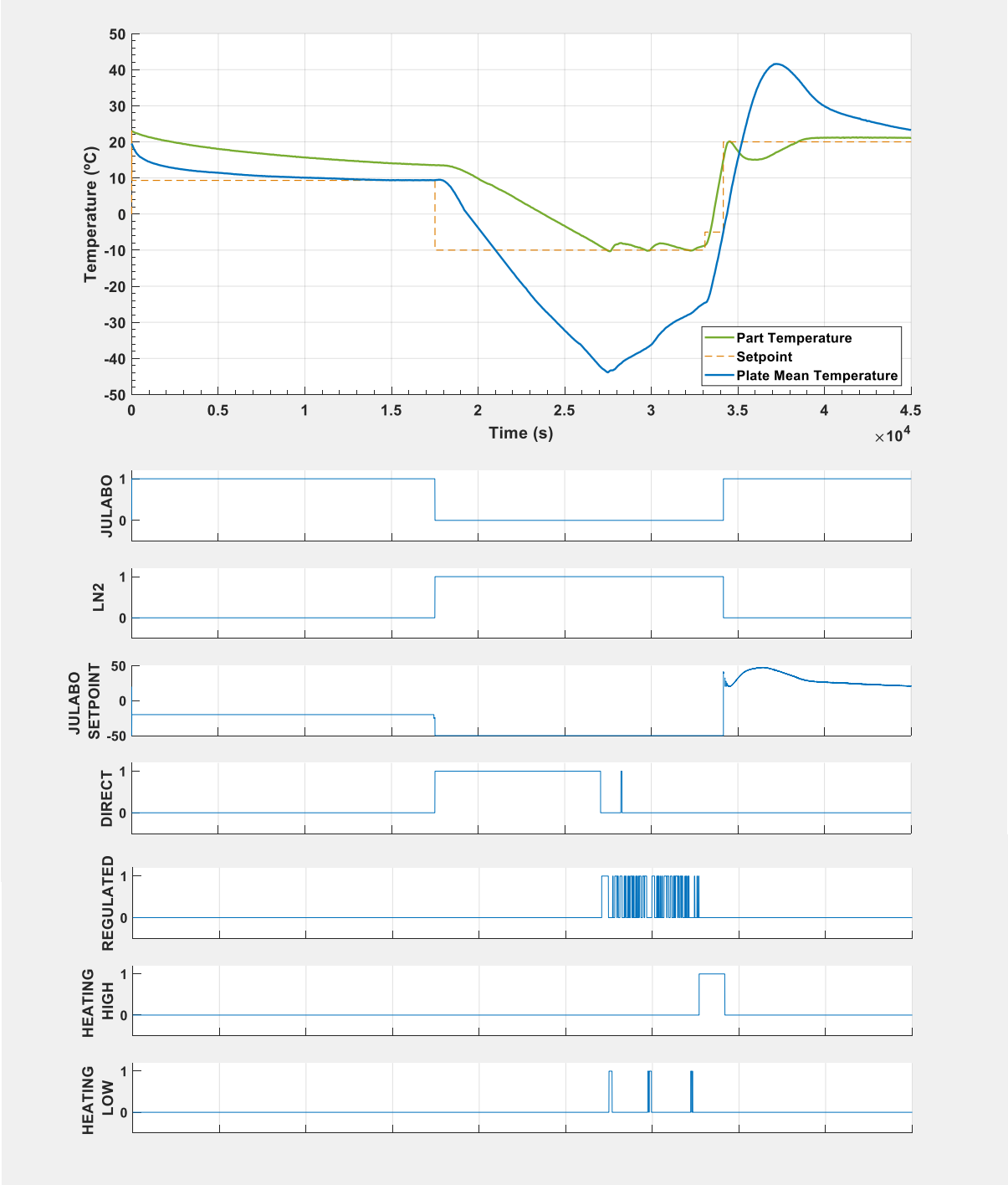

Figure 111- Complete cycle

It is also important to show the full cycles, to better understand the phenomena that lead to the PI response.

The part was at negative temperatures, and the plate at even lower temperature. When the heating was tuned on, it had more effect on the part due to its smaller size and proximity to the irradiating surface. This lead to an increase in temperature much more accentuated than the heating of the copper plate. As a result, when the part achieved the setpoint, and the thermal bath system was turned on, the temperature differential was big enough to reduce the part temperature with the heat absorption by the plate.

When this occurred, the PI controller started correcting the bath temperature to compensate for such behaviour. And, as its seen at the end of the test, the final temperature is stable and with a small error to the setpoint, while the cooling is still occurring.

Consequently, the PI controller performed its job and adapted to disturbances of the system and controlled accordingly.

When transitioning from the sub-zero temperatures to the above zero ones, while done successfully and in a controlled manner, the behaviour may be smoothened by limiting the heating to facilitate the transition and avoid such abrupt part temperature drop. This becomes even more critical at lower temperatures, where the differential between part and plate is higher.

Therefore, this test validates the implemented solution regarding both the temperature control and thermal cycling, while at the same time foreseeing improvements that can be done to a future iteration of the controller.

9 CONCLUSIONS AND FURTHER WORK

9.1 Conclusions

The main objective of this work was the development of a control system for the thermal vacuum chamber at INEGI. The objective was the creation of an automatic temperature cycling system, that is robust and reliable for long term testing.

From a control system stand point, this project was very unique since it required two completely different approaches for the different heat exchange systems: for the above zero system a common PID controller was used, while the sub-zero system required a more custom and experimental method. The programming component was very significant in this project, mainly in LabVIEW, and due to the type of programming used, it set some challenges in creating the control algorithm.

The instrumentation and signal processing element were also very demanding, resulting from all the temperature and pressure sensors that need to be monitored and the control signals being sent to all the auxiliary systems, through the DAQ board. Two new electronic boards had to be developed, for the control of the solenoid valves and control of the heating element.

The thermal bath modelling was successful and proved to be a good approximation to the real behaviour and was essential for the controller parameter estimation. The tests run for the modelling of the chamber allowed for a better understanding of the dynamics involved and influence of outside variables, such as room temperature and chamber pressure, on the part temperature evolution.

A new solution for the heat exchange circuits was designed, and all the parts acquired, assembled and tested both separately and after integration with the other systems. Four new cryogenic solenoid valves and a heating element were added to the system.

Besides the installation of the physical system and implementation of the control system, a graphical user interface and data acquisition program was developed for controlling and monitoring the functions of the chamber.

The goals set at the beginning of this project were achieved, and the control system is able to operate within the established requirements while cycling with no human intervention, except for the exchange of the liquid Nitrogen (N2) bottle.

9.2 Future work

Although all the goals were achieved, and the controller operates correctly and is completely suited for the current project objectives and requirements, some modifications may be implemented in the future in case of need.

A complete modelling of the chamber-plate-part dynamics can be made, to better understand the heat exchanges occurring in the system. As the objective of this dissertation was only focused on the development of a controller, the model used was an approximation to the system behaviour, which was appropriate for such task. Understanding the influence of the various systems and solutions in the temperature control may also emphasize the need for the following solutions.

Even though fully working, the access to internal variable of the thermal bath and faster communication options, instead of a closed heating system, may render the upgrade of the thermal bath a viable idea, with the main objective of having the full control of the process and not be dependent on drivers and software from the manufacturers. This type of solution was discussed in section 4.5 and some examples detailed.

Furthermore, though a topic out of the scope of this project, but directly related to it, the improvement of contact interface with the copper plate should also be studied and possibly improved, by using highly conductive material. The addition of a heat exchange shroud to the inside of the chamber, to promote better heat exchange may also be a solution to consider and evaluate, since it is a common solution in thermal vacuum chambers and could promote more temperature homogeneity in comparison to the copper plate and passive shroud currently used.

Lastly, and looking back at decisions made during the execution of the project, the system is fully operational but other approaches could have been followed. If a more complex controller is required for future projects, the use of two solenoid ON/OFF valves for the liquid nitrogen system may be swapped for a continuous control of the liquid Nitrogen flow, exchanging a binary control system with a continuous one, having in mind the complexity of said system and components involved.

10 BIBLIOGRAPHY

[1] C. Perestrelo, “Reusable and Non-Explosive Actuator for Hold Down and Release Mechanisms,” SPIN-RUNE-TN5.2.

[2] Spin.Works, “Proposta de candidatura- Parte B (Anexo Técnico)”.

[3] U.Porto, "Noticias UP," 2016. [Online]. Available: https://noticias.up.pt/inegi-reune-lideres-para-debater-o-futuro-em-materia-de-inovacao/. [Accessed February 2018].

[4] INEGI, 2011. [Online]. Available: http://www.inegi.pt/instituicao.asp?idm=1&idsubm=5&LN=EN. [Accessed February 2018].

[5] R. S. S. Chisabasa, E. E. Bürger and G. Loureiro, “Space Simulation Chambers State-Of-The-Art,” in *International Astronautical Congress (IAC)*, Guadalajara, Mexico, 2016.

[6] A. Chambers, Basic Vacuum Technology, 2nd edition, CRC Press., 1998.

[7] K. Harrison, “Engineering a Better Vacuum Chamber,” [Online]. Available: http://www.gnbvalves.com/pdf/EngineeringaBetterVacuumChambe.pdf. [Accessed February 2018].

[8] D. M. Hoffman , B. Singh and J. H. Thomas, III , Handbook of vacuum science and technology., Elsevier Science, 1997.

[9] “Vac Aero,” January 2016. [Online]. Available: https://vacaero.com/. [Accessed February 2018].

[10] Osaka Vacuum, “Turbo Molecular Pumps (Compound Molecular Pumps) Exhaust Theory,” 2010. [Online]. Available: http://www.osakavacuum.co.jp/en/products/pump_turbo/genri.html.

[11] Osaka Vacuum, “Turbo Molecular Pumps (Compound Molecular Pumps) Exhaust Theory,” 2010. [Online]. Available: http://www.osakavacuum.co.jp/en/products/pump_turbo/index.html. [Accessed February 2018].

[12] Pfeiffer Vacuum, “5.1 Fundamentals of total pressure measurement,” 2018. [Online]. Available: https://www.pfeiffer-vacuum.com/en/know-how/vacuum-measuring-equipment/fundamentals-of-total-pressure-measurement/. [Accessed February 2018].

[13] Pfeiffer Vacuum, “5.1.1 Direct, gas-independent pressure measurement,” 2018. [Online]. Available: https://www.pfeiffer-vacuum.com/en/know-how/vacuum-measuring-equipment/fundamentals-of-total-pressure-measurement/direct-gas-independent-pressure-measurement/. [Accessed February 2018].

[14] Pfeiffer Vacuum, “5.1.2 Indirect, gas-dependent pressure measurement,” 2018. [Online]. Available: https://www.pfeiffer-vacuum.com/en/know-how/vacuum-

measuring-equipment/fundamentals-of-total-pressure-measurement/indirect-gas-dependent-pressure-measurement/. [Accessed February 2018].

[15] VAC AERO, “Proper Selection and Use of Vacuum Gauges – Part Two,” February 2016. [Online]. Available: https://vacaero.com/information-resources/vacuum-pump-technology-education-and-training/1029-proper-selection-and-use-of-vacuum-gauges-part-two.html. [Accessed February 2018].

[16] VACOM, “Hot Cathode Ionization Vacuum Gauges,” 2017. [Online]. Available: https://www.vacom.de/en/products/total-pressure-measurement/ionization-vacuum-gauge/hot-cathode-ionization-vacuum-gauges. [Accessed February 2018].

[17] Kurt J. Lesker Company, “Pressure Measurement Technical Notes,” 2018. [Online]. Available: https://www.lesker.com/newweb/gauges/gauges_technicalnotes_1.cfm. [Accessed February 2018].

[18] RBD Instruments, “Finding Vacuum chamber leaks,” May 2016. [Online]. Available: https://www.rbdinstruments.com/blog/finding-vacuum-chamber-leaks/. [Accessed February 2018].

[19] Agilent Technologies, “Leak Checking Large Vacuum Chambers,” September 2017. [Online]. Available: https://www.agilent.com/cs/library/technicaloverviews/public/5991-7606EN.pdf. [Accessed February 2018].

[20] ECSS, “Space Engineering - Testing,” February 2002. [Online]. Available: https://eop-cfi.esa.int/Repo/PUBLIC/DOCUMENTATION/SYSTEM_SUPPORT_DOCS/ECSS%20Standards%20for%20Ground%20Segments/ECSS-E-10-03A%20Testing%20.pdf. [Accessed February 2018].

[21] Gary S. Ash, “Manufacturing of Cryoshroud Surfaces for Space Simulation Chambers,” [Online]. Available: http://www.dynavac.com/wp-content/uploads/2015/12/Space-simulation-Conference-2008-2.pdf. [Accessed February 2018].

[22] N. M. Strickland, C. Hoffmann and S. C. Wimbush, “A 1 kA-class cryogen-free critical current characterization system for superconducting coated conductors,” November 2014. [Online]. Available: https://www.researchgate.net/publication/268877470_A_1_kA-class_cryogen-free_critical_current_characterization_system_for_superconducting_coated_conductors?enrichId=rgreq-7c2372e1b6a0aef02da279cc9e1fbc94-XXX&enrichSource=Y292ZXJQYWdlOzI2ODg3NzQ3MDtBUzo0MT. [Accessed March 2018].

[23] Dynavac, “Thermal Control,” [Online]. Available: http://www.dynavac.com/systems/thermal-vacuum/thermal-control/. [Accessed February 2018].

[24] Telstar, “Thermal Conditioning Unit for Space Simulation,” 2013. [Online]. Available: http://www.telstar-vacuum.com/files/BR-THERMAL-CONDITIONING-UNITS-EN-1215_0.pdf. [Accessed February 2018].

[25] Bemco Inc, “Space Simulation and Thermal Vacuum Systems,” 2007. [Online]. Available: http://www.bemcoinc.com/AH.htm. [Accessed February 2018].

[26] Brooks , “P-102 Cryocooler,” 2018. [Online]. Available: http://www.brooks.com/products/cryopumps-cryochillers/cryochillers/p-102-cryocooler. [Accessed February 2018].

[27] Laco technologies, “Custom Solution | Space Simulation System for Satellite Component Testing,” 2017. [Online]. Available: https://www.lacotech.com/products/customer-project-space-simulation-testing-chamber-system?from=33. [Accessed February 2018].

[28] JULABO GmbH, “Bath fluids,” 2018. [Online]. Available: https://www.julabo.com/en/products/accessories/bath-fluids. [Accessed 1 June 2018].

[29] Air Liquide, “The TR, TP, AGIL range,” November 2003. [Online]. Available: http://www.ninolab.se/fileadmin/Ninolab/bilder/air_liquide/TR_TP-GB.pdf. [Accessed February 2018].

[30] Ametherm, “AMETHERM,” 2013. [Online]. Available: https://www.ametherm.com/. [Accessed February 2018].

[31] PTOA, March 2016. [Online]. Available: https://www.ametherm.com/blog/thermistors/temperature-sensor-types. [Accessed February 2018].

[32] P. A. Bemporad, “System identification,” 2010. [Online]. Available: http://cse.lab.imtlucca.it/~bemporad/teaching/ac/pdf/AC2-08-System_Identification.pdf . [Accessed March 2018].

[33] Dewesoft, “PID Control,” 2018. [Online]. Available: https://dewesoft.pro/online/course/pid-control. [Accessed May 2018].

[34] Android developers, “PWM,” 18th April 2018. [Online]. Available: https://developer.android.com/things/sdk/pio/pwm. [Accessed June 2018].